The Genetics of Sexually Selected Male Reproductive Traits in Mice (Mus and Peromyscus Species)

The genetics of sexually selected male reproductive traits in mice (*Mus* and *Peromyscus* species)

A dissertation presented

by

Emily Jacobs-Palmer

to

The Department of Organismic & Evolutionary Biology

In partial fulfillment of the requirements
for the degree of
Doctor of Philosophy
in the subject of

Biology

Harvard University
Cambridge, Massachusetts

April, 2015

Dissertation Advisor: Professor Hopi Hoekstra Emily Jacobs-Palmer

THE GENETICS OF SEXUALLY SELECTED MALE REPRODUCTIVE TRAITS IN MICE (*MUS* AND *PEROMYSCUS* SPECIES)

ABSTRACT

Sexual selection is rampant in Nature, and has produced some of the most beautiful and bizarre traits on Earth. Because females are often promiscuous, sexual selection can continue even after mating, as the sperm of multiple males race to fertilize a limited number of eggs. Though post-copulatory sexual selection is ubiquitous and drives both rapid adaptation and divergence between lineages, we know little about the genetic basis of phenotypes subject to this force. To illuminate one of the important mechanisms by which evolution produces a remarkable diversity of traits, we must identify the genetic loci targeted by post-copulatory sexual selection.

Here we determine the genes or genomic regions underlying particular male reproductive traits—sperm development and morphology, age to male sexual maturity, and segregation distortion—that were likely shaped by post-copulatory sexual selection in the ancestors of mice from the genera *Peromyscus* and *Mus*. We measure phenotype at the organismal and cellular levels, and then employ quantitative trait locus mapping, RNA sequencing, and bulk DNA sequencing to pinpoint loci influencing the aforementioned traits.

We first identify a single locus of large effect controlling sperm midpiece length, a trait relevant to sperm competition success that differs between promiscuous and monogamous sister species of *Peromyscus* mice. We then show that regions of the genome underlying polymorphism in sperm morphology within species are entirely distinct from those determining divergence in the same traits between species. Next, we determine differences in age to male sexual maturity in closely related species with disparate mating systems, and characterize the role of *cis*-regulatory evolution in the timing of male reproductive development. Additionally, we develop a novel method to identify segregation distortion systems that may have been shaped by historical selection at multiple levels, but find none in hybrids of *Mus musculus.* Finally, we characterize the role of a non-coding RNA locus in male fertility, discovering that it mediates separation of spermatids from collective cytoplasm. In sum, we reveal links between particular genes or genomic regions and male reproductive phenotypes that may influence success in post-copulatory competition, thereby clarifying the mechanistic basis of evolution by sexual selection.

TABLE OF CONTENTS

ACKNOWLEDGEMENTS

My deepest gratitude goes to Hopi. It has been almost a decade since the day I met her and caught her infectious enthusiasm for scientific research. She has been a great mentor and dear friend; I admire her, and I revel in the opportunities I've had to learn from her and think alongside her. I hope that there will be many more!

I am grateful to Jonathan Losos, Dan Hartl, and David Haig, who served on my committee and with whom I had the pleasure of teaching and learning throughout my time in OEB. Each of them applied their expertise to improve my research and did so in the kindest and most patient and genuine manner imaginable.

I sincerely appreciate my colleagues in the Hoekstra Lab. What a wonderful, brilliant, crazy group of people! In particular, the mentorship of Heidi Fisher, captain of Team Sperm, has been instrumental to my growth as a scientist. And I am a happier individual and clearer thinker as a result of conversations with Sacha Vignieri, Jesse Weber, Rowan Barrett, Emily Kay Delaney, Hillery Metz, Evan Kingsley, Nicole Bedford, Kyle Turner, Ricardo Mallarino, and Andrés Bendesky, among so many others.

I am very fortunate to be a member of the OEB, Harvard, and Somerville communities: personal relationships are an essential context for scientific progress. In particular, I thank G1 students in OEB 399 with whom I had the pleasure to work closely, as well as Nikki Hughes, Alison Pirie, and Chris Preheim, who make getting it done easy and fun. I appreciate Mona, Jesse, Eny, and Joe, who have been good friends, and who are excellent at what they do. My students at Harvard College, Harvard Extension

School, and the Boys and Girls Club at the Healey School in Somerville have taught me and helped to keep my life balanced. The mice also deserve mention: I respect their lives and appreciate their contribution to our understanding of biology.

Finally, I thank many good friends and family who have seen me into my PhD, will see me out again, or both. Kate Chabot, Nick Coffin, Ryan Kelly, Lindsey Reed, Adina Bricklin, Mel McCrea, Nina Eichacker, Beck and Emily Straley, Maude Baldwin, Shane Campbell-Staton, Susie Gagliardi, and other good friends have celebrated life with me. Callin Switzer fills my days with laughter and love. Diana Reno, Cliff Lerner, Uncle Larry Palmer, and Manju Hingorani lured me onto the path of scientific research with their excellent teaching. My grandfather Martin Jacobs was a tireless supporter of my education and development. My grandmother Laura Vajda is my constant champion and inspiration. My parents are two amazing individuals who give so much of themselves, bringing opportunity and joy to the world around them, and me in it; I thank them with all of my heart.

INTRODUCTION

Sexual selection—the subset of natural selection involving organisms' ability to reproduce, rather than to simply survive—has produced some of the most bizarre and beautiful traits on Earth (Figure 0.1). This type of selection can influence any sexually reproducing species in which there is competition between members of the same sex over access to the opposite sex (intrasexual selection), or in which at least one sex exercises a degree of mate choice, preferring particular characteristics in the opposite sex (intersexual selection) (Bradbury & Davies 1987). Because a sexually reproducing organism's biological fitness is closely tied to how many times it mates, and with whom (Bateman, 1948; Darwin, 1871; Fisher, 1930), both intra- and intersexual selection are common and widespread.

Sexual selection has unique features that render it particularly important as a factor shaping the diversity, outward appearance, and behavior of living things (Andersson 1994). In contrast to the environmental elements producing natural (i.e., non-sexual) selective forces, which are often (though certainly not always) abiotic, the forces determining an organism's reproductive success—the traits of competitors and potential mates—are biotic. Thus, while selection by an environmental factor may drive adaptation towards a particular optimum, traits driven by sexual selection chase moving targets; an organism must not simply be 'large' or 'strong' if only the largest and strongest reproduce, and the size and strength of competitors evolves constantly. Traits thus produced may rapidly become extreme unless checked by natural selection, when

the benefit of attractiveness or competitive superiority causes a cost of greater magnitude to survival (Fisher, 1930). Additionally, the sexually-selected characteristics that determine an individual's reproductive success within a population often limit mating between populations, spurring speciation (Ritchie 2007). Sexual selection is therefore an important force in the production of biodiversity worldwide, helping to create "endless forms most beautiful" (Darwin 1859).

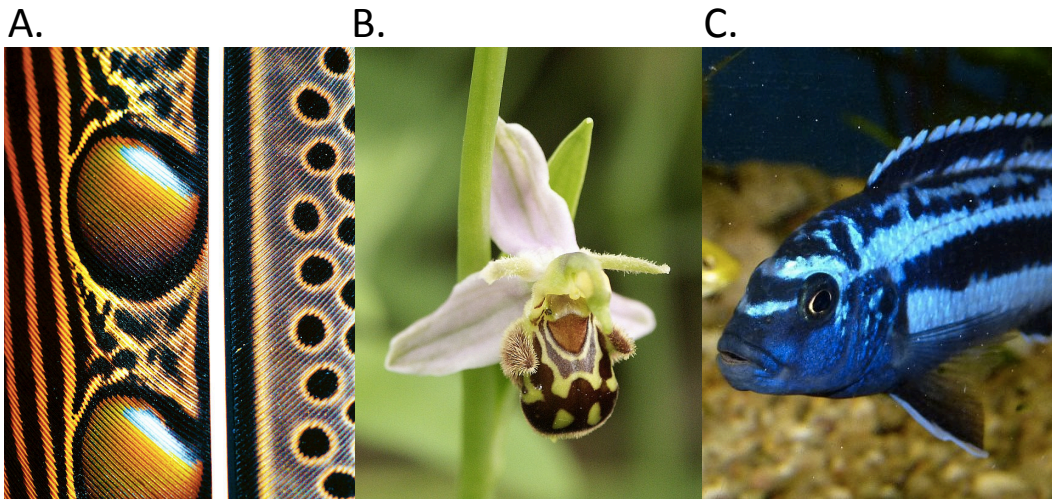

Figure 0.1: Bizarre and beautiful traits shaped by sexual selection

Images of traits shaped by sexual selection in a bird, a bee, a flower, and a fish. A. The feather shown here (Johnson 2012) prompted Charles Darwin to state in *Descent of Man and Selection in Relation to Sex*, "I know of no fact in natural history more wonderful than that the female Argus pheasant should appreciate the exquisite shading of the ball-and-socket ornaments and the elegant patterns on the wing-feather of the male" (1871). Needless to say, Charles Darwin had no shortage of natural history facts

to admire. B. Sexual selection on both a bee (genus *Eucera*) and a bee orchid (*Ophrys apifera*; Berndh, 2005) help determine the appearance and scent of the latter. The orchid resembles a female bee and produces chemicals similar to her pheromones (themselves sexually selected), enticing the male bee to approach the flower and attempt copulation (Schiestl *et al.* 1999). The attempted copulation deposits pollen onto the bee, which is then transferred to the next flower he visits, increasing the fecundity of the original orchid. The plant's sneaky technique highlights potential for complexity in traits shaped by sexual selection. C. This brilliant blue fish (*Melanochromis cyaneorhabdos*; Rehschuh, 2011) is a cichlid of the African Great Lakes, where sexual selection (in combination with ecological opportunity (Wagner *et al.* 2012)) has formed hundreds of species in the short evolutionary time-scale of a few hundred thousand years (Genner *et al.* 2007).

Post-copulatory sexual selection

For approximately a century, from the publication of Darwin's treatise on sexual selection, *Descent of Man* (1871), until the 1970s, the scientific community broadly assumed that sexual selection acted only during the period prior to copulation (in internally fertilizing species such as our own). Once mates were won or chosen, the battle was over (Birkhead 2010). These assumptions went hand-in-hand with the presumption of female monogamy in animals (Knight 2002). More recent research, however, has shown that females are often promiscuous, and that sexual selection is thus rife even after 'the act' occurs (e.g. in insects (Arnqvist & Nilsson 2000), birds

(Petrie & Kempenaers 1998), reptiles (Uller & Olsson 2008), and mammals (Soulsbury 2010)). Competition among sperm from multiple males may follow mating (Parker 1970), continuing or replacing the process of competition among male individuals, and the female reproductive tract may favor particular sperm (Eberhard 1996), allowing female individuals to bias paternity regardless of their ability to select mates. Because they occur after mating, these two phenomena—sperm competition and cryptic female choice, respectively—together are termed post-copulatory sexual selection (Birkhead & Pizzari 2002).

Just as pre-copulatory sexual selection has resulted in a dazzling array of traits visible to the naked eye (Figure 0.1), so post-copulatory selection has driven similarly fantastic traits not typically observed by the casual naturalist. For example, sperm of certain mammalian species cooperate: gametes from one male aggregate together, out-swimming lone cells in the race for ova (Fisher & Hoekstra, 2010; Jenkins et al. 2002; Pizzari & Foster, 2008). In one species of fruit fly, the testes comprise more than ten percent of a male's adult body weight, and sperm are almost six millimeters long, many times the length of the male (Bjork et al. 2007). Lastly, in some ducks, females form a bond with one male, but are forced into copulation by others. Multiple blind-end pouches in the female tract may allow a hen to shunt sperm of aggressors away from her eggs, thus retaining control over the paternity of her offspring (Brennan *et al.* 2007). Furthermore, post-copulatory sexual selection appears to drive extremely rapid adaptive change in reproductive proteins (Swanson & Vacquier 2002), and is often responsible for shaping the traits (e.g. genitalia) used to differentiate closely-related

taxa that are otherwise indistinguishable (Hosken & Stockley 2004), suggesting that selection acting upon these structures may be critical to the isolation of lineages.

The importance of post-copulatory sexual selection in the evolution of gametes and reproductive organs, and in the divergence of incipient species, is now widely appreciated by the scientific community (Birkhead & Pizzari 2002; Ritchie 2007). Yet the genetic regions underlying adaptation to post-copulatory sexual selection in natural populations are known in only a very few cases (primarily selfish genetic elements that mediate fertility, e.g. *SD* in fruit flies (Larracuente & Presgraves 2012) and the *t*-haplotype in house mice (Manser *et al.* 2011)). Techniques such as quantitative trait locus (QTL) mapping and genome-wide association studies (GWAS) have revealed the genetic basis for many naturally selected traits (reviewed in Anderson, Willis, & Mitchell-Olds, 2011; Nadeau & Jiggins, 2010; Stapley et al., 2010); by applying these methods to the study of traits modified by post-copulatory sexual selection, we can address fundamental questions about the nature of this force. For example, does phenotypic change in response to post-copulatory sexual selection typically involve many genes, or few? How does polymorphism in the responding traits (and in the underlying genomes) among populations translate to divergence between species? Are regulatory changes particularly important in shaping these phenotypes, or protein coding changes, or both? In sum, identifying the genetic basis of traits molded by post-copulatory sexual selection will illuminate the precise mechanisms by which sexual selection drives rapid adaptation and speciation.

Study system and dissertation outline

Here we examine the genetic basis of sexually selected traits in wild-derived and domesticated strains of mice from the genera *Peromyscus* and *Mus.* These animals exhibit natural variation in ecologically relevant phenotypes, or induced variation in male fertility. Their close relation to the laboratory mouse (*Mus musculus*) allows us to take advantage of associated molecular tools and genetic resources. Additionally, because mice have become models for health and disease, our work on the reproductive traits of these small mammals can contribute to a greater understanding of human fertility (and lack thereof), despite our clear focus on the genetic response to post-copulatory sexual selection.

In the first chapter of this thesis, we study two closely-related sister species of deer mice (genus *Peromyscus*) common in North America, one of which is promiscuous and the other, monogamous. We characterize differences in sperm morphology between these species, and demonstrate that midpiece length is adaptive in sperm competition. We then identify differences in transcript-specific gene expression underlying variation in this important trait, thereby linking natural variation at a genetic locus to changes in phenotype with relevance to organismal fitness.

In Chapter 2, we measure sperm attributes in an additional subspecies of the promiscuous deer mouse examined in Chapter 1, and determine the intraspecific genetic architecture of variation in these traits. We then compare the loci underlying polymorphism in sperm morphology within species to those determining divergence between species. We find that entirely distinct regions of the genome control sperm

midpiece and tail length at the inter- and intraspecific levels.

In Chapter 3, we characterize differences in the age to sexual maturity between promiscuous and monogamous deer mice, and establish potential fitness consequences of this shift. We then analyze allele-specific expression in testes of hybrid animals over development to determine the prevalence of *cis*-regulatory changes that might mediate the timing of reproductive maturity. We find that, at a minimum, hundreds of loci show evidence of evolution in *cis*-regulation since divergence of these two species, and may thus contribute to differences in age to sexual maturity. Additionally, large clusters of genes exhibit differential allele-specific expression over time, suggesting that many recently evolved *cis*-regulatory changes are cell-type and context specific.

Chapter 4 addresses a phenomenon known as segregation distortion, in which different sperm cells within an individual male may sabotage one another (with subsequent effects on male fertility and sperm-competitive ability). Using a novel methodology, we search for segregation distorters in hybrids of wild-derived lab mouse subspecies in an attempt to understand their potential contribution to speciation. To our surprise, despite excellent power to detect segregation distorters of small effect, we find none in this study. Nevertheless, our method is highly applicable to the search for such selfish genetic elements in other taxa.

Finally, in Chapter 5, we investigate the role of the locus encoding *Tug1*, a long non-coding RNA essential for male fertility. By examining sperm, testes, and epididymides of animals lacking the *Tug1* locus, we discover that this lncRNA mediates separation of individual spermatids from their collective cytoplasm in the final stage of

spermatogenesis. This study is the second to characterize the role of a lncRNA in male fertility, and the first to implicate any gene in the process of sperm individualization in mammals.

Post-copulatory sexual selection is a powerful evolutionary force that promotes rapid adaptation and speciation. However, we know little about the response to post-copulatory sexual selection on a genetic level, either within or between species. Here we characterize the genetic basis of multiple traits shaped by this force: sperm morphology, age to sexual maturity, segregation distortion, and sperm development. It is our hope that this detailed study is practically applicable to mammalian fertility, and that it may increase basic knowledge of the genetic mechanisms by which sexual selection drives evolutionary change.

CHAPTER 1: THE CAUSES AND CONSEQUENCES OF ADAPTIVE SPERM MORPHOLOGY IN DEER MICE

Co-authors: Heidi Fisher, Jean-Marc Lassance, and Hopi Hoekstra

ABSTRACT

An extraordinary array of reproductive traits is shaped by sexual selection, yet the mechanisms that enable divergence, often over short evolutionary timescales, remain elusive. In natural systems it is frequently unclear which genes are responsible for variation in sexually selected traits and how changes in those genes directly modulate reproductive success. Here we examine two sister-species of *Peromyscus* mice, one that mates promiscuously and one monogamously, which experience disparate levels of sperm competition, a form of post-copulatory sexual selection. We show that these species differ in sperm morphology, and that the most competitive sperm have flagella with longer midpiece regions. In second-generation hybrids, we find that midpiece length is positively correlated with sperm swimming velocity and with paternity. We then use a forward-genetics approach to identify a gene associated with midpiece size: *Prkar1a*, whose protein product we show localizes to the sperm flagellum in *Peromyscus.* We confirm the role of this locus by demonstrating that lab mice with a dominant negative mutation in *Prkar1a* have shorter midpiece than their wild-type brothers. While we find no *Prkar1a* coding changes between the two

Peromyscus **species, we observe differential mRNA expression in the testes but not in other tissues, including the epididymis where mature sperm are stored, suggesting that** ***Prkar1a*** **regulation affects sperm development. Finally, we show that genetic variation at this locus also accurately predicts male reproductive success – hybrid males carrying at least one** ***Prkar1a*** **allele from the promiscuous species are more likely to sire offspring than males carrying only monogamous-species** ***Prkar1a*** **alleles. By examining the molecular basis of reproductive traits directly related to fertility, we demonstrate that rapid evolution of sexually selected traits can occur through tissue-specific changes to ubiquitously expressed genes that act during development and can, in turn, affect fitness.**

INTRODUCTION

The rapid evolution of elaborate male displays and weaponry, traits that maximize the potential for reproductive success prior to mating, are classic examples of sexual selection (Darwin 1871; Andersson 1994). However, when females mate with multiple partners within a reproductive cycle, male competition can continue long after mating has occurred as sperm compete for fertilization of a limited number of ova (Birkhead & Pizzari 2002). Although the phenotypic targets of post-copulatory sexual selection can vary tremendously across taxa, even slight trait modifications can lead to a measurable increase in an individual's fitness. By contrast, these changes can also result in a failure to reproduce at all or lead to negative pleiotropic consequences in either the

opposite sex or in other tissues, as most genes expressed in reproductive organs (e.g. testes) are also expressed elsewhere in the body (Shima *et al.* 2004; Chalmel *et al.* 2007). Despite these constraints, reproductive phenotypes show striking and often rapid divergence (Birkhead *et al.* 2008). Since the genetic basis of many sexually selected traits is poorly understood, the mechanisms by which genetic changes enable reproductive traits to respond so quickly to changes in the selective regime remain unclear.

The strength of post-copulatory sexual selection is largely determined by female mating strategy (Birkhead & Pizzari 2002). We examine two closely related *Peromyscus* rodents with highly divergent mating systems—monogamy and promiscuity. Within the genus, sperm competition is predicted to be greatest in *P. maniculatus*: both sexes mate with multiple partners, often in overlapping series just minutes apart (Dewsbury 1985), and females frequently carry multiple-paternity litters in the wild (Birdsall & Nash 1973). By contrast, its sister species *P. polionotus* is strictly monogamous on the basis of both behavioural (Dewsbury 1981) and genetic data (Foltz 1981). Moreover, relative testes size is roughly three times larger in *P. maniculatus* than in *P. polionotus* (Linzey & Layne 1969), consistent with the relationship between relative testis size and level of sperm competition in rodents (Ramm *et al.* 2005). Therefore the post-copulatory environments experienced by *P. maniculatus* and *P. polionotus* males represent divergent selective regimes, yet the phenotypic and genetic targets of this selection are unknown.

METHODS

Animals and breeding scheme

We performed all pure species experiments and measurements using wild-derived outbred stocks of *P. polionotus* and *P. maniculatus* obtained from the Peromyscus Genetic Stock Center (Columbia, South Carolina). To generate second-generation (F2) hybrid progeny of these species, we bred two *P. polionotus* males with two *P. maniculatus* females to produce 38 first-generation (F1) hybrids, and then intercrossed F1 siblings to produce 300 F2 male mice. All animals were produced and used in accordance with the Hoekstra Laboratory IACUC Protocol 27-23.

Male sperm motility, sperm morphology, and fertility phenotypes

To determine sperm motility parameters of pure species and hybrids, we sacrificed animals and collected sperm by dissecting out the cauda epididymis, bisecting it, and suspending the tissue in a solution of Biggers-Whitten-Whittingham (BWW) sperm media (Biggers *et al.* 1971) at 37 degrees Celsius. After approximately 15 minutes, we mounted 20uL of sperm between a plastic slide and coverslip, and took a five-second video of live cells on an upright microscope (AxioImager.A1, Zeiss, Jena, Germany). We measured sperm motility parameters (including total number of motile sperm, straight-line velocity (VSL), curvilinear velocity (VCL), and average path velocity (VAP) from these videos using the Computer Assisted Sperm Analysis (CASA) plugin for ImageJ. To measure sperm morphology, we fixed sperm suspended in BWW in 2% paraformaldehyde, and mounted 20 uL suspended cells in Fluoromount media

(Southern Biotech). We measured sperm midpiece and total flagellum lengths from 10 cells per male using the curve spline tool in the AxioVision software package. To determine the fertility of F2 males, we paired each F2 male with an F2 female for at least one week, and recorded resultant offspring (or lack thereof) as a measure of reproductive success. We performed all statistical tests in R (R Core Team 2014).

Competitive swimup assays

To assess the association of sperm midpiece length with success in sperm competition, we performed a series of swim-up assays. We removed and incubated the sperm of two males as above, diluted the more concentrated sperm sample with buffer to ensure approximately equal numbers of sperm entering the competition, and placed equal volumes of sperm from the two males in a single 1.5 mL tube (Eppendorf). We then added polyvinylpyrrolidone (PVP, which increases the sample density, producing more discriminating swimming conditions) to a final concentration of ten percent. We retrieved and fixed (as above) an initial sample of sperm, representative of the population of cells entering the competition, before centrifuging in a 37°C warmed rotor at 250xg for five minutes. During centrifugation, the most motile cells remain in suspension, while those with low or no motility collect at the tube bottom; we thus took and fixed a second sample of sperm, representative of the population with high motility, from near the tube's surface immediately following centrifugation. We then measured sperm midpiece length for 20 morphologically normal sperm entering, and 20 with high motility, per competition.

DNA extraction and linkage map construction

We extracted genomic DNA from liver tissue using either phenol chloroform (Automated DNA Extraction Kit, AutoGen, Holliston, MA) or DNeasy Kits (Blood & Tissue Kit, Qiagen, Hilden, Germany). We identified single nucleotide polymorphisms (SNPs) and assigned genotypes for each study subject by double digest Restriction-site Associated DNA Sequencing (ddRADseq; (Peterson *et al.* 2012)). Briefly, we digested ~1µg of gDNA for each individual with two restriction endonucleases: EcoR1 and Msp1 (New England BioLabs, Ipswich, MA). We ligated the resulting fragments to sequencing adapters containing a unique barcode for each individual male. We then pooled these barcoded fragments from multiple individuals and isolated the fragments in the size range of 280-320bp using a Pippin Prep (Sage BioSciences, Beverly, MA). Finally, we amplified the remaining fragments using a Phusion High Fidelity PCR Kit (ThermoFisher Scientific, Waltham, MA) and sequenced the resulting libraries on a Genome Analyzer IIx or a HiSeq 2500 (Illumina, San Diego, CA). We recovered 1753 informative SNP markers that consistently differed between the two parental strains used to generate the hybrid population, and which were additionally confirmed as heterozygous in the first generation hybrids (F_1). We then pruned our marker set to exclude any markers genotyped in fewer than 100 individuals or with genotype information identical to another marker; 516 markers remained after pruning.

We conducted all genetic mapping analyses using R/qtl software (Broman *et al.* 2003), an add-on package for R statistical software (R Core Team 2014). To construct a

genetic linkage map, we first calculated linkage distances based on the fraction of recombination events and Logarithm of Odds (LOD) scores between all SNP marker pairs. Next, we grouped markers by varying the recombination parameters until we recovered a map with 23 linkage groups containing at least 5 markers each (the karyotypes of both species are known [n = 24 chromosomes], however we are unable to recover the majority of the Y chromosome with the cross design employed in this study). Any markers not included in the 23 linkage groups were excluded. Finally, we refined this map by ordering the markers within each linkage group in overlapping windows of 8 markers and minimizing the frequency of recombination events between markers in each window. The resulting genetic linkage map contained 504 markers grouped into 23 linkage groups.

QTL mapping

To identify quantitative trait loci (QTL) contributing to sperm morphology, we performed Haley-Knott regression and interval mapping analyses sequentially in R/qtl (Broman *et al.* 2003). To fine-scale map the midpiece QTL, we scanned the 20 cM region of the genome surrounding the marker most strongly associated with sperm midpiece length. The resulting region of interest was syntenic to chromosome 11: 97–114 Mb in *M. musculus* and chromosome 10: 91–104 Mb in *R. norvegicus* (Karolchik *et al.* 2014). We designed markers in eight genes – *Foxj1, Kcnj16, Prkar1a, Prkca, Fmnl1, Klhl10, Slc25a39*, and *Ttll6* – based on position and prioritized those implicated in male fertility, spermatogenesis, cytoskeletal organization, mitochondrial function, and/or specifically

or highly expressed in the testes or during spermatogenesis (Kanz *et al.* 2005; Eppig *et al.* 2012; Karolchik *et al.* 2014; The Uniprot Consortium 2014; Shimoyama *et al.* 2015). We genotyped all F_2 males for informative SNPs residing in each of these genes using custom designed TaqMan SNP Genotyping Assays (Invitrogen, Carlsbad, CA), except in the case of *Ttll6*, where we used a restriction enzyme digest assay (all primers and TaqMan probe sequences are available in Supplementary Table S1.1; methods followed manufacturer's instructions).

Prkar1a sequencing

To investigate genetic differences between *P. maniculatus* and *P. polionotus* within *Prkar1a*, we sequenced the protein-coding region by extracting mRNA from the decapsulated testis tissue of *P. maniculatus* and *P. polionotus* males using an RNeasy Mini Kit (Qiagen, Hilden, Germany), converting the mRNA to cDNA using SuperScript II Reverse Transcriptase (Invitrogen, Carlsbad, CA) and a polyT primer (T16). We amplified the entire coding sequence (1,146bp) using primers listed in Supplementary Table S1.4.

Gene expression

To determine *Prkar1a* mRNA abundance, we performed RNA-Seq on testis tissue of 8 adult *P. maniculatus* and adult *P. polionotus*, and on hypothalamus tissue from a subset of 3 individuals per species. In brief, we purified RNA from fresh tissue with TRIzol reagent (Life Technologies), used RNeasy spin columns (Qiagen) to remove impurities, and then enriched for Poly-A mRNA using a TruSeq RNA isolation kit

(Illumina). We created libraries with a TruSeq Library prep kit and sequenced them on a HiSeq 2000 instrument (Illumina) in the Harvard Bauer Core Facility.

To confirm the results of RNA-Seq, we examined *Prkar1a* mRNA abundance by qPCR. We created cDNA from testis and spleen tissue using an RNeasy Mini Kit (Qiagen, Hilden, Germany), converting the mRNA to cDNA by SuperScript II Reverse Transcriptase (Invitrogen, Carlsbad, CA) using a poly-T primer (T16). We then designed primers to amplify short (100-200bp) fragments crossing at least one exon boundary (Supplementary Table S1.5), ensuring that primer-binding sites were identical in *P. maniculatus* and *P. polionotus*. We conducted assays in triplicate, calculated ΔCT values with *beta actin* (*ActB*), a standard housekeeping gene, and compared relative differences in gene expression in *P. maniculatus* and *P. polionotus* using two-tailed unpaired t-tests with Bonferroni correction.

For untranslated *Prkar1a* exon E1b, we placed forward primers in this exon and a reverse primer in the first translated exon, E2. We then used the KAPA SYBR FAST qPCR system (KAPA Biosystems, Woburn, MA) to determine expression level in both species. Conditions were as recommended by KAPA Biosystems, except that we added 3% DMSO to the reaction and performed the annealing step at 67°C to disrupt the extensive secondary structure in this amplicon.

Quantitative mass spectrometry

We performed quantitative mass spectrometry to determine the levels of PKA R1α protein in the testis of 5 *P. maniculatus* and 5 *P. polionotus* individuals. We

homogenized fresh or flash frozen (in liquid nitrogen) testis tissue with a TissueLyser LT (Qiagen) in buffer containing 100mM NaPO4 pH 7.0, 250mM Sucrose, 150mM NaCl, 1mM EDTA, 4mM EGTA, 4mM DTT, 0.5% Triton-X 100, 1mM PMSF (diluted in ethanol), and 1X Protease inhibitor cocktail (AMRESCO). We then centrifuged the homogenate at 4 degrees Celsius for 20 minutes at 12,000rpm, and removed the soluble protein-containing supernatant. We assayed the protein concentration of this supernatant with Bradford reagent (BioRad), ran it on a TGX precast gel (BioRad), and excised bands corresponding to the molecular weight of the PKA R1α protein. We washed the gel slices in 50% acetonitrile, and submitted samples to the Harvard Mass Spectrometry and Proteomics Resource Laboratory, where they were subjected to proteolytic digestion and microcapillary reverse-phase HPLC nano-electrospray tandem mass spectrometry (μLC/MS/MS) on a Thermo LTQ-Orbitrap mass spectrometer.

Protein Localization

We performed immunohistochemistry on mature epididymal sperm fixed in 2% paraformaldehyde and 1.25% glutaraldehyde for 15 min. We first washed the cells in phosphate-buffered saline with 0.1% Tween 20 (PBT) for 15 min, and blocked in PBT with 3% bovine serum albumin (BSA) for 1 hr at room temperature (RT). Next we incubated the cells overnight at 4°C with the primary antibody, PKA R1α (Santa Cruz Biotechnology #18800, Dallas, TX), which we diluted 1:100 in PBT with 3% BSA. The following day we washed cells in PBT for 1 hr at RT 3 times, and incubated with the secondary antibody, Alexa Fluor 546 (Invitrogen #A11056, Carlsbad, CA), diluted 1:500

in PBT with 3% BSA, for 1hr at RT. Cells were then washed in PBT for 1 hr at RT 3 times, stained with DAPI (Invitrogen, Carlsbad, CA) to visualize DNA within cells for 15 min at RT, washed a final time in PBT for 15 min, and mounted in Fluoromount-G (Southern Biotech Birmingham, AL). In addition, we controlled for non-specific binding of the secondary antibody by performing a side by side comparison with cells processed identically to the above methods except that instead of treating with the primary antibody, cells were solely treated with PBT with 3% BSA, the secondary antibody and DAPI. We viewed cells at 400X and 1000X magnification on an upright microscope (AxioImager.A1, Zeiss, Jena, Germany).

RESULTS and DISCUSSION

The factors regulating reproductive success are complex, yet when sperm from multiple males compete for a limited number of ova, sperm motility can be a key determinant of paternity (Birkhead *et al.* 2008). Indeed, sperm from the promiscuous *P. maniculatus* swim with greater velocity (straight-line velocity [VSL]) than sperm of the monogamous *P. polionotus* (Supplementary Figure S1.1; t-test: $P = 0.017$, $df = 8$, $n = 76$-549 sperm/male). Although velocity is influenced by many traits, sperm morphology and size are known to be under intense sexual selection in rodents (Gomendio & Roldan 2008; Tourmente *et al.* 2011). In our laboratory colonies, we found that sperm head size does not differ between these species (Supplementary Figure S1.2A-B), but *P. maniculatus* sperm have longer flagella than *P. polionotus* (Supplementary Figure S1.2C;

t-test: $P = 8x10^{-11}$, n = 10 sperm/male). Moreover, the midpiece region of the flagellum (Figure 1.1A) is significantly longer in *P. maniculatus* sperm than in *P. polionotus* (Supplementary Figure S1.2D; t-test: $P = 3x10^{-7}$, n = 10 sperm/male), consistent with differences observed in wild-caught individuals (Linzey & Layne 1974). The midpiece houses the mitochondria of the cell and size is predicted to positively influence flagellar thrust and velocity of mammalian sperm (Cardullo & Baltz 1991); furthermore, comparative data from murine rodents both within (Firman & Simmons 2010) and between (Gomendio & Roldan 2008) species support this prediction. To assay the relationship of *Peromyscus* midpiece length and swimming performance in a competitive context we conducted a series of swim-up assays (Holt *et al.* 2010). We found that the most motile sperm in each assay had the longest midpiece; this result was true when the competitions contained sperm from two heterospecific males (*P. maniculatus* vs. *P. polionotus*), two conspecific males (*P. maniculatus* vs. *P. maniculatus*), and even within-male competitions (*P. maniculatus*) (Supplementary Figure S1.3; $\text{t-test}_{\text{heterospecific}}$: $P = 3.28x10^{-4}$; $\text{t-test}_{\text{conspecific}}$: $P = 0.001$; $\text{t-test}_{\text{within-male}}$: $P = 0.014$; n = 20 sperm/trial). Taken together, these results suggest that sexual selection is likely driving the evolution of sperm morphology under a competitive regime.

To dissect the genetic basis of sperm performance and morphology, we performed a genetic intercross between *P. maniculatus* and *P. polionotus* to produce 300 second-generation hybrid (F_2) male offspring. We found that in the F_2 hybrid males, sperm midpiece length (but not total flagellum length) is significantly and positively correlated with velocity across males (Figure 1.1B; linear regression: $R^2 = 0.028$, P =

0.0057). These results show not only that sperm velocity is correlated with midpiece length in *Peromyscus*, but that these two traits share a genetic mechanism or are influenced by tightly linked genes in the genome.

We next measured reproductive success of the F_2 males and found that those who sired pups after being paired with a female had sperm with significantly longer midpiece than those that did not reproduce (Figure 1.1C; t-test: $P = 0.041$). Importantly, these pairings test the effect of midpiece length on male fertility without being compromised either by pre-copulatory selective forces (e.g., male competition for access to females and female mate choice), cryptic female choice, or the false positives that arise from methods designed to bypass reproductive barriers (e.g., artificial insemination and *in vitro* fertilization). Theory predicts that differences in reproductive success due to trait variation in monogamous mating regimes should be amplified in the presence of sperm competition (Birkhead & Pizzari 2002). Moreover, this is a conservative estimate of male fertility because many false negatives were likely included (e.g., pairs that failed to mate, female infertility, missed litters due to infanticide, and other unrelated physiological or behavioural conditions of the animals). These results, in combination with the competitive *in vitro* swim-up assays, directly test the two components of fitness at the focus of this study – reproductive success and competitive ability – and thus indicate that midpiece length is important for competitive fitness in *Peromyscus*.

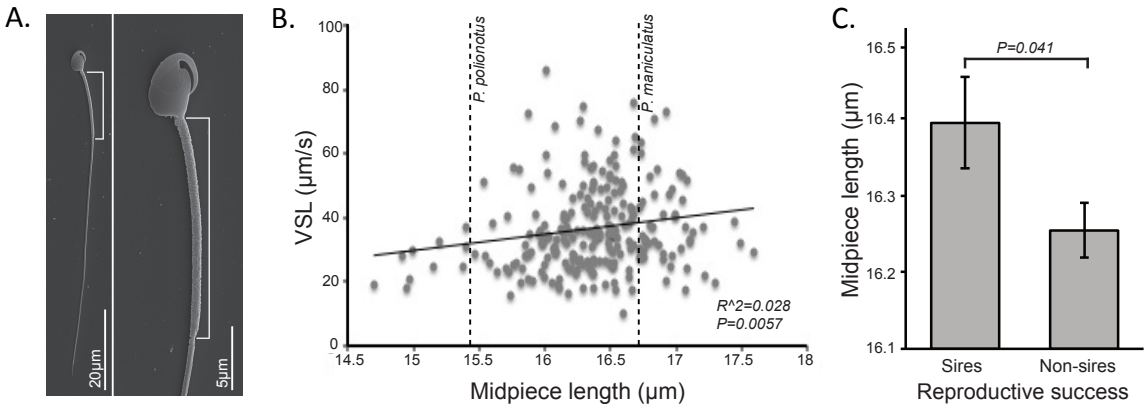

Figure 1.1. Variation in sperm midpiece length.

A. Scanning electron micrographs of a mature *P. maniculatus* sperm cell; the midpiece is indicated by brackets. B. Association between midpiece length and straight-line velocity of F_2 hybrid males (*n* = 233). Midpiece length of each parental species is plotted as a dashed line. Mean ± standard error (SE): *P. maniculatus* = 16.70 ± 0.014µm, *P. polionotus* = 15.43 ± 0.24µm, *n* = 10 males, *n* = 10 sperm/male. C. Mean ± SE sperm midpiece length of F_2 males that did (*n* = 85) and did not (*n* = 173) sire offspring. Note truncated y-axis. **P*<0.05.

Next, to identify quantitative trait loci (QTL) associated with the adaptive difference in sperm morphology, we genotyped each F_2 male at 504 loci throughout the genome. While total sperm flagellum length and velocity had no significant genomic associations (Figure 1.2A), we identified one chromosomal region significantly associated with midpiece length variation on linkage group 4 (Figure 1.2A; on the basis of logarithm of odds (LOD), significance determined by a genome-wide permutation test with $\alpha = 0.01$).

This single region of the genome explains 33% of sperm midpiece length variation in the F_2 hybrids, and largely recapitulates differences in midpiece length observed between the pure species (Supplementary Figure S1.4). Furthermore, we found that F_2 males carrying at least one *P. maniculatus* allele at this locus have a significantly longer midpiece than those with none (Supplementary Figure S1.4; t-test: $P = 4.44 \times 10^{-15}$). Thus, a single large-effect locus explains much of the difference in sperm midpiece length between these two species.

To further refine the QTL and identify a causal locus, we enriched marker coverage in the 20cM region surrounding the marker of highest association by genotyping each F_2 male for 8 additional single nucleotide polymorphisms (SNPs; Supplementary Table S1.1). This improved our QTL signal and reduced the 1.5-LOD support interval to 3.3cM and the 99% Bayes credible interval to a single locus: *Prkar1a* (Figure 1.2B-C). The *Prkar1a* gene encodes the R1α regulatory subunit of the Protein Kinase A (PKA) holoenzyme, which we found is abundant and localized in the flagellum of *Peromyscus* sperm (Figure 1.3A), and is the only gene within the broader 3.3cM confidence interval implicated in male fertility, sperm morphology or sperm motility (Burton 2006; Matzuk & Lamb 2008). Using a genetic breakpoint analysis and two additional SNPs, we confirmed support for *Prkar1a* by narrowing the 3.3cM interval to 0.8cM (Supplementary Table S1.2), a region with only four other known genes that are unlikely candidates on the basis of their function (Supplementary Table S1.3). Our findings therefore strongly implicate the *Prkar1a* gene as a major determinant of the sperm midpiece length differences observed in *Peromyscus*.

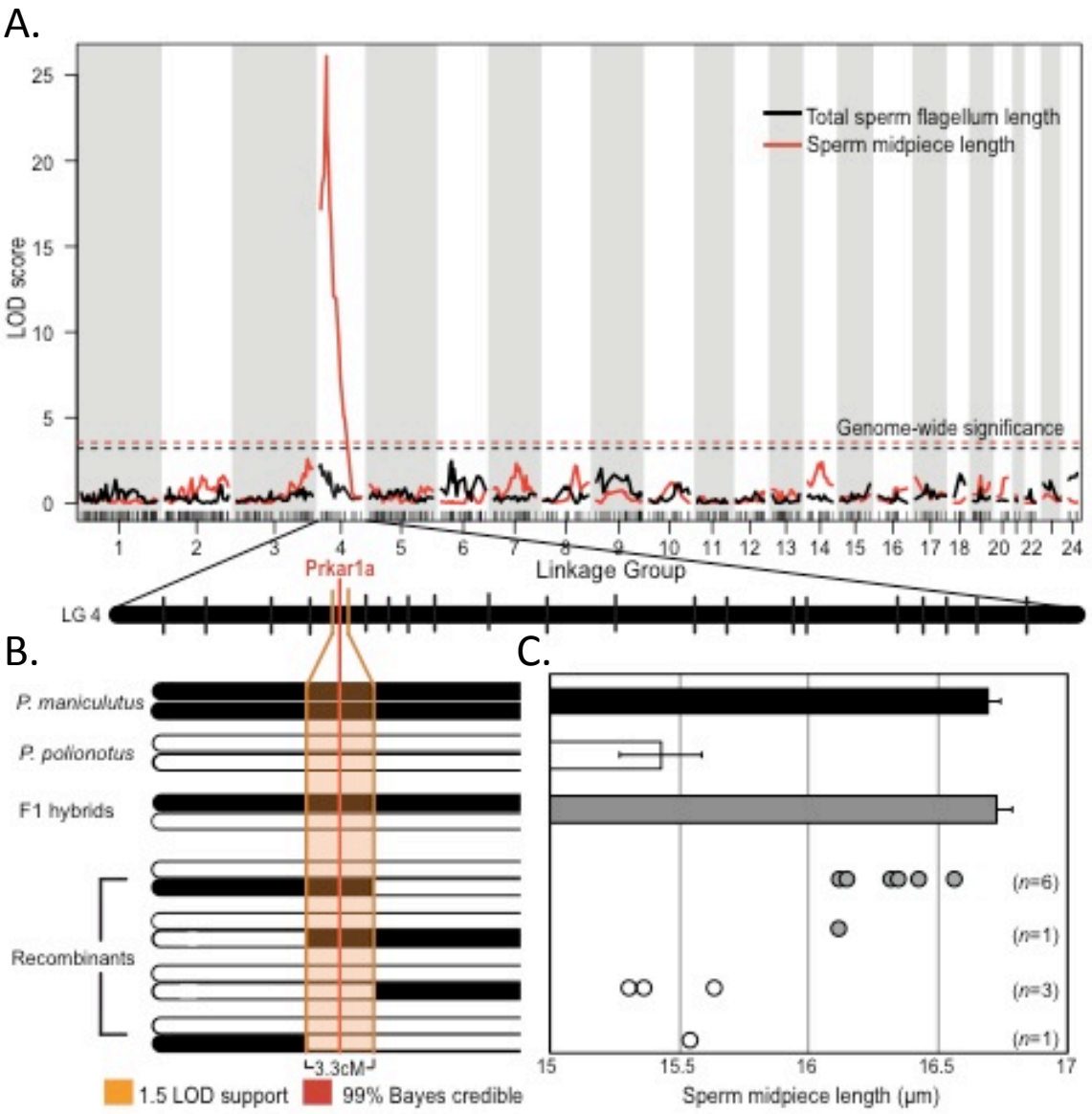

Figure 1.2. Genetic mapping of sperm morphology

(a) Association between genome-wide SNP markers and total sperm flagellum length (black) or midpiece length (red). Genome-wide significant LOD thresholds for each trait (from 10,000 permutations; $\alpha = 0.01$) indicated by dashed lines. (b) Recombinant

breakpoint analysis of Linkage Group 4 (LG4) indicates confidence thresholds for QTL associated with midpiece length. (c) Bar graphs represent mean±SE midpiece length for parental and F_1 hybrid males, circles represent midpiece length (*n* = 10 males, *n* = 10 sperm/male) of F_2 hybrids with recombination events within the 1.5-LOD support threshold. Colour indicates genotype of individual(s) at the *Prkar1a* allele (*AA* = black, *Aa* = grey, *aa* = white), note truncated x-axis.

Successful fertilization requires precise temporal and spatial regulation of PKA activity, the main downstream effector of cellular cyclic AMP concentrations (Burton & McKnight 2007). The R1α subunit is known to influence gross sperm morphology, motility, and fertility in humans presenting Carney Complex (a disease associated with mutations in *Prkar1a*) and in *Mus musculus Prkar1a* mutants (Burton 2006). To confirm the influence of *Prkar1a* on sperm midpiece length in particular, we examined *Mus musculus* C57BL/6 animals with only a single functional copy of the gene (Willis *et al.* 2011) and found that the midpiece of *Prkar1a*$^{+/-}$ males' sperm is significantly shorter than wild type brothers (Figure 1.3B; t-test: *P* = 3.67x10^{-8}, *n* = 10 sperm/male and n = 8-9 males/genotype).

We found no non-synonymous differences between species in the 10 coding exons (1,146 bp) and no differences in overall mRNA or protein abundance of *Prkar1a* in adult testis tissue by quantitative mass spectrometry. However, *Prkar1a* has three distinct testis-expressed transcripts. These differ in their 5' untranslated exons, which confer spatial and temporal specificity (Dahle *et al.* 2001). The most highly expressed

transcript, E1b, shows significantly greater expression in *P. maniculatus* testis tissue, relative to *P. polionotus,* by both RNA-Seq (Figure 1.3C; t-test: $P = 0.006$, $n = 8$ males/species) and qPCR (Figure 1.3D; t-test: $P = 0.005$, $n = 8$ males/species). Although the magnitude of E1b expression differences between species is not large, measures of transcription in adult testis tissue depict the combined activity of reproductive cells participating in multiple stages of spermatogenesis. The degree to which expression differs between species in any particular cell type (such as elongating spermatids undergoing midpiece development) may therefore be underestimated here. Additionally, although *Prkar1a* E1b also appears in both spleen and brain, there are no significant differences in transcript levels between *P. maniculatus* and *P. polionotus* in these somatic tissues (Supplementary Figure S1.6). Taken together, these findings suggest that sexual selection may operate via spatially-restricted transcript regulation of a ubiquitously expressed gene, and therefore without compromising non-reproductive functions in either males or females.

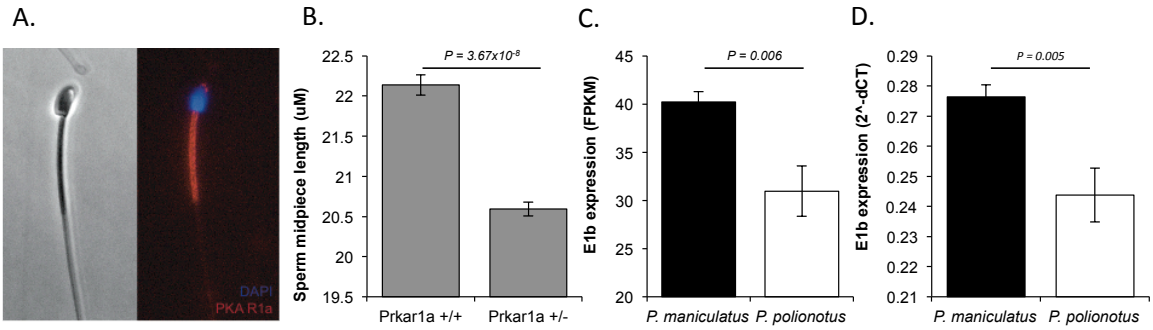

Figure 1.3. *Prkar1a* in sperm development

A. PKA R1α protein localization in cross-section of *P. maniculatus* testis (400X); immunofluorescence of anti-PKA R1α (green) and DAPI (blue). B. Mean±SE sperm midpiece length of *Mus musculus* wild type (n = 8) and *Prkar1a*$^{+/-}$ (n = 9) males. Note truncated y-axis. C. Mean ± SE expression of Prkar1a E1b transcript (RPKM) in *P. maniculatus* (black) and *P. polionotus* (white) by RNA-Seq. D. Mean ± SE expression of Prkar1a E1b transcript (*n* = 8) relative to a housekeeping gene, *beta actin*, in *P. maniculatus* (black) and *P. polionotus* (white) by qPCR. Note truncated y-axes.

We next examined how variation at the *Prkar1a* locus predicts sperm morphology, performance and male reproductive success in the F_2 hybrid population. Sperm midpiece of first generation hybrids (F_1 mean ± SE = 16.7 ± 0.06μm) are phenotypically indistinguishable from *P. maniculatus* (t-test: *P* = 0.97, *n* = 10 sperm/male,), suggesting the *P. maniculatus* allele segregates in a dominant fashion. Indeed, we found that F_2 males carrying at least one *P. maniculatus Prkar1a* allele (*AA* or *Aa*, as defined by the *Prkar1a* SNP (Supplementary Table S1.1) not only produce sperm with significantly longer midpiece (Supplementary Figure S1.4; t-test: $P = 4.44 \times 10^{-15}$), but their sperm swim with greater velocity than sperm from males homozygous for *P. polionotus Prkar1a* allele (*aa*; mean VSL ± SE: *AA* = 78.7 ± 1.9μm/s, *Aa* = 77.5 ± 1.1μm/s, *aa* = 73.1 ± 1.8μm/s, t-test: $P_{AA\text{-}aa} = 0.040$, $P_{Aa\text{-}aa} = 0.044$). These results show that variation at the *Prkar1a* locus, therefore, has a major effect on both sperm morphology and on speed.

The question remains, however: does the *Prkar1a* genotype predict reproductive

success? To test this we compared the genotype of F_2 males that did and did not sire offspring. We found that 45.2% of males homozygous for the *P. maniculatus* allele, but only 25.7% of those homozygous for the *P. polionotus* allele, sired pups ($\chi^2_{AA\text{-}Aa\text{-}aa} = 6.35$, $P = 0.042$). These analyses indicate that males carrying two copies of the *P. maniculatus Prkar1a* allele not only produce significantly faster sperm but also benefit from greater reproductive success, suggesting a direct link between fitness, phenotype and genetic variation at this locus.

Here we showed that *P. maniculatus* produce sperm with a longer midpiece than *P. polionotus*, which confers a reproductive advantage to males in sperm performance and male fertilization success. However, if this simple relationship between midpiece length and fitness exists, it is unclear why monogamous species would not share the same sperm morphology as promiscuous species. The functional relevance of the midpiece, in both evolutionary and human fertility studies, is controversial (Mukai & Okuno 2004; Piomboni *et al.* 2012), and many closely-related species vary extensively in this trait (Immler & Birkhead 2007; Tourmente *et al.* 2009, 2011). While drift and selection acting on pleiotropic traits could lead to shorter midpiece, sperm cells with more or larger mitochondria afforded by the larger midpiece may experience greater oxidative stress, which is known to increase mutagenesis in germ cells (Aitken & Baker 2004). When sperm competition is absent, such as in monogamous *P. polionotus*, the benefits conferred by producing faster sperm may not outweigh the associated costs. However, in the highly competitive environment that *P. maniculatus* sperm experience, even small increases in quality could differentiate those that reproduce and those that do not

(Birkhead *et al.* 2008). Thus, the balance between negative and positive effects of cellular respiration in sperm may determine the relative roles of natural and sexual selection as drivers of interspecific midpiece variation seen in *Peromyscus*, and across animals more generally.

The rapid evolution of reproductive protein-coding regions is a well-known response to post-copulatory sexual selection (Swanson & Vacquier 2002); we demonstrate here that changes to the reproductive-tissue-specific expression of an otherwise broadly-expressed gene is also a target of sexual selection. Over 50% of mammalian genes are expressed in the testis and most of these genes are also expressed in other tissues (Shima *et al.* 2004; Chalmel *et al.* 2007); therefore, changes to testis-specific expression are likely to be a common mechanism by which post-copulatory sexual selection in males can operate with swiftness and without deleterious effects in other tissues or in females. By continuing to elucidate both the phenotypic effects of sexual selection and their genetic basis, we can identify the ways in which evolution acts on variation in the genome to shape the extraordinary diversity of reproductive traits in nature.

CHAPTER 2: THE GENETIC BASIS OF ADAPTATION TO SPERM COMPETITION WITHIN AND BETWEEN SPECIES

Co-author: Hopi Hoekstra

ABSTRACT

Traits that vary both between and within closely related species present an opportunity to study the relationship between adaptive polymorphism and divergence, and more specifically, to determine whether the same genetic regions control similar phenotypes at inter- and intraspecific levels. Sexually selected traits are particularly useful in this pursuit because they evolve rapidly, generating significant variation on a time-scale similar to (or faster than) species formation. Here we use a quantitative trait locus (QTL) mapping approach to identify the genomic regions underlying sperm morphology of *Peromyscus* mice in two sets of genetic crosses: one between a monogamous and a promiscuous species, and a second between two subspecies of the latter. Although we identify a total of six QTL for sperm midpiece and tail length, we find no overlap in the loci underlying sperm morphology within and between species, despite the close relation of all three taxa. This surprising finding may suggest that evolution of variation within species contributes less to variation among species than we might expect, or that sexual selection, in particular, tends to employ different raw genetic material as it promotes evolution at intra- and interspecific levels.

INTRODUCTION

The genetic basis of phenotypic convergence in both closely and distantly-related taxa has received much recent attention in the field of evolutionary biology (Hoekstra & Price 2004; Manceau *et al.* 2010; Stern 2013). As a result of this focus, there are now many examples in which the same genes, and even the same nucleotide changes, are known to control convergent evolution towards similar phenotypes in highly diverged taxa (e.g. Mc1r in cryptic coloration of lizards, mice, and mammoths (Nachman *et al.* 2003; Hoekstra *et al.* 2006; Rosenblum *et al.* 2010; Workman *et al.* 2011). Likewise, genetic changes may occur independently or spread via introgression to produce comparable phenotypes in sister species (e.g. *Ectodysplasin* in adaptation of stickleback fish (*Gasterosteus*) to fresh water (Colosimo *et al.* 2005), *FRIGIDA* in adaptation of mousear cress (*Arabidopsis*) to climate (Johanson et al. 2000), and *Optix* in adaptation of butterflies (*Heliconius*) to mimic sympatric species (Heliconius Genome Consortium 2012)). However, the degree to which the same loci control natural variation at both inter- and intraspecific levels is less clear.

Are phenotypes similarly encoded between and within species? The answer to this question may yield important insights regarding the mechanistic nature of evolutionary change. Comparing the loci responsible for species- and subspecies-level variation in selected traits – adaptive polymorphism and divergence, respectively – can reveal whether (1) there are few or many genetic paths to similar phenotypes within a given genomic context, (2) selection is strong enough to repeatedly fix the same ancestral genetic variation, and (3) microevolution leads predictably or stochastically to

macroevolution. However, for only a handful of traits are both the inter- and intraspecific genetic bases known (see Wittkopp et al. 2009).

The evolution of sexually selected traits within and between species is particularly compelling because natural and sexual selection differ in a number of important ways. First, sexual selection may be stronger, on average, than viability selection in natural populations (Kingsolver *et al.* 2001), driving more rapid evolution of phenotypic traits (Lande 1981). Second, sexual selection may be a more constant force than natural selection (Hoekstra *et al.* 2001), due to fitness conflicts between the sexes that remain unresolved over long periods of time (Parker & Partridge 1998; Chapman *et al.* 2003). Finally, because sexual selection may be an important driver of speciation, at least in certain cases (Ritchie 2007), loci underlying sexually selected phenotypic targets may create barriers to gene flow as they evolve (e.g. Hawaiian cricket male calls and female acoustic preferences (Shaw & Lesnick 2009)) whereas naturally selected alleles may move more freely amongst populations (e.g. stickleback plate morphs, (Colosimo *et al.* 2005)). Therefore, we may have different expectations for the genetic basis of naturally versus sexually-selected traits evolving within and between species.

Sexual selection can occur both before and after mating. In any species in which females mate promiscuously, the potential exists for post-copulatory sexual selection (Birkhead & Pizzari 2002), in which the sperm of multiple males compete for ova (sperm competition; (Parker 1970)), and females may influence the outcome of this competition (cryptic female choice; Eberhard 1998). Although post-copulatory sexual selection is not readily visible, rapid evolution of male reproductive traits, such as sperm

count, sperm morphology, and seminal fluid characteristics suggest that this force is strong and widespread (Birkhead *et al.* 2008). Thus, adaptation of similar traits to post-copulatory sexual selection within and between closely-related taxa may be a common but underappreciated occurrence, and its genetic basis at the inter- and intraspecific levels may shed light on the process of evolution by sexual selection more broadly.

Here we investigate the evolution of traits subject to post-copulatory sexual selection within and between two species of wild-derived mice, *Peromyscus polionotus* and *P. maniculatus*. *P. polionotus*, the oldfield mouse, lives exclusively in the southeastern United States. Populations of this species in which mating system has been studied are socially monogamous (Dewsbury 1981), and single paternity of all offspring in a given litter has been demonstrated genetically (Foltz 1981). By contrast, its sister species, *P. maniculatus*, the deer mouse, is comprised of well over 50 described subspecies (Hall & Kelson 1959) distributed across North America. Data on mating system is available for only a few subspecies, though females of the subspecies *P. maniculatus bairdii* are known to be highly promiscuous, mating multiple times in a span of minutes (Dewsbury 1985). Thus, *P. polionotus* and *P. m. bairdii* experience differing sperm competition regimes; indeed, differences in male reproductive traits (specifically, male reproductive tract and sperm morphology) thought to be driven by post-copulatory sexual selection have been observed previously between these species (Linzey & Layne 1969; Linzey & Layne 1974; Chapter 1).

A second subspecies of *P. maniculatus*, the cloudland deer mouse (*P. maniculatus nubiterrae* (Rhoads)) inhabits forests of the Appalachian mountain range in

the eastern United States. Although genetic data on paternity is not available in this subspecies, paternal behavior (pup retrieval, nesting with pregnant females and females with newborn pups, and formation of longer associations with females (Wolff & Cicirello 1991) suggests that *P. m. nubiterrae* may be less promiscuous than *P. maniculatus bairdii*, or perhaps even monogamous. The examination of differences in male reproductive traits between *P. m. bairdii* and *P. m. nubiterrae,* as well as between *P. m. bairdii* and *P. p. subgriseus,* therefore present an opportunity to compare phenotypes that have evolved between and within species, likely in response to post-copulatory sexual selection.

To characterize the genetic architecture of these male reproductive differences at both inter- and intraspecific levels, we employ a QTL mapping approach. A cross previously conducted between *P. m. bairdii* and *P. p. subgriseus* allows us to determine the genetic basis of sperm morphology differences between sister species. Using similar methodology, we then cross *P. m. bairdii* with *P. m. nubiterrae* and examine the genetic basis of variation in the same sperm morphological characters. With these two crosses, we are thus able to compare the relationship of genetic regions underlying post-copulatory sexually-selected traits within species to those between species in wild-derived *Peromyscus* mice.

METHODS

Animal collection

We purchased wild-derived outbred stocks of *P. maniculatus bairdii* and *P. polionotus subgriseus* animals from the *Peromyscus* Genetic Stock Center (Columbia, South Carolina). Additionally, we collected 9 male and 9 female *P. maniculatus nubiterrae* from the Powdermill Nature Reserve in Westmoreland Co. Pennsylvania, USA in 2010. We identified these animals by morphological characters (Bruseo *et al.* 1999) and a mitochondrial marker (Avise *et al.* 1979), and imported them into an animal care facility at Harvard University (IACUC protocols 11-05 and 27-23).

Pure species phenotypes

We sacrificed second- and later-generation progeny of wild-caught *P. m. nubiterrae* parents and measured animal body mass. We next removed the entire male reproductive tract, placed it in phosphate buffered saline (PBS), and took images of the testes and seminal vesicles with a dissecting microscope (Discovery.V8, Zeiss, Jena, Germany). We used the curve spline tool in the AxioVision software package to determine the area of these organs, and took the mean of the two measurements for each male. Additionally, we collected sperm by dissecting out the cauda epididymis, bisecting it, and suspending the tissue in a solution of Biggers-Whitten-Whittingham (BWW) sperm media at 37 degrees Celsius. After approximately 15 minutes, we fixed sperm in 2% paraformaldehyde in PBS, and mounted 20 uL suspended cells in Fluoromount media (Southern Biotech). We took images of sperm at 400X magnification on an upright microscope (AxioImager.A1, Zeiss, Jena, Germany) and measured sperm midpiece and sperm tail (principal piece and endpiece) from 10 cells per male using the

curve spline tool in the AxioVision software package. We collected the same phenotypes from laboratory colonies of *P. maniculatus bairdii* and *P. polionotus subgriseus* (Chapter 1) with identical methodology. We performed all statistical tests for pure species trait values in R, determining significance by Wilcoxon rank-sum test and adjusting *p*-values to control family-wise error rate with the Holm-Bonferroni method (R Core Team 2014).

F2 intercrosses

At the interspecific level, we previously crossed *P. maniculatus bairdii* and *P. polionotus subgriseus* (Chapter 1). Briefly, we mated 2 *P. maniculatus bairdii* dams and 2 *P. polionotus subgriseus* sires to complete the cross in one direction only, because *P. polionotus subgriseus* dams mated to *P. maniculatus bairdii* sires produce very large pups (if any), due to aberrant imprinting effects (Vrana *et al.* 1998) and frequently experience dystocia (obstructed labor; Dawson 1965). We generated 38 first-generation (F1) offspring, which we mated with siblings to produce 300 F2 male offspring, 265 of which produced sperm.

At the intraspecific level, we crossed *P. maniculatus bairdii* and *P. m. nubiterrae.* We mated a single *P. m. nubiterrae* dam with single *P. m. bairdii* sire to generate 7 male and 7 female first-generation (F1) progeny, which were then mated with siblings to produce 211 second-generation (F2) progeny, 106 of which were male. Next, we mated a single *P. m. bairdii* dam with a single *P. m. nubiterrae* sire to again generate 7 male and 7 female F1s, and mated these animals with siblings to produce 303 F2 progeny, 162 of

which were male. A total of 239 F2 males produced sperm. We took sperm samples and measurements (as for pure species above) for 239 F2 males with sperm.

We measured F2 sperm in the interspecific cross using an AxioCam MRc camera and in the intraspecific cross using an AxioCam MRm camera on the same microscope (Zeiss, Jena, Germany). Because slight differences in the calibration of these two cameras caused small but noticeable differences in sperm morphology measurements, we measured *P. m. bairdii* and *P. p. subgriseus* sperm morphology with the AxioCam MRc camera alongside *P. m. bairdii* x *P. p. subgriseus* F1 and F2 hybrids, and then again with the AxioCam MRm camera alongside *P. m. nubiterrae* and *P. m. bairdii* x *P. m. nubiterrae* F1 and F2 hybrids, such that all comparisons between species, subspecies, and their hybrids could be performed using measurements taken with an identical setup. For this reason, sperm morphology means for *P. polionotus* and *P. maniculatus* are not always identical from figure to figure or panel to panel; however, they are always comparable within figure panels, and within paragraphs of text.

Genotyping and QTL mapping

We obtained the genotype of cross parents and all F2 intercross animals throughout the genome using ddRADseq technology (Peterson *et al.* 2012). We obtained linkage maps for both crosses using R/qtl software (Broman *et al.* 2003). The *P. maniculatus bairdii* x *P. polionotus subgriseus* cross map was 2309.7 cM in length, containing 482 markers on 23 linkage groups (Chapter 1). The *P. m. bairdii* x *P. m. nubiterrae* cross map was 1,826 cM in length, containing 2618 markers on 25 linkage

groups.

Using identical methodology in both the *P. maniculatus bairdii* x *P. polionotus subgriseus* and the *P. m. bairdii* x *P. m. nubiterrae* crosses, we mapped sperm midpiece and tail length using the EM algorithm of the scanone function in R/qtl (Broman *et al.* 2003). We determined genome-wide significance thresholds for each trait (alpha = 0.05) by permutation test (1000 permutations). To search for epistatic interactions between traits, we performed the scantwo function in R/qtl (Broman *et al.* 2003) using the recommended significance thresholds for a mouse intercross (Broman 2006). To identify genes within QTL peak 95% Bayes credible intervals that are expressed in *Peromyscus* testes, we performed RNA-Seq on the testis tissue of *P. m. bairdii* x *P. p. subgriseus* first generation hybrids at ten time-points throughout development (Chapter 3). We obtained the maximum expression (RPKM) of each locus between days 16 and 64, and determined a cutoff for biologically relevant expression (RPKM = 3.1) by plotting a histogram of log(maximum RPKM) values and identifying the upper bound of the lower expression peak.

RESULTS

Male reproductive traits in P. poliontous, P. maniculatus bairdii *and* P. m. nubiterrae

Male tract morphology varies at both inter- and intraspecific levels in *Peromyscus* mice. Specifically, both testis and seminal vesicle size is significantly greater in *P. m. bairdii* ($mean_{testis} \pm SE = 41.27 \pm 1.39$ mm^2; $mean_{seminal\ vesicle} \pm SE = 52.65 \pm 2.05$

mm^2; n=7) than in *P. p. subgriseus* ($mean_{testis}$ ± SE = 27.63 ± 2.05 mm^2; $mean_{seminal\ vesicle}$ ± SE = 27.10 ± 1.86 mm^2; n = 10; p_{testis} = 0.0003; $p_{seminal\ vesicle}$ = 0.0002; Figure 3.1C-D). Within *P. maniculatus, P. m. bairdii* testes and seminal vesicles are significantly larger than those of *P. m. nubiterrae* ($mean_{testis}$ ± SE = 35.60 ± 1.15 mm^2; $mean_{seminal\ vesicle}$ ± SE = 29.62 ± 2.31 mm^2; n = 14; p_{testis} = 0.004 and $p_{seminal\ vesicle}$ = 5.2E-05; Figure 3.1C-D).

Sperm morphological traits also differ between species (Chapter 1) and subspecies, though midpiece and tail length differences are not all consistent in direction. Both sperm midpiece and tail are longer in *P. m. bairdii* ($mean_{midpiece}$ ± SE = 15.87 ± 0.07µm; $mean_{tail}$ ± SE = 57.64 ± 0.20µm; n = 8) than in *P. p. subgriseus* ($mean_{midpiece}$ ± SE = 14.74 ± 0.17µm; $mean_{tail}$ ± SE = 54.34 ± 0.36µm; n = 8; $p_{midpiece}$ = 0.0005 and p_{tail} = 3.2E-05; Figure 3.1E-F)). At the intraspecific level, however, sperm midpiece are shorter in *P. m. bairdii* than in *P. m. nubiterrae* (mean ± SE = 16.28 ± 0.07µm; n = 8; p = 0.008; Figure 3.1E), but tails are longer in *P. m. bairdii* than in *P. m. nubiterrae* (mean ± SE = 57.32 ± 0.17µm; n = 8; p = 0.001; Figure 3.1F).

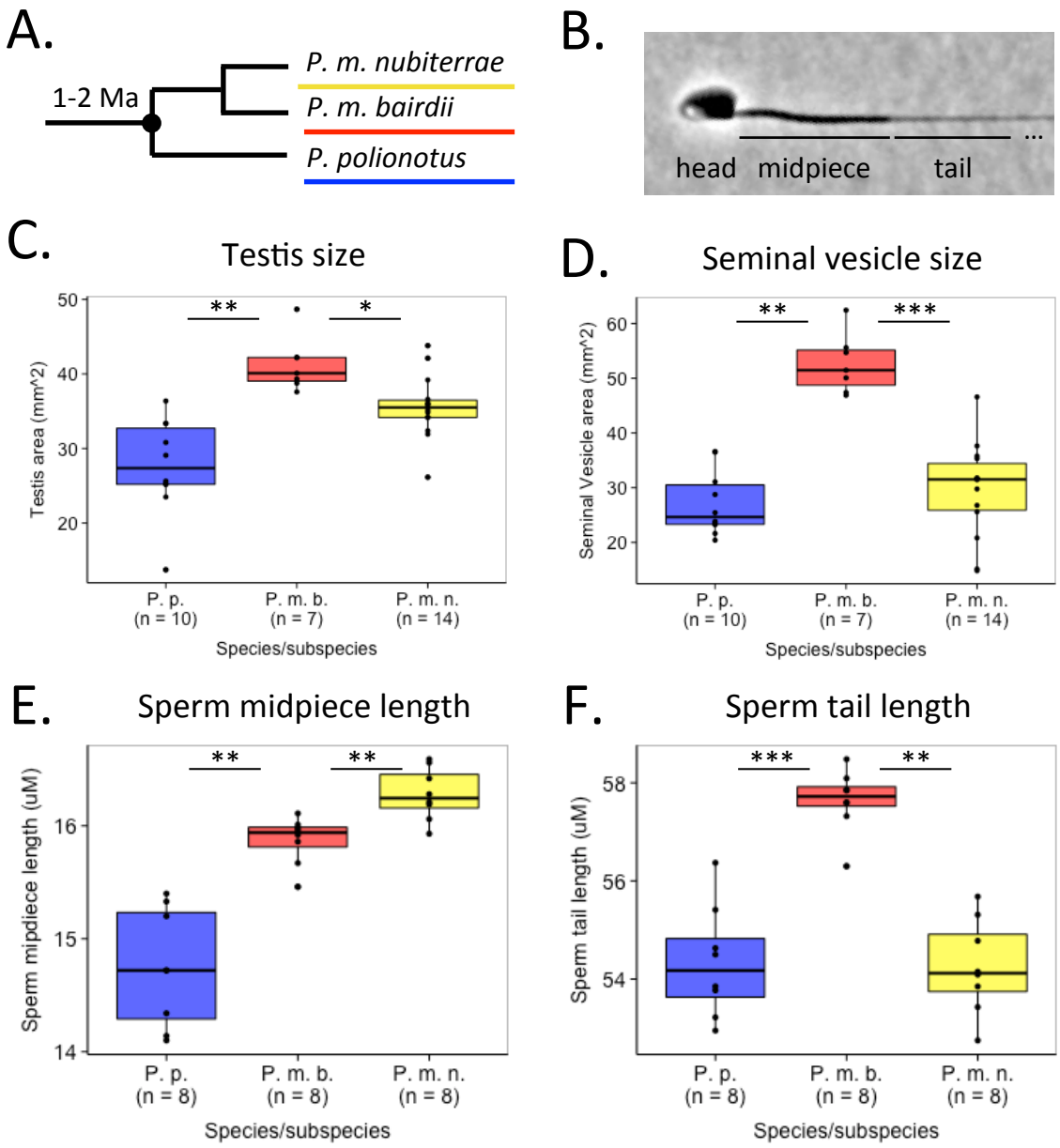

Figure 2.1. *P. polionotus, P. maniculatus bairdii* and *P. m. nubiterrae* male reproductive tract and sperm morphology

Blue elements denote *P. polionotus subgriseus* (P. p.), red elements denote *P. m. bairdii* (P. m. b.), and yellow elements denote *P. m. nubiterrae* (P. m. n.). A. Phylogenetic tree depicting the relationships between *P. m. nubiterrae* and *P. m. bairdii*, two subspecies of

the widespread and common species *P. maniculatus*; *P. polionotus* is the species sister to *P. maniculatus*. B. Brightfield images of *P. m. nubiterrae* x *P. m. bairdii* F1 sperm; sperm midpiece is the thickened portion of the sperm flagellum immediately adjacent to the head; sperm tail is the remaining portion of the flagellum distal to the midpiece. In box plots, box denotes median (horizontal line) and interquartile range, all points are shown. Significance was determined by Wilcoxon rank-sum test with *p*-values adjusted to control family-wise error rate (Holm-Bonferroni method); * = $p < 0.01$, ** = $p < 0.001$, *** = $p < 0.0001$. Note truncated axis in all plots. C. Testis size, and D. seminal vesicle size, reported as the average area (mm^2) covered by a male's left and right organs; sample sizes are given below species abbreviation. E. Sperm midpiece length, and F. sperm tail length, each reported as the average of 10 sperm per male; sample sizes given below species abbreviation.

Inheritance of sperm midpiece and tail length between and within species

The inheritance of sperm morphological components differs in the inter- and intraspecific crosses. As reported previously, *P. m. bairdii* x *P. p. subgriseus* F1 hybrid sperm midpiece (mean ± SE = 16.73 ± 0.06, n = 11) are statistically indistinguishable in length from *P. m. bairdii* midpiece (mean ± SE = 16.70 ± 0.04µm, n = 10; $p = 0.62$), but significantly longer than *P. polionotus* midpiece (mean ± SE = 15.43 ± 0.16µm, n = 10; $p = 1.7E\text{-}05$; note that *P. m. bairdii* and *P. p. subgriseus* sperm morphology was measured using two cameras that differed slightly in calibration (see methods) but that values for all species, subspecies, and hybrids are comparable within panels). Additionally, the

median F2 sperm midpiece length (16.37µM) more closely resembles *P. m. bairdii* than *P. p. subgriseus* parental sperm midpiece length. In contrast, *P. m. bairdii* x *P. p. subgriseus* F1 hybrid tail length (mean ± SE = 57.47 ± 0.15, n = 11) is intermediate to the two parental species (mean$_{P.\ maniculatus}$ ± SE = 59.02 ± 0.17µm, n = 10; mean$_{P.\ polionotus}$ ± SE = 55.36 ± 0.33µm, n = 10; Figure 2.2A-B) and significantly different from both ($p_{F1\ v.\ P.\ p.\ subgriseus}$ = 1.7E-05; $p_{F1\ v.\ P.\ m.\ bairdii}$ = 6.8E-05). Finally, the median F2 sperm tail length (57.69µM) is also intermediate between *P. m. bairdii* and *P. p. subgriseus.* In sum, sperm midpiece length is *P. m. bairdii* dominant, but sperm tail length is additively inherited between species.

In the intraspecific cross, sperm midpiece length in F1 animals (mean ± SE = 16.12 ± 0.06 µm, n = 8) is greater than in *P. m. bairdii* (mean ± SE = 15.87 ± 0.06µm, n = 8) but less than in *P. m. nubiterrae* (mean ± SE = 16.28 ± 0.07µm, n = 8; Figure 2.2C) though not significantly different from either ($p_{F1\ v.\ P.\ m.\ bairdii}$ = 0.13; $p_{F1\ v.\ P.\ m.\ nubiterrae}$ = 0.21), and the median F2 sperm midpiece length (16.16µm) is also intermediate. Sperm tail length in F1 individuals (mean ± SE = 57.32 ± 0.17 µm, n = 8) is similar to the *P. m. bairdii* parental subspecies (mean ± SE = 57.64 ± 0.20µm, n = 8; p = 0.19) but longer than *P. m. nubiterrae* (mean ± SE = 54.26 ± 0.31µm, n = 8; p = 0.0005; Figure 2.2D). Similarly, median sperm tail length of F2 animals in the intraspecific cross (56.70µm) resembles sperm tail length in *P. m. bairdii* more closely than those of *P. m. nubiterrae.* Thus, sperm midpiece is additively inherited within species, but sperm tail length is *P. m. bairdii* dominant, and the inheritance of these sperm morphological traits differs at the inter- and intraspecific levels.

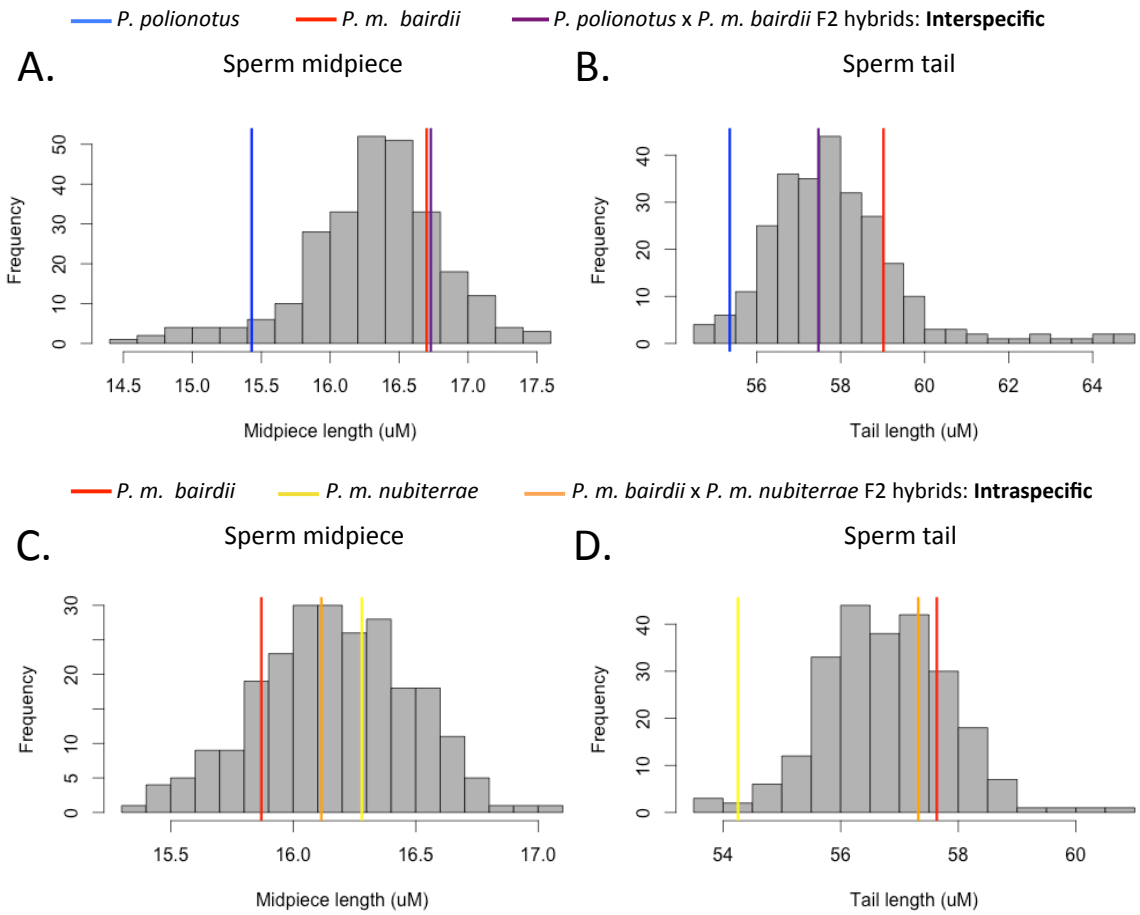

Figure 2.2. Sperm midpiece and tail length of intra- and interspecific F1 and F2 hybrids

Blue elements denote *P. polionotus,* red elements denote *P. m. bairdii*, yellow elements denote *P. m. nubiterrae,* purple elements denote *P. polionotus* x *P. m. bairdii* interspecific hybrids, and orange elements denote *P. m. bairdii* x. *P. m. nubiterrae* intraspecific hybrids. A. Histogram of *P. polionotus* x *P. m. bairdii* F2 sperm midpiece lengths and B. sperm tail lengths, each an average of 10 sperm per male, with parental species and F1 sperm midpiece length medians shown as vertical bars. C. Histogram of *P. m. bairdii* x. *P. m. nubiterrae* F2 sperm midpiece lengths and D. sperm tail lengths,

each an average of 10 sperm per male, with parental subspecies and F1 sperm midpiece length medians shown as vertical bars.

Correlation of sperm morphological traits between and within species

Sperm morphological traits also differ in their correlation structure within and between species. While in the interspecific cross, sperm midpiece and sperm tail length are significantly and negatively correlated ($R^2 = 0.17$, $m = -1.34$, $p < 0.001$; Figure 2.3A), these two traits show no correlation in the intraspecific cross (Figure 2.3D). Conversely, sperm midpiece length has no correlation with total flagellum length in the F2 offspring of *P. polionotus* and *P. m. bairdii* (Figure 2.3B), yet these traits are significantly and positively correlated in the F2 offspring of *P. m. bairdii* and *P. m. nubiterrae* ($R^2 = 0.12$, $m = 1.29$, $p < 0.001$; Figure 2.3E). Finally, sperm tail and total flagellum lengths are strongly and positively correlated in both crosses ($R^2_{interspecific} = 0.88$, $m_{interspecific} = 0.88$, $p_{interspecific} < 0.001$, Figure 2.3C; $R^2_{interspecific} = 1.02$, $m_{interspecific} = 0.93$, $p_{interspecific} < 0.001$, Figure 2.3F).

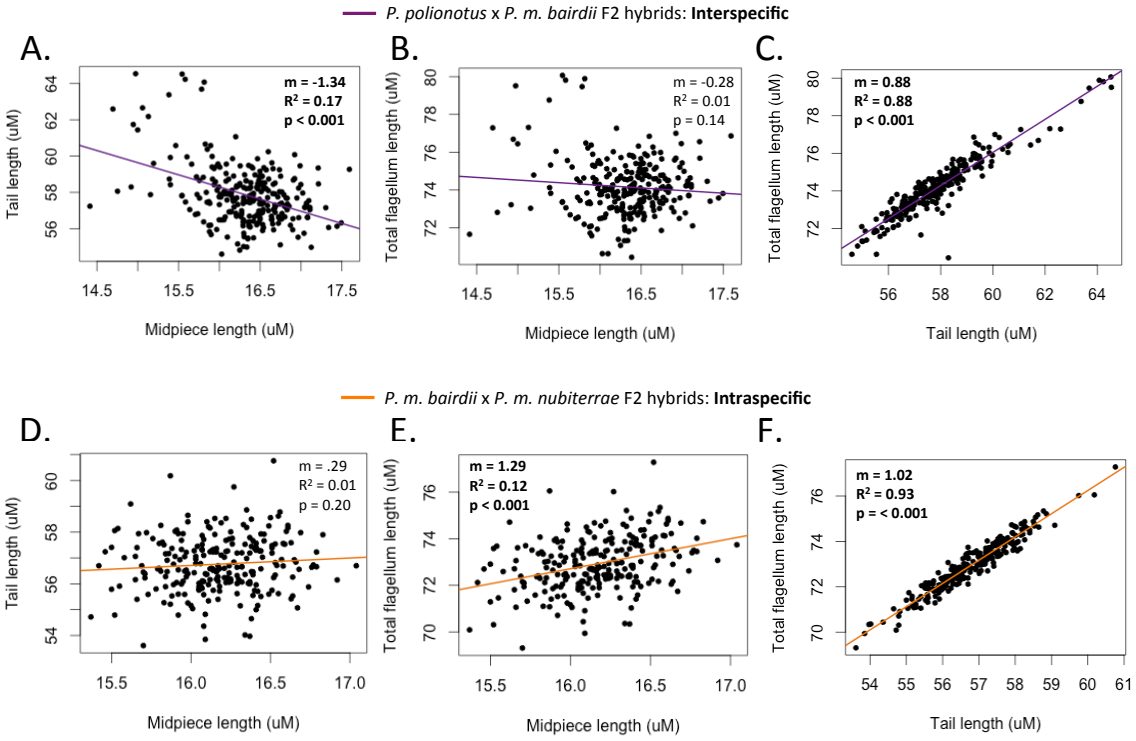

Figure 2.3. Sperm morphological correlations in intra- and interspecific F2 hybrids

Purple elements denote *P. polionotus* x *P. m. bairdii* interspecific hybrids and orange elements denote *P. m. bairdii* x. *P. m. nubiterrae* intraspecific hybrids. Least squares regression lines are given, with slope, R^2 value, and p-value reported in insets, in bold if significant. Correlations of A. sperm midpiece length (x) and tail length (y), B. sperm midpiece length (x) and sperm total flagellum length (y), and C. sperm tail length (x) and total flagellum length (y) are given for interspecific F2 hybrids of *P. polionotus* and *P. m. bairdii*. Correlations of D. sperm midpiece length (x) and tail length (y), E. sperm midpiece length (x) and sperm total flagellum length (y), and F. sperm tail length (x) and total flagellum length (y) are given for intraspecific F2 hybrids of *P. m. bairdii* and *P. m.*

nubiterrae.

Genetic architecture of sperm morphological traits between and within species

The genetic architecture and loci underlying sperm morphological traits are not similar between and within species. A QTL peak for sperm midpiece length on linkage group 4 explains 33% of the interspecific variance between *P. p. subgriseus* and *P. m. bairdii* (Figure 2.4A; Table 2.1; Chapter 1). Sperm tail length maps to a similar location (Figure 2.4B-C) that explains 13 % of the variance between parental species in this cross. The peaks for sperm midpiece and tail length overlap in their 95% Bayes credible intervals at one locus, *Prkar1a*, with synteny to *Mus musculus* chromosome 9 (Table 2.1).

In the subspecific cross, loci on linkage group 10 (which maps to *Mus musculus* chromosome 1) and on the X-chromosome explain 9.4% and 6.1% of the variance in intraspecific sperm midpiece length, respectively (Figure 2.4D; Table 2.1). These two QTL act in opposite directions (Supplementary Figure S2.1) and there is no evidence for epistasis between them. Loci on linkage groups 1, 4, and 16 (with synteny to segments of *Mus musculus* chromosomes 19, 4, and 17, respectively) explain between 7.7 and 8.5 percent of the within-species variance in sperm tail length (Figure 2.4E; Table 2.1). Although all three produce change in the same direction (Supplementary Figure S2.1), epistatic interactions are also not detectable between these regions. A subset of genes under each peak are expressed in the developing and adult testes of *Peromyscus* mice, and candidate loci are identifiable from these groups, based on known association with

sperm morphology in the literature (Table 2.1). Notably, there is no overlap between inter- and intraspecific crosses in the loci underlying sperm midpiece or tail length (note that linkage group 4 in the interspecific cross and linkage group 4 in the intraspecific cross do not have synteny to one another; Figure 2.4F; Table 2.1).

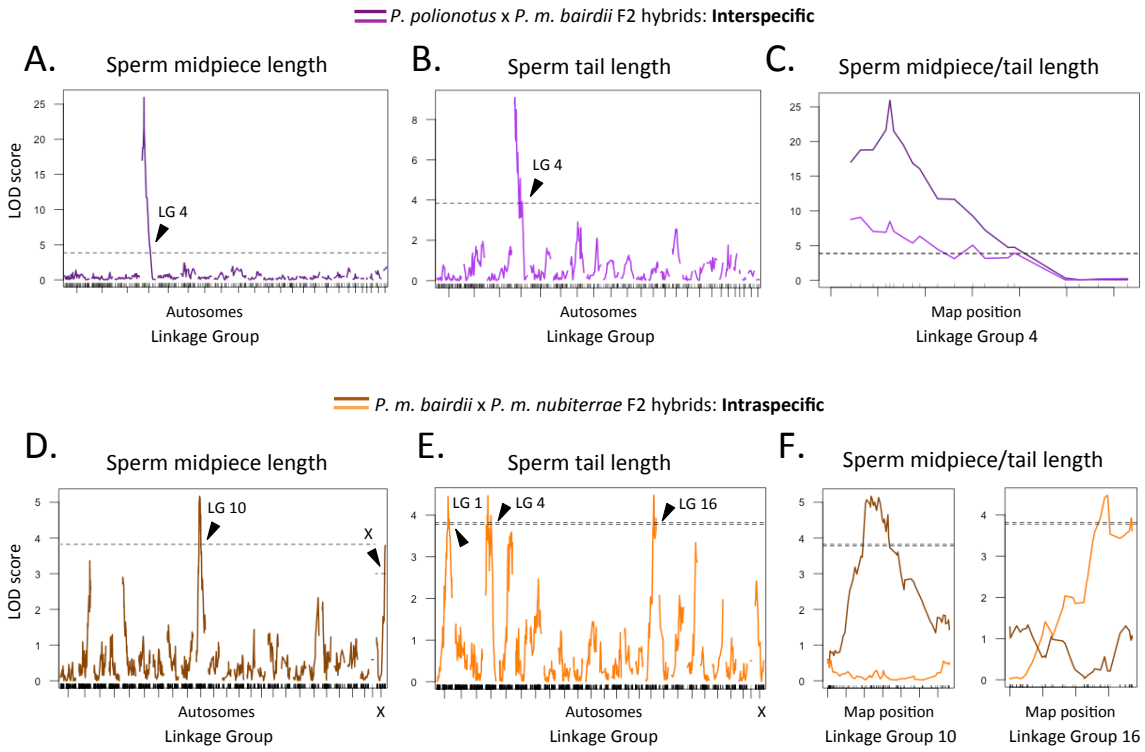

Figure 2.4. Intra- and interspecific genetic architecture of sperm morphology

Purple elements denote *P. polionotus* x *P. m. bairdii* interspecific hybrids and orange elements denote *P. m. bairdii* x. *P. m. nubiterrae* intraspecific hybrids. Genome-wide significance thresholds (α = 0.05) are indicated with dashed horizontal black lines. Position within the genome or linkage group is shown on the x-axis; Likelihood of Odds Density (LOD) score is given on the y-axis. Interspecific genome-wide scan for A. sperm

midpiece length and B. sperm tail length QTL, and C. close-up of overlapping QTL peaks for sperm midpiece length (dark purple) and sperm tail length (light purple) on linkage group 4. Intraspecific genome-wide scan for D. sperm midpiece length and E. sperm tail length QTL, and E. close-ups of non-overlapping QTL peaks for sperm midpiece length (dark orange) and sperm tail length (light orange) on linkage groups 10 and 16, respectively.

Table 2.1. Genetic regions and candidate loci underlying inter- and intraspecific QTL peaks for sperm morphological traits

Cross	Trait	LG	Chr.	Peak LOD	PVE	Genes in CI	Testis-expressed	Top candidates	References
Interspecific	Midpiece	4	9	25.97	33	1	1	*Prkar1a*	(Burton 2006)
Interspecific	Tail	4	9	9.09	13	NA	NA	*Prkar1a*	" "
Intraspecific	Midpiece	10	1	5.17	9.4	72	43	*Aspm, Kif14*	(Ponting 2006; Noguchi *et al.* 2011)
Intraspecific	Midpiece	X	X	3.79	6.1	92	49	*Rpgr, Cdk16, Elk1*	(Cesari *et al.* 2004; Brunner *et al.* 2008; Mikolcevic *et al.* 2012)
Intraspecific	Tail	1	19	4.22	7.7	402	280	*Tmem216, Map3k11, Spata6l*	(Jamsai *et al.* 2008; Reiter *et al.* 2012; Yuan *et al.* 2015)
Intraspecific	Tail	4	4	4.35	8.0	760	460	*Aqp7, wdr78, Fhl5*	(Kotaja 2004; Saito *et al.* 2004; Pazour *et al.* 2006)
Intraspecific	Tail	16	17	4.65	8.5	143	97	*Tcte3, Pacrg, Katna1*	(Dawe 2005; Rashid *et al.* 2010; O'Donnell *et al.* 2012)

Cross: Interspecific refers to the cross between *P. m. bairdii* and *P. polionotus*; intraspecific refers to the cross between *P. m. bairdii* and *P. m. nubiterrae.*

LG: linkage group (note that linkage group numbers differ for syntenic regions in the inter- and intraspecific crosses).

Chr.: *Mus musculus* chromsome with synteny to *Peromyscus* linkage group.

Peak LOD: Highest Logarithm of the Odds (LOD) score for each chromosome with a QTL peak that surpassed the genome-wide significance threshold ($\alpha = 0.05$).

PVE: Percent phenotypic variance explained by genotypes at the marker of highest association with phenotype for each chromosome with significant QTL.

Genes in CI: Number of genes with the Bayes 95% credible interval for each significant QTL peak.

Testis-expressed: Number of genes with the Bayes 95% credible interval for each significant QTL peak that also had testis expression in developing F1 hybrids of *P. m. bairdii* and *P. polionotus* that surpassed background noise levels (see methods).

Top candidates: Testis expressed genes chosen on the basis of sperm morphological phenotypes reported in the literature.

DISCUSSION

Male reproductive tract differences are known to be associated with mating system in rodents (Ramm *et al.* 2005), and *Peromyscus* in particular (Figure 2.1B-C; Chapter 1; (Linzey & Layne 1969)). Significantly smaller mean testis and seminal vesicle size in *P. m. nubiterrae* relative to *P. m. bairdii* (Figure 2.1B-C) is consistent with the hypothesis that females of forest-dwelling *P. m. nubiterrae* may be monogamous, or at least less promiscuous than female prairie-dwelling *P. m. bairdii* (Wolff & Cicirello 1991). More broadly, these observations suggest that sexual selection pressures may be of different magnitude and/or direction in subspecies of *P. maniculatus*.

In addition to male reproductive tract variation, significant differences in sperm morphology exist both between and within species (Figure 2.1E-F). The adaptive relevance of sperm midpiece and tail length, as well as their expected direction of change in response to sexual selection for sperm competitiveness, are hotly contested (Mukai & Okuno 2004; Immler & Birkhead 2007; Gomendio & Roldan 2008; Piomboni *et al.* 2012). Measurable divergence of these traits such closely related taxa (Figure 2.1A), however, suggests that sexual selection (or relaxation of selection) may play a role in determining sperm morphology within *P. maniculatus*. Regardless, the existence of variation both between and within species provides an opportunity to compare the genetic architecture of traits at inter- and intraspecific levels.

Patterns of inheritance can yield information about the genetic basis of phenotypic traits. The observation that sperm midpiece is inherited dominantly between but not within species, and that the reverse is true for sperm tail length (Figure 2.2A-D), suggests that the loci underlying sperm morphological variation at the species and subspecies levels may differ. Alternatively, however, the pattern of inheritance of similar loci may differ in the genetic context of the inter- and intraspecific crosses. Thus, patterns of inheritance alone cannot be used to distinguish whether a common or disparate genetic mechanism underlies sperm morphology between and within species.

Correlation among phenotypes in F2 individuals of a single cross, in whom regions of the genome from the parental taxa are recombined and inherited separately, indicate traits that may share a common (or linked) genetic basis. The negative correlation of sperm midpiece and tail length in the intercross between *P. polionotus*

and *P. m. bairdii* (Figure 2.3A) indicates that these two structures may be shaped by the same or neighboring loci, and that a tradeoff exists in their sizes. During spermatid development, the annulus, a small ring-like structure, travels down the sperm axoneme and stops at a location where the boundary ultimately appears between midpiece and tail (Toure *et al.* 2011). Differences in the rate or destination of annulus migration may thus influence differences in *P. m. bairdii* and *P. p. subgriseus* sperm morphology. In contrast, no correlation exists between sperm midpiece and tail in the intraspecific cross (Figure 2.3C), suggesting that a different developmental process may mediate the length of these structures. Indeed, within *P. maniculatus* F2 hybrids, midpiece length is positively correlated with total flagellum length (Figure 2.3E), indicating that factors affecting the entire axoneme may instead underlie variation in this trait between subspecies. The distinct correlation structure of sperm morphological traits in the inter- and intraspecific crosses therefore provides further tentative support for the control of similar traits by disparate genetic mechanisms within and between species.

QTL mapping results confirm that the genetic architecture of sperm midpiece and tail length differ at the inter- and intraspecific levels. Notably, variation in both morphological traits are controlled by the same single locus of large effect between species, and thus have a simpler genetic basis than within species, where sperm midpiece and tail are controlled by multiple loci of smaller effect (Figure 2.4). However, it is important to note that because we could not conduct the species-level cross in both directions, we are not able to detect any X-linked loci that might contribute to the genetic basis of sperm midpiece length between *P. m. bairdii* and *P. polionotus*. Under

QTL in the intraspecific cross are a series of candidate genes that merit further study. Examples include *Kif14*, which promotes crosslinking of microtubules in sperm and whose absence causes elongation defects (sperm midpiece length QTL, linkage group 10; Table 2.1 (Noguchi *et al.* 2011; Fabian & Brill 2012)) and Parkin co-regulated gene product (*Pacrg*), an axonemal component in whose absence flagella are structurally aberrant (sperm tail length QTL, linkage group 16; Table 2.1 (Dawe 2005)). Adding genetic markers and F2 individuals to this cross may narrow the QTL confidence intervals and help us to determine which gene(s) may underlie sperm morphology within species.

Completely non-overlapping sets of loci determine the length of sperm midpiece and tail within and between *Peromyscus* species. This is surprising given a) the close genetic relation of *P. polionotus*, *P. m. bairdii*, and *P. m. nubiterrae*, and b) the observation that the same genes are known to control similar phenotypes in vastly divergent organisms and in many groups of closely-related species (Hoekstra & Price 2004; Manceau *et al.* 2010; Stern 2013). However, a review of the few cases in which adaptive traits have been studied at both the inter- and intraspecific levels suggests that only about half of the reported QTL overlap between and within species ((Wittkopp *et al.* 2009; Chenoweth & McGuigan 2010), with the important caveat that overlapping QTL are not necessarily evidence of a shared genetic basis (Korstanje & Paigen 2002)). Previous studies in animals were conducted exclusively in insects, but our work indicates that mammalian systems may show a similar lack of concordance in the genes underlying natural variation within species and divergence between them (Table 2.2).

Table 2.2. Prior studies comparing intra- and interspecific QTL

Adapted and updated from Wittkopp et al. (2009).

Trait	**S/N**	**Intraspecific (species)**	**QTL_1**	**$Reference_1$**	**Interspecific (species)**	**Approx. div. time**	**QTL_2**	**Over-lap**	**$Reference_2$**
Sex comb tooth number	S	*Drosophila melanogaster*	2	(Nuzhdin & Reiwitch 2000)	*D. simulans* *D. mauritania*	0.8 Ma	≥5	1	(Coyne 1985)
Male courtship song	S	*Drosophila melanogaster*	3	(Gleason *et al.* 2002)	*D. simulans* *D. sechellia*	0.8 Ma	6	0	(Gleason & Ritchie 2004)
Abdominal pigmentation	S	*Drosophila melanogaster*	3	(Kopp *et al.* 2003)	*D. melanogaster* *D. willistoni*	32 Ma	N/A	1	(Williams *et al.* 2008)
Sex comb tooth number	S	*Drosophila simulans*	7	(Tatsuta & Takano-Shimizu 2006)	*D. simulans* *D. mauritania*	0.8 Ma	2	2	(True *et al.* 1997)
Abdominal pigmentation	S	*Drosophila americana* and *D. novamexicana*	≥2	(Wittkopp *et al.* 2009)	*D. americana* *D. novamexicana*	0.3 – 0.5 Ma	6	2	(Wittkopp *et al.* 2002)
Pheromone production	S	*Heliothis subflexa*	1	(Groot *et al.* 2013)	*H. subflexa* *H. virescens*	2 Ma	2	1	(Sheck *et al.* 2006)
Pupariation site preference	N	*Drosophila simulans*	≥3	(Erezyilmaz & Stern 2013)	*D. simulans* *D. sechellia*	0.8 Ma	2	2?	(Erezyilmaz & Stern 2013)
Male genital arch lobe	S	*Drosophila melanogaster*	≥3	(McNeil *et al.* 2011)	*D. simulans* *D. mauritania*	0.8 Ma	4	1?	(Masly *et al.* 2011)
Sperm midpiece length	S	*Peromyscus maniculatus*	2	This work	*P. maniculatus* *P. polionotus*	1-2 Ma	1	0	Chapter 1; this work
Sperm tail length	S	*Peromyscus maniculatus*	3	This work	*P. maniculatus* *P. polionotus*	1-2 Ma	1	0	Chapter 1; this work

Approximate dates for *Drosophila* spp. divergence were obtained from Obbard et al. (2012) and Wittkopp et al. (2009). Traits in bold were added to the original table.

S/N: Indication of whether natural (N) or sexual (S) selection is most likely the primary force acting on the trait.

Intraspecific (species): The single species in which variation in a trait was mapped (between populations, strains, or subspecies).

QTL_1: Number of intraspecific QTL mapped.

$Reference_1$: Reference in which intraspecific QTL was reported.

Interspecific (species): The two species between which variation in a trait was mapped.

Approx. div. time: Approximate time, in millions of years before present, of species divergence.

QTL_2: Number of interspecific QTL mapped.

Overlap: Number of QTL mapped at both the intra- and interspecific levels. "?" indicates particularly broad QTL, for which there was little evidence that similar genes were involved.

$Reference_2$: Reference in which interspecific QTL was reported.

However, a bias exists in the subset of traits examined thus far in intra- versus interspecific (and higher) taxonomic comparisons. Studies of the genetic basis of adaptive phenotypes within species have focused predominantly on sexually selected traits (e.g. sex comb tooth number in *Drosophila* (Nuzhdin & Reiwitch 2000; Tatsuta & Takano-Shimizu 2006) and pheromone blend in *Heliothis* (Groot *et al.* 2013)). In contrast, the traits best known for convergence between species are primarily naturally selected (Manceau *et al.* 2010; Stern 2013). It is possible that the strong (Kingsolver *et al.* 2001) and constant (Hoekstra *et al.* 2001) nature of sexual selection may cause rapid fixation of all available genetic variation, such that ancestral polymorphism for sexually

selected traits is rare. This could produce a pattern like the one we observe here, in which differences in sexually selected traits within and between species are not determined by the same loci.

Future work to determine the genetic underpinnings of convergent sexually-selected traits at the inter- and intraspecific levels in a wider taxonomic sampling of organisms is clearly necessary. Additionally, the genetic basis of naturally selected traits must be examined within as well as between species to fill substantial gaps in our knowledge of the transition from polymorphism to divergence. These studies will help to clarify whether disparate intra- versus interspecific genetic control is a common feature of adaptive traits, or whether sexual selection in particular often employs different raw genetic material within and between species.

CHAPTER 3: *CIS*-REGULATORY EVOLUTION MODIFIES THE TIMING OF SEXUAL MATURITY IN *PEROMYSCUS* MICE

Co-authors: Carlo Artieri, Hunter Fraser, and Hopi Hoekstra.

ABSTRACT

When life is short and females mate multiply, a race for the fertilization of their eggs ensues. This competition among males, and among their sperm, may drive more precocious reproductive investment in males from promiscuous compared to monogamous taxa. Here we compare the timing of sexual maturity in males from two interfertile sister species of *Peromyscus* mice that differ in mating system, and we characterize *cis*-regulatory evolution underlying differences in male reproductive development. We first demonstrate that the onset of spermatogenesis occurs earlier in the promiscuous deer mouse (*P. maniculatus*) than the monogamous oldfield mouse (*P. polionotus*), leading to earlier sperm production and fertility. Next, we examine allele-specific expression in hybrid testes at ten points across post-natal development. We find that expression levels of the *P. maniculatus* and *P. polionotus* parental alleles are at least two-fold different at hundreds of loci throughout the genome. Thus, many *cis*-acting regulatory changes have occurred in the testis over the short evolutionary time period since these two species diverged. Additionally, clusters of genes show disparate levels of allele-specific expression across spermatogenesis. Our results thus implicate a role for *cis*-regulatory mutations in the evolution of

reproductive development, and showcase the context-specificity of such *cis*-regulatory changes, which alter expression during particular time periods and in distinct cell-types.

INTRODUCTION

Mating systems, and in particular, female mating habits, determine the strength of post-copulatory sexual selection within species. Multiple mating by females within a single reproductive cycle (i.e. reproductive promiscuity) results in direct competition among the gametes of different males; no such sperm competition exists when females mate monogamously (Parker 1970). Much attention has been given to the evolution of sexually-selected adult male traits that improve sperm competitive ability. For example, testis size and sperm count show strong correlations with mating system in diverse vertebrate taxa such as fish (Stockley *et al.* 1997; Stoltz & Neff 2006), birds (Moller 1988), and mammals (Moller 1989), including rodents (Ramm, Parker, and Stockley 2005; Montoto et al. 2011). Additionally, recent work has begun to uncover the genetic bases of these traits (Chapters 1 and 2).

By comparison, the timing of male sexual maturation in relation to female promiscuity has received far less attention, despite the potential for large effects on fitness. Evidence exists suggesting that reproductive development is accelerated in promiscuous relative to monogamous species (Kleiman 1977), and that the relative lengths of pre-reproductive and reproductive stages may be subject to particularly

strong selection in organisms with brief adult lifespans (Harvey & Zammuto 1985). Although the growth and developmental processes leading to sexual maturation are well-studied in mammalian model systems – from physiological (e.g. Bronson 1979), hormonal (e.g. Nef and Parada 2000), and neurological (e.g. Clarkson and Herbison 2006) perspectives – we know relatively little about how changes in reproductive timing may evolve at the molecular level.

Here we study two sister species of deer mice (genus *Peromyscus*) with divergent mating systems and short adult lives in the wild (Blair 1948; Howard 1949; Sadleir 1965; Dapson 1972; Smith *et al.* 1972; Rave & Holler 1992). *Peromyscus maniculatus* females are highly promiscuous, sometimes mating multiple times only minutes apart (Dewsbury 1985), while *P. polionotus* are strictly monogamous, both socially and genetically (Dewsbury 1981; Foltz 1981). Consistent with their differing reproductive strategies, these two species have differences in adult male reproductive morphology (i.e. testes and seminal vesicles are larger in *P. maniculatus* than *P. polionotus*; (Linzey & Layne 1969)) and in sperm morphology (i.e. sperm are longer in *P. maniculatus*; (Linzey & Layne 1974)). In other species of mammals, and rodents specifically, males of promiscuous species also tend to reach sexual maturity earlier than those of monogamous species (e.g. Rood 1972; Montoto et al. 2012)). Here we quantify differences in the timing of male reproductive maturity in *P. maniculatus* and *P. polionotus,* which diverged recently over the short evolutionary time-scale of approximately 1-2 million years (Avise *et al.* 1983; Van Zant & Wooten 2007).

Comparison of these *Peromyscus* sister species provides a unique opportunity to

study the evolution of sexual maturation. Although geographically separated in the wild, in the lab they can be crossed to produce viable and fertile hybrids, providing a window into the genetic changes underlying differences in reproductive development. To pinpoint the regulatory mechanisms responsible for this divergence, we perform transcriptomic analyses of the developing testes of *P. maniculatus* x *P. polionotus* hybrid offspring. We compare the allele-specific expression (ASE) levels of transcripts at ten developmental time-points, beginning in early puberty, when spermatogonia divide mitotically to form spermatocytes, through meiosis and the differentiation of spermatids, to adulthood, when mature sperm are produced and released by the testis. Together with our characterization of reproductive development, these genetic data allow us to investigate divergence in regulatory networks driving rapid evolution in the timing of sexual maturation.

METHODS

Animals

We obtained wild-derived *P. maniculatus* and *P. polionotus* from the Peromyscus Genetic Stock Center at the University of South Carolina, which were housed in Harvard University's Biological Research Infrastructure and maintained as outbred lines. To raise animals of a known age, we checked breeding pairs daily for new litters. Pups remained with their parents until day 23, after which we weaned and housed them with same-sex litter-mates or individuals of the same species and similar age. We produced F1 hybrids

by mating *P. maniculatus* females with *P. polionotus* males (because imprinting effects preclude the production of F1 hybrids with *P. polionotus subgriseus* dams and *P. maniculatus bairdii* sires (Dawson 1965; Vrana *et al.* 1998). We performed all procedures involving *Peromyscus* mice according to IACUC protocol number 27-23 at Harvard University.

Age to sexual maturity

To first determine age at sexual maturity, we sacrificed males every four days late in development, ranging from day 40, at which time no male of either species ever bred successfully or produced mature sperm, to day 90, at which time both species' males breed and produce sperm at levels similar to older adults from the same colonies (post-natal day: 40, 44, 48, 52, 56, 60, 64, 68, 72, 76, 80, 90, and adult). Exactly seven days before sacrifice, we paired males with a female of the same species (sufficiently longer than the five-day estrus cycle to ensure that females were fertile at least once during the assay). We checked paired females 21-28 days later for a resulting litter, noting the presence of pups to confirm male fertility. Upon sacrifice of the males, we took testis and body weight, and also removed the left cauda epididymis and bisected it in 1.5mL of Biggers-Whitten-Whittingham (BWW) sperm media at 37 degrees Celsius. After approximately 15 minutes, we fixed 500uL sperm in 400uL 4% paraformaldehyde (PFA) in phosphate buffered saline (PBS), for a final concentration of 2% PFA in PBS. To determine sperm count, we diluted fixed sperm 1:1 in Trypan Blue (Life Technologies) and counted sperm cells on a Countess automated cell counter (Life Technologies) using

the following settings: sensitivity = 5, minimum size = 2µM, maximum size = 16µM, circularity = 45%.

Developmental testis mass and body mass

To determine the trajectory of somatic and testis development, we sampled along a second time series. At each point (post-natal day: 16, 20, 24, 28, 32, 36, 40, 44, 50, 64, and adult >90), we sacrificed males by CO2 overdose, took the animal's weight, and dissected out the reproductive tract. We immediately took left testis weight with a fine-scale balance, fixed the right testis in Bouin's solution overnight, and then transferred this fixed testis to 70% ethanol for storage.

Histology

To determine the precise timing of the initial round of spermatogenesis in juvenile mice of *P. polionotus*, *P. maniculatus*, and their F1 hybrids, we examined testis histology at the 10 early time-points between day 16 and 64 mentioned above. We first embedded one Bouin's-fixed testis per male in paraffin and sectioned the tissue at 6uM onto glass microscope slides (Harvard Medical School Rodent Histopathology Core). We then cleared the slides, hydrated the testis sections, and stained with Periodic Acid (VWR), Schiff's Reagent (VWR), and Mayer's hematoxylin (VWR). Next, we took bright-field images of each testis at 100X magnification using an upright microscope (AxioImager.A1, Zeiss, Jena, Germany). Finally, we determined which of 6 broad cell types (spermatogonia, early [leptotene/zygotene/diplotene] spermatocyte, pachytene

spermatocyte, round spermatid, elongating spermatid, and elongated spermatid) was the most abundant mature cell type present in each tubule of a single testis section.

RNA-Seq

To measure differences in transcript abundance across post-natal development in *P. maniculatus* and *P. polionotus,* we sacrificed two F1 male offspring from each of the ten early time-points, spanning days 16 to 64 (see above). We removed a single testis, deposited it immediately into liquid nitrogen, and stored the tissue at -80 degrees Celsius. We used the animal tissues protocol of the RNeasy RNA extraction kit (Qiagen) to extract RNA and stored it at -80 degrees Celsius. We then purified the RNA using the Ribo-Zero Gold Kit (epicenter), created stranded libraries with a PrepX kit on the Apollo 324 NGS Library Prep System (Wafergen Biosystems), and sequenced paired-end 125 base pair reads on an Illumina HiSeq in the Harvard Bauer Core Facility.

***P. maniculatus* x *P. polionotus* variant calling**

To identify fixed single nucleotide polymorphisms (SNPs) between *P. maniculatus* and *P. polionotus*, we combined RNA-seq data derived from each of the parental strains as well as interspecific F1 hybrids (see Supplementary Table S3.1). We removed adapters and overlapping segments between mate-pairs using SeqPrep (https://github.com/jstjohn/SeqPrep) and mapped reads to the *P. maniculatus bairdii* genome assembly Pman_1.0 (NCBI genome assembly accession GCF_000500345.1) using Tophat 2 version 2.0.9 (Kim *et al.* 2013) in very-sensitive mode and trimming the

first 6 nucleotides off of the 5' ends of reads. We removed duplicate reads using the PICARD tools (http://broadinstitute.github.io/picard), then pooled all mapped reads into three groups based upon their origin – *P. maniculatus* parental, *P. polionotus* parental or F1 hybrid. We first realigned INDELs within each pool using the Genome Analysis Toolkit version 3.3 (McKenna *et al.* 2010), and then called variants relative to the reference sequence via the unified genotyper with the following arguments: -nt 12 -ploidy 2 -glm BOTH -stand_call_conf 30 -stand_emit_conf 10.

After removing all low confidence SNP calls, we excluded all SNPs that were within 125 bp (the read length) of an insertion/deletion (INDEL) as improper alignment of INDELs can lead to reference allelic bias. We retained remaining SNPs for ASE calling if neither parent showed evidence of polymorphism at the SNP site and parental base calls at a site supported the alleles observed in the hybrids. In cases where *P. polionotus* parental coverage was insufficient to confirm a SNP detected in the hybrids, we retained heterozygous sites in the hybrid that contained the *P. maniculatus* reference allele and one other.

Calling ASE in F1 hybrids

We generated a reference *P. maniculatus* genome with all potential SNPs, including those of low confidence, masked by 'N'. We mapped reads from each replicate to this reference using STAR version 2.4.0i (Dobin *et al.* 2013), with the following options: --outFilterMultimapNmax 1 --outSAMtype BAM SortedByCoordinate --outSAMattributes MD --clip3pNbases 6. We removed duplicates from the resulting

mapped files using the PICARD tools, and calculated allelic counts for each individual SNP using custom PERL and Python scripts. Each read and its paired-end mate contributed a count only to a single SNP, and in cases where a read/mate overlapped multiple SNPs, we randomly assigned its allelic count to a single SNP. We then further excluded any SNPs that (1) lacked any counts in all hybrid samples, (2) lacked counts in either of the two parental alleles in all hybrid samples, or (3) had ≥90% of counts summed across all replicates and time points favoring one parental allele. Our final SNP set comprised 138,889 SNPs, allowing estimation of ASE in 16,842 of genes in the annotation (65%).

We then computed gene-level counts by summing across individual SNPs within the longest isoform. In cases where SNPs overlapped multiple annotated features, they were not included in allele counts. As the data were generated using a stranded library preparation method, we calculated ASE counts only from reads mapping to the appropriate strand. Variance in $\log_2$(*P. maniculatus*/*P. polionotus*) allelic counts is negatively correlated with the total number of allele-specific counts at any gene. Therefore, we performed variance stabilizing normalization as implemented in the DESeq R package (Anders & Huber 2010) in pooled mode, which uses the inter-replicate variance to parameterize scaling.

Finally, to identify set of genes for which our power to detect ASE is high, we selected all loci with detectable expression during all 10 time points and with an average raw SNP count of at least 100 per species per time-point. We plotted the allelic expression levels of these genes by determining the proportion of the total number of

allele-specific counts from *P. maniculatus* and from *P. polionotus* in the two replicates per time point, and multiplying these two proportions by the average RPKM value for that gene, i.e. *P. maniculatus* allelic expression gene A, replicate 1, day 16 = ([*P. maniculatus* allele-specific counts gene A, replicate 1, day 16] / [*P. maniculatus* + *P. polionotus* allele-specific counts gene A, replicate 1, day 16])*(Average RPKM gene A, day 16).

Soft-clustering and gene ontology analysis

To explore how patterns of ASE varied over the developmental time-course, we applied fuzzy c-means soft-clustering as implemented in the 'Mfuzz' package (Futschik 2014) in R (R Core Team 2014) with a set of genes for which our power to detect ASE is high (described above). Mfuzz is an unsupervised machine learning method designed to find hidden structure in time series gene expression data by allowing each gene's expression pattern to exhibit partial membership in a number of naively-determined dominant cluster patterns. We performed clustering over a range of values of the 'm' parameter (the 'fuzzifier,' which determines the degree to which genes cluster together despite differences in expression pattern) in increments of 0.1 between 1.29 and 1.35. For each value of m, we used the highest number of clusters possible, in which no cluster contained zero genes with maximum membership in that cluster. We then examined the clusters produced (between 4 and 30), and found that four distinct cluster shapes (each of which had many genes with strong membership ≥0.75) exist for all values of m except the highest (m=1.29-1.34; c = 8-30).

We then further inspected representative genes with membership ≥0.5 in these four robust cluster shapes in c = 10 (m = 1.33). To determine the enrichment of genes underlying particular cellular processes, functions, and components with these patterns of ASE, we performed gene ontology (GO) term analysis using the online Gene Ontology enRIchment anaLysis and visuaLizAtion tool (GOrilla) (Eden *et al.* 2007, 2009). We compared two unranked lists of genes for each cluster (those with membership ≥0.5 in a cluster, and those in the entire set of genes subjected to soft-clustering analysis) using the *Mus musculus* organism setting, and searched for all ontologies available.

RESULTS

Age to sexual maturity, testis mass, and body mass

P. maniculatus and *P. polionotus* males differ dramatically in their age to sexual maturity. *P. maniculatus* begin to produce sperm as early as day 40 (consistent with previous observations; Clark 1938), and achieve a sperm count statistically indistinguishable from adults by day 60 (sperm count, day 60 = 1.2E07 cells/mL; mean sperm count, adult ± SE = 1.3E07 ± 3.68E05 cells/mL; 1 sample t-test, p = 0.06; Figure 3.1A). In contrast, *P. polionotus* males do not begin to produce sperm until day 56 and show greater variation in count over the course of development (Figure 3.1A). In accordance with sperm count, *P. maniculatus* males begin to impregnate females in days 41-48, but the first *P. polionotus* males to impregnate a female in this study did so not until days 73- 80 (Figure 3.1A). However, no age group of *P. polionotus* routinely

reproduced, consistent with this species' overall lower rate of reproduction in the lab (in five adult pairings of each species used to quantify adult sperm count (Figure 3.1A), 2 pairs of *P. polionotus* reproduced, whereas all 5 pairs of *P. maniculatus* produced offspring; these results are typical of our colonies).

Given these substantial differences in the timing of sexual maturity, we next measured testis mass across development. *P. maniculatus* males' testes increase in mass steadily between days 16 and 64, reaching 50% of adult mass by day 36, whereas *P. polionotus* median testis mass increases only slowly until day 36, varies widely between individuals thereafter in development, and reaches 50% of adult mass only on day 50 (Figure 3.1B). To determine whether earlier attainment of sexual maturity and more rapid testis development in *P. maniculatus* might simply be due to greater overall precociality, rather than mating system *per se*, we also measured body mass of the two species over time. *P. maniculatus* and *P. polionotus* male pups increase in body mass similarly over the course of development relative to adults of the same species (Figure 3.1C).

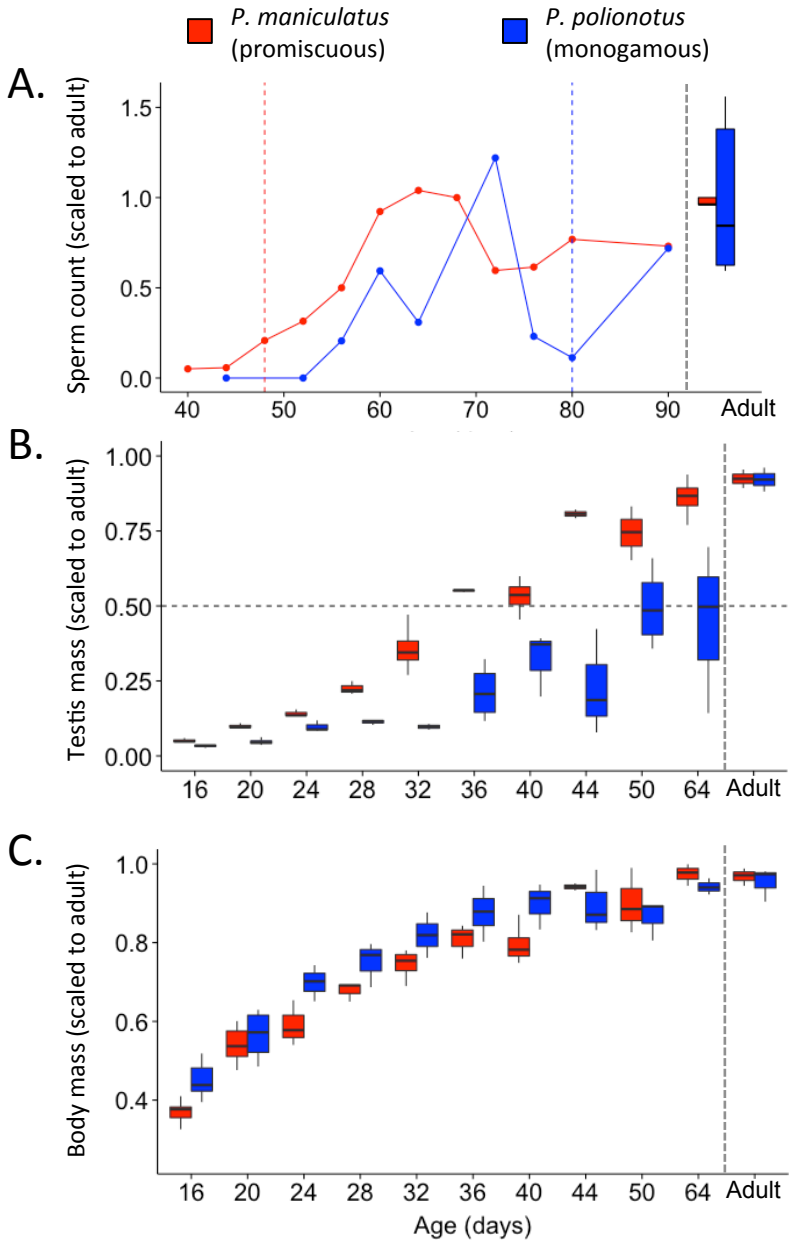

Figure 3.1. Age to sexual maturity, testis mass, and body mass in *P. maniculatus* and *P. polionotus*

Age in days (postnatal) is given on the x-axis. Red elements denote *P. maniculatus*; blue elements denote *P. polionotus*. For all plots, vertical grey dashed line separates developing from adult samples. For all box plots, sample median is the horizontal line

within the box, box outer bounds denote the two inner quartiles; whiskers give the last datum within 1.5 times the interquartile range. A. Sperm count in developing animals (points, n = 1-2) and adults (boxes, n = 5) scaled to adult means; vertical dashed lines denote age at which a male first impregnated a female in the week prior to count measurement. B. Testis mass in developing animals (n = 2-3) scaled to mean testis mass of adults (n = 5); horizontal dashed line denotes 50% of adult testis mass.
C. Body mass in developing animals (n = 3-5) scaled to mean body mass of adults (n = 5).

Testis histology

To determine the cellular basis for differences in age to sexual maturity, we examined histology of *P. maniculatus* and *P. polionotus* testes across development (Figure 3.2A-B). At day 16, nearly half (44%) of the tubules in *P. maniculatus* testes contain spermatocytes (Figure 3.2A), in contrast to a very small fraction (4%) of *P. polionotus* cells (Figure 3.2B). Similarly, by day 24, approximately one-third (28%) of the cells in *P. maniculatus* testes have undergone meiosis I and II to produce round spermatids, the first of which are seen in a small fraction (7%) of *P. polionotus* tubules only on day 32. The final cell type, elongated spermatid, appears in a substantial fraction (>5%) of *P. polionotus* tubules (21% on day 50), ten days later than *P. maniculatus* (12% on day 40). Finally, *P. polionotus* testis tubules tend to occupy a greater variety of stages in spermatogenesis at a single time-point, especially in the middle of this first round of spermatogenesis (such as days 32 and 40; Figure 3.2B).

To determine the inheritance of differences in timing of spermatogenesis, we

examined the histology of testes from *P. polionotus* x *P. maniculatus* F1 hybrids across development (Figure 3.2C). During the first two time-points in spermatogenesis, F1 testes have a greater proportion of tubules containing spermatocytes (35% and 78% on days 16 and 20, respectively) than *P. polionotus* (4% and 18%), but a smaller proportion than *P. maniculatus* (44% and 98%). In later time-points, after the first post-meiotic cells appear in F1 testes (days 28-64), the proportion of tubules of each cell type more closely resembles *P. maniculatus* than *P. polionotus* (Figure 3.2A-C). Finally, F1 testis tubules typically occupy only two to three stages at any one time-point; hybrids therefore also resemble *P. maniculatus* in that they have lower variation in the timing of spermatogenesis than *P. polionotus* (Figure 3.2A-C).

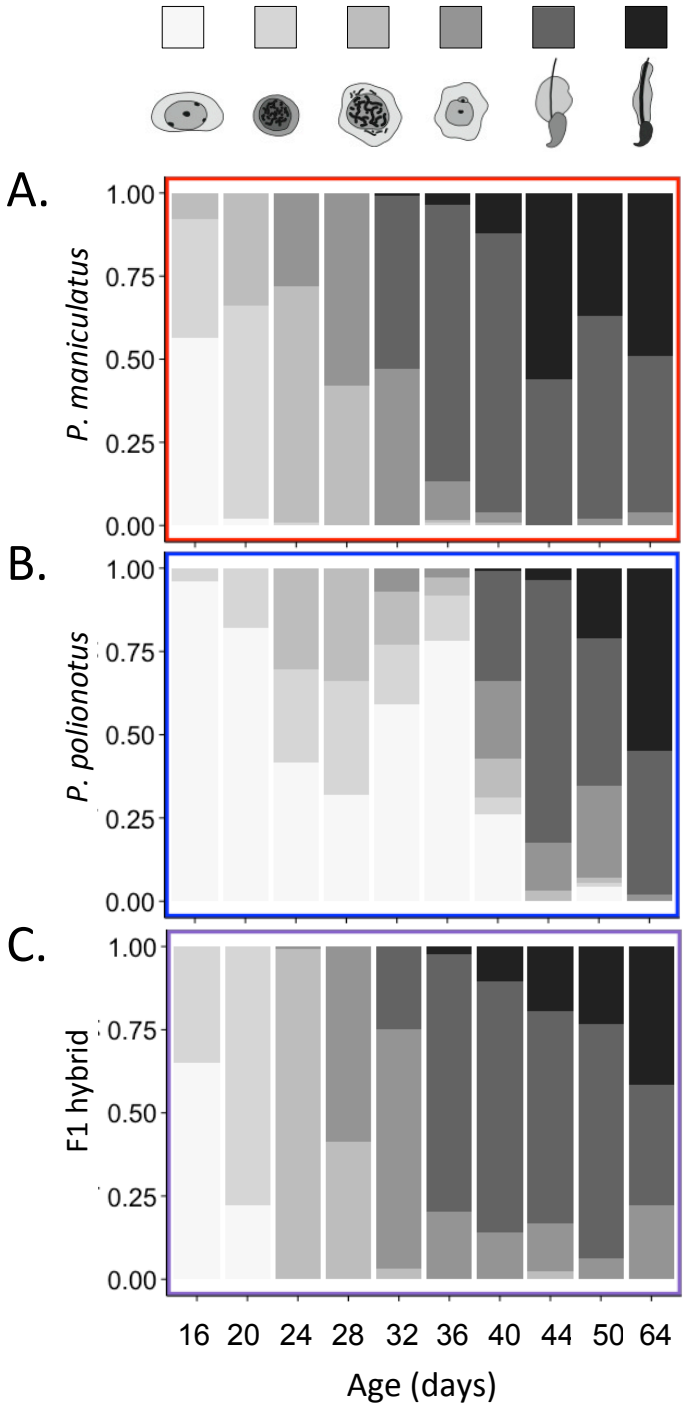

Figure 3.2. Histology of developing testes in *P. maniculatus*, *P. polionotus*, and their F1 hybrids

Age in days (postnatal) is given on the x-axis (note non-linear scale in last two time-

points). For each time-point, the proportion of testis tubules with mature cells falling into one of six types (spermatogonia, early spermatocyte, pachytene spermatocyte, round spermatid, elongating spermatid, and elongated spermatid; respective cartoons across top of figure) are denoted with vertical bars of various shades (light = early cell types, dark = late cell types; see legend at top). A. *P. maniculatus* (n = 2-3 animals per time-point), B. *P. polionotus* (n = 2-3 animals per time-point), and C. *P. maniculatus* x *P. polionotus* F1 hybrids (n = 1 animal per time-point).

Gene expression and allele-specific expression

To investigate the possibility that *cis*-regulatory evolution contributes to the differences in the age to sexual maturity in these two sister species, we performed RNA-Seq on the testes of *P. maniculatus* x *P. polionotus* F1 hybrids between 16 and 64 days of age. Of the 4,337 loci for which we had strong power to detect ASE, we identified 702 with 2-fold (or greater) differences in the expression of *P. maniculatus* and *P. polionotus* alleles at one or more time-points (16.2% of genes examined). At single time-points over the course of spermatogenesis, the fraction of genes with ≥2-fold ASE ranged from 3.3 to 6.9% (Figure 3.3A). Alleles over-expressed in *P. maniculatus* comprised 1.6-3.5% of this gene set, and similarly, those over-expressed in *P. polionotus*, 1.7-3.4% (Figure 3.3A). An extremely small number of loci for which we had strong power to detect ASE displayed ≥2-fold differences in allelic expression at all time-points (14 of 4,337, or 0.3%). Of these, four are not annotated in *Peromyscus*, and one (*Igf2r*) is a known imprinted gene in *Mus musculus*; thus, the ASE observed at this locus is likely related to

epigenetic, rather than genetic differences between species. Five of the nine remaining genes have known or suspected associations with testis development, spermatogenesis, or sperm phenotype (*Tyro-3* (Lu *et al.* 1999), *Lgals3bp* (Freour *et al.* 2013), *Myl6* (Mizuno *et al.* 2009), *Npm1* (Okuwaki *et al.* 2012), *Atrnl1* (Li *et al.* 2009)), and only two of these, *Npm1* and *Tyro3*, have well-characterized functions related to male fertility. *Npm1* is expressed more highly from *P. maniculatus* than from *P. polionotus* alleles in F1 hybrids and *Tyro3* exhibits the reverse bias, but both show constant levels of ASE over time (Figure 3.3B-C).

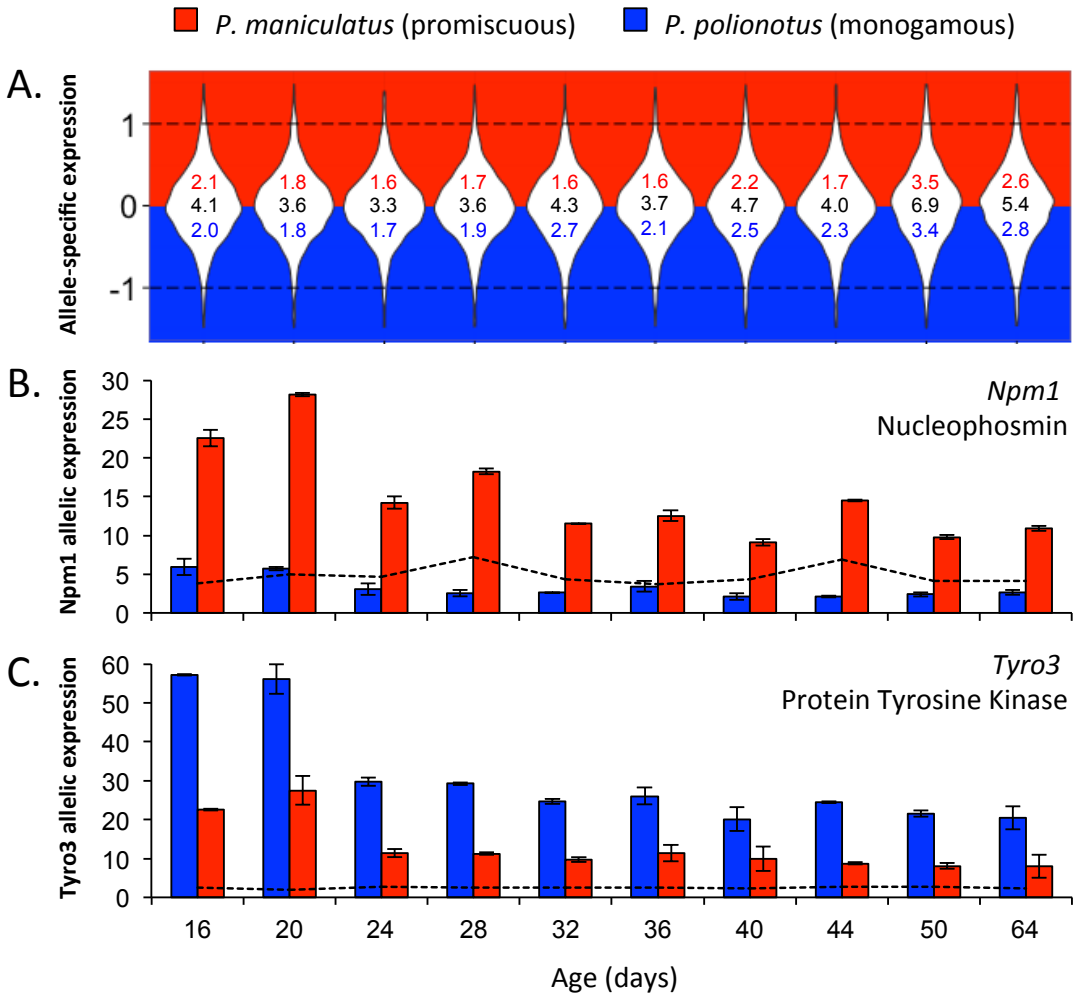

Figure 3.3. Allele-specific expression during testis development in *P. polionotus* x *P. maniculatus* F1 hybrids

Age in days (postnatal) is given on the x-axis (note non-linear scale in last two time-points). Red elements denote *P. maniculatus*-biased ASE, blue elements denote *P. polionotus*-biased ASE, and black elements denote the sum of ASE in both directions. A. $\log_2$(*P. maniculatus*/*P. polionotus*) allelic counts in the subset of genes for which we had high power to detect ASE; ASE ratios falling above or below horizontal dashed lines indicate ≥2-fold differences in expression between *P. polionotus* (negative) and *P. maniculatus* (positive) alleles; in violin plots, width of plot denotes density of ASE values; numbers within plots indicate the percentage of this gene set in which ≥2-fold ASE occurred in *P. maniculatus* (top), *P. polionotus* (bottom), and both species combined (middle). B. Mean ± SE of expression from *P. polionotus* and *P. maniculatus* alleles for the Nucleophosmin gene (*Npm1*) and C. the Protein Tyrosine Kinase (*Tyro3*), both of which show ≥2-fold ASE during all time-points over development; dotted lines denote ratio of *P. maniculatus* : *P. polionotus* and *P. polionotus* : *P. maniculatus* alleles, respectively.

Gene clustering by ASE pattern

To identify groups of genes with specific patterns in the direction and magnitude of ASE across spermatogenesis, we performed soft-clustering analysis. We found four consistent clusters containing many genes with strong membership (Supplementary

Figure S3.1); all four of these clusters show substantial change in ASE across time, with a dramatic shift in the level of ASE before but not after F1 testes tubules begin to undergo their first meiosis, on day 28 (Figure 3.4). The four clusters can be further broken into two sets in which each cluster is a mirror image of the other. For example, cluster 2 contains genes with ASE changing in the direction of *P. polionotus*-bias (though it is important to note that genes in each cluster may favor expression of the same allele across the entire course of spermatogenesis, though the degree to which that allele is more highly expressed grows weaker or stronger; Figure 3.4A). Cluster 10 has a similar shape to cluster 2 but contains genes with increasing ASE in the direction of *P. maniculatus*-bias over reproductive development (Figure 3.4B). Clusters 6 and 7 also share a common shape, yet exhibit opposing changes in ASE-bias with time (Figure 3.4C-D). Thus, many genes show variation in ASE magnitude across spermatogenesis, with the most rapid shifts occurring prior to meiosis, and with major patterns reflected in both directions of allelic bias.

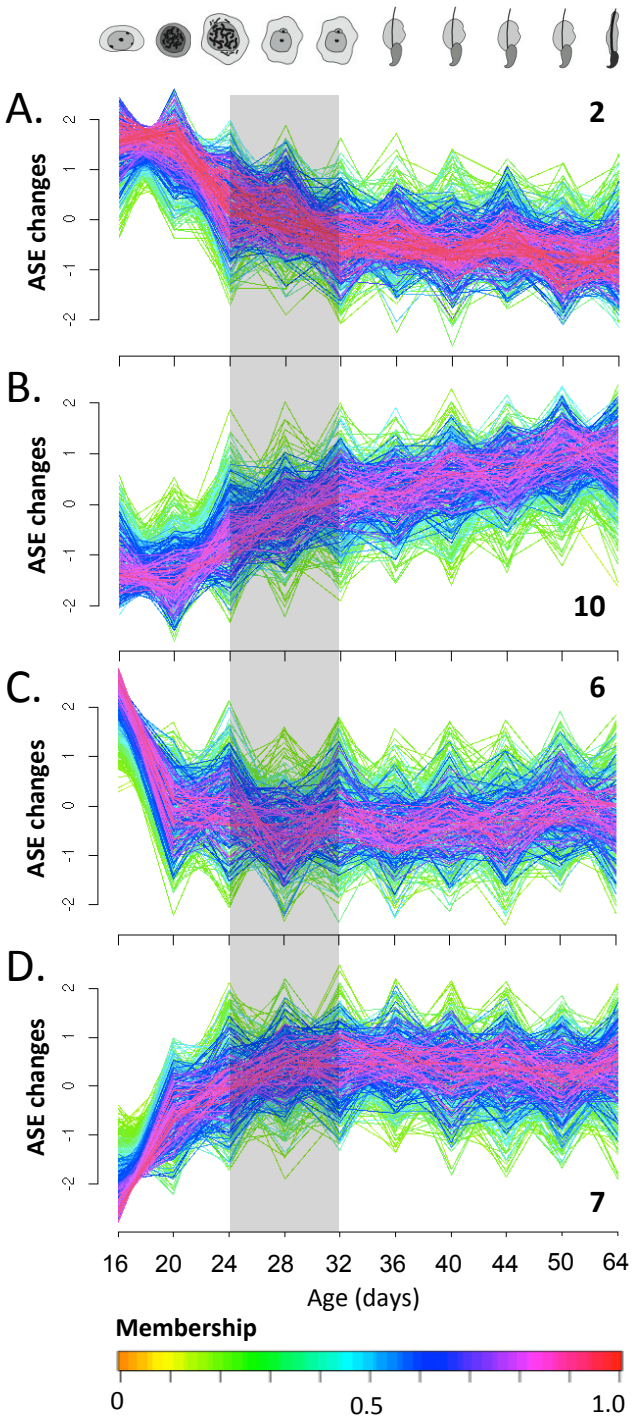

Figure 3.4. ASE patterns during spermatogenesis

Membership in soft clusters of genes according to their patterns of ASE during

spermatogenesis. Age in days (postnatal) is given on the x-axis (note non-linear scale in last two time-points). All $\log_2$(*P. maniculatus*/*P. polionotus*) allelic counts are standardized to have mean = 0 and standard deviation = 1 on the y-axis. Cluster membership is denoted by color, with genes of highest alignment to a given cluster pattern shown in pink-red (see scale at bottom). The cartoons at top show the most mature cell type present in a majority of tubules within F1 testes at each time-point. The translucent grey bar represents the time-period in which the most mature cells within F1 testis tubules undergo meiosis. A. Cluster 2. B. Cluster 10. C. Cluster 6. D. Cluster 7.

To determine which aspects of development may be influenced by genes with these four distinct patterns of ASE, we examined loci with ≥50% membership in each cluster. cAMP Responsive Element Modulator (*CREM*) and Ribonuclease Type III (*DROSHA*) are two important regulators of spermatogenesis (Sassone-Corsi 1998; Wu *et al.* 2012) with strong membership (0.82 and 0.86) in clusters 2 and 10, respectively; their allelic expression levels are depicted in Figure 3.5A-B. Additionally, we performed GO-term analysis to determine the enrichment of genes associated with particular cellular processes, functions, and components in the four clusters (Table 3.1). We found that cluster 2 contains significantly more genes involved in synthesis of cholesterol, a precursor of testosterone, than would be expected by chance. Clusters 6 and 7 comprise an abundance of loci that regulate anoikis (a form of programmed cell death) and immune function, respectively. Finally, cluster 10 includes loci that perform post-translational modification of other proteins, likely regulating their activity and/or

localization. In sum, sets of genes known to impact particular cellular functions are over-represented in each of the four gene clusters identified here, but no two clusters are enriched for loci underlying a single function.

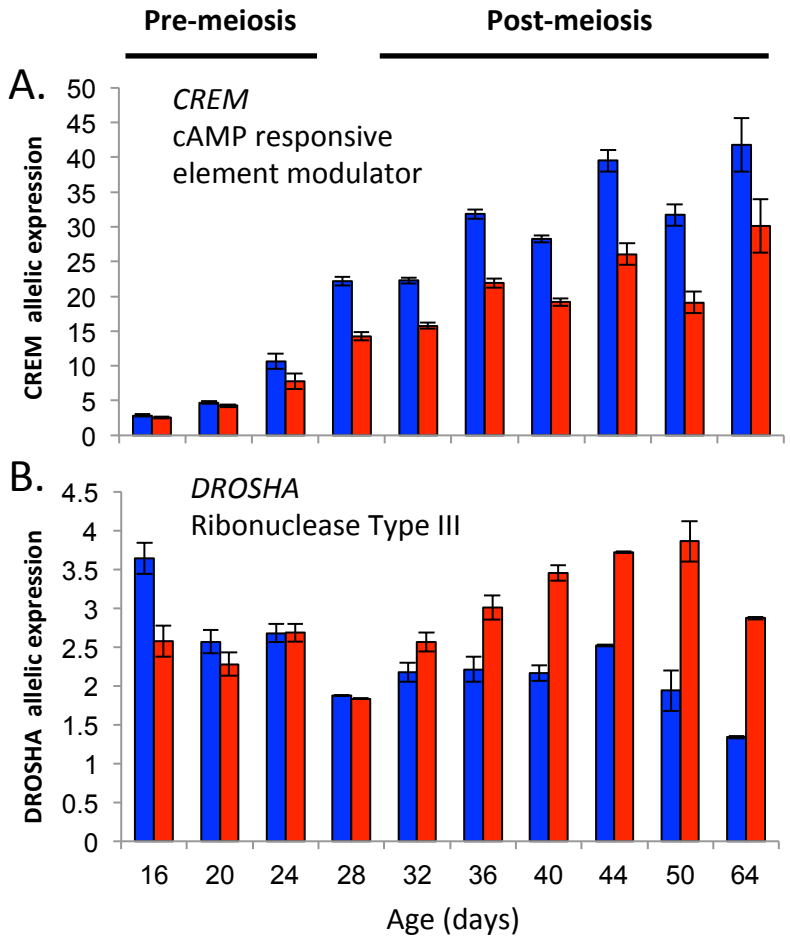

Figure 3.5. Two regulators of spermatogenesis with changing ASE over development

Mean ± SE of expression from *P. polionotus* and *P. maniculatus* alleles for A. the cAMP Responsive Element Modulator (*CREM*) and B. Ribonuclease Type III (*DROSHA*), both of which show changing ASE over development.

Table 3.1. GO term analysis of genes with membership ≥0.5 in clusters 2, 6, 7, and 10.

Cluster	GO term	Description	Genes
2	GO:0008933	lytic transglycosylase activity	*Man2c1, Glb11, Edem3, St8sia4*
2	GO:000820 GO:0016125	cholesterol metabolic process sterol metabolic process	*Pctp, Cftr, Dhcr24, Sorl1, Insig2, Lrp5, Lrp1*
6	GO:2000209	regulation of anoikis	*Mybbp1a, Mcl1, Ptk2*
7	GO:0045582 GO:0045621 GO:1902107 GO:0045580	positive regulation of T cell differentiation positive regulation of lymphocyte differentiation positive regulation of leukocyte differentiation regulation of T cell differentiation	*Hsp90aa1, Socs5, Itpkb, Ap3d1*
7	GO:0046638 GO:0046637 GO:0046635 GO:0046634	positive regulation of alpha-beta T cell differentiation regulation of alpha-beta T cell differentiation positive regulation of alpha-beta T cell activation regulation of alpha-beta T cell activation	*Socs5, Itpkb, Ap3d1*
7	GO:0002475 GO:0019884	antigen processing and presentation via MHC class Ib antigen processing and presentation of exogenous antigen	*B2m, Ap3d1*
7	GO:0044431	golgi apparatus part	*Man2a1, Zdhhc17, Inpp5k, Stk24, Vps53, Ap3d1, Creb3, Scfd1, Tmed2, Dennd5a, Slc35a5, Scamp1, Nucb2, Sppl2b*
10	GO:0010800	positive regulation of peptidyl-threonine phosphorylation	*Cab39, Gsk3b, Mapk1*
10	GO:1902108	regulation of mitochondrial membrane permeability involved in apoptotic process	*Rhot1, Them4, Mtch2*
10	GO:0018410	C-terminal protein amino acid modification	*Atg4b, Atg12, Icmt*

DISCUSSION

P. maniculatus males begin to produce sperm sixteen days before *P. polionotus* males. This may be a conservative approximation of the difference in age to sexual maturity, given a more than 30-day difference in the time at which males of these two species begin to impregnate adult females. An estimation of four months for the average male lifespan in both *P. maniculatus* and *P. polionotus* is generous, though mortality varies among populations (Blair 1948; Howard 1949; Sadleir 1965; Dapson 1972; Smith *et al.* 1972; Rave & Holler 1992). Thus, a difference of sixteen days in the age to reproductive maturity may greatly alter the time available for reproduction in

average males of *P. maniculatus* and *P. polionotus* by more than twenty percent, assuming reproduction is equally likely at all ages following maturation. The magnitude of this difference between sister-species thus suggests that strong selection (and/or its relaxation) likely drives the timing of sexual maturation in these mice.

Histology of the developing testis in these two species corroborates delays in sperm production in *P. polionotus* relative to *P. maniculatus* (Figure 3.2A-B). The intermediate rate of spermatogenesis in immature *P. maniculatus* x *P. polionotus* F1 hybrids (Figure 3.2C) early in spermatogenesis demonstrates that inheritance of developmental timing is, to some degree, additive. Divergent *trans*-acting regulators have been shown to exhibit more completely dominant effects on gene expression in hybrids than *cis*-acting regulators (Lemos & Araripe 105AD). To examine the contribution of such *cis*-acting regulators to the evolution of reproductive development, we searched for ASE in the F1 hybrid testis transcriptome.

In a subset of genes for which we had high power to detect ASE, we saw hundreds of loci with greater than 2-fold differences in expression from the *P. maniculatus* and *P. polionotus* parental alleles (Figure 3.3A) at some point in development, suggesting that a corresponding (or higher) number of *cis*-acting regulatory changes have therefore occurred in testis-expressed loci on the short evolutionary timescale since isolation of these sister species. However, the frequency of ASE observed here is not unusually high. Larger proportions of genes exhibit ASE or *cis*-regulatory divergence between closely-related species or subspecies in genome-wide studies similar to our own (for example, 13.5% of loci show ASE in hybrids of geographically remote *A. thaliana* accessions

(Zhang & Borevitz 2009), and 51% of genes show *cis*-regulatory changes in hybrids of *D. melanogaster* x *D. sechellia* species (McManus *et al.* 2010)), though the amount of ASE detected depends on the divergence of parental groups as well as the technology and significance thresholds employed. Although it is important to note that not all of the *cis*-regulatory changes we infer between *P. maniculatus* and *P. polionotus* are necessarily the result of selection acting on reproductive development, our results indicate that differences in the timing of sexual maturity between *P. maniculatus* and *P. polionotus* are not likely caused by one or a few strong *trans*-acting regulatory changes acting in isolation. Instead, evolution at many hundreds of loci scattered throughout the genome may have some influence on developmental rate.

An extremely small proportion of the genes in which we have strong power to detect ASE exhibited consistently strong bias over the entire course of F1 reproductive development, and only two of these have reasonably well-characterized roles related to male reproduction: *Npm1* and *Tyro3* (Figure 3.3B-C). Nucleophosmin (*Npm1*) is known to contribute to sperm chromatin remodeling, but only that which occurs upon oocyte entry immediately after fertilization (Okuwaki *et al.* 2012). Perhaps this locus also affects chromatin state during spermatogenesis, or perhaps the allele-specific expression of *Npm1* during sperm development is a pleiotropic consequence of selection on its post-fertilization phenotype. Male mouse knockouts of *Tyro3* and two closely-related protein kinases *Axl* and *Mer* display aborted spermatogenesis and cell death in testis tubules (Lu *et al.* 1999), and regulate the phagocytic function of Sertoli cells (Xiong *et al.* 2008), although this family of protein kinases is also thought to play

important immune (Lu & Lemke 2001) and nervous system functions (Prieto *et al.* 2000) as well. Thus, the most striking changes in *cis*-regulation between *P. maniculatus* and *P. polionotus* across development are not necessarily in well-known regulators of spermatogenesis. Additionally, when ASE is consistently strong, it is difficult to implicate individual genes in the process of development, *per se*, because constitutively operating changes to *cis*-regulation may instead have been selected for their effects on non-reproductive tissues or adult phenotypes.

The low proportion of loci with strong ASE at any particular day relative to the total proportion of genes with strong ASE in at least one time-point (Figure 3.3) suggests that the differential expression of alleles is often transient over the course of developmental processes, and that many *cis*-regulatory mutations act in a highly context-specific manner. Notably, had we examined animals at day 64 only (Figure 3.3A), we would have identified less than one-third of all loci with significant ASE during spermatogenesis. Additionally, although expression bias in F1 testis tissue does not show strong trends in magnitude or direction across spermatogenesis as a whole, clusters of genes do exhibit specific patterns of changing ASE over time (Figure 3.4). These genes have experienced *cis*-regulatory divergence between *P. maniculatus* and *P. polionotus* that likely mediates interaction with *trans*-acting factors limited to particular developmental time-points.

CREM and *DROSHA* (Figure 3.5) are two such genes. *CREM* is a transcription factor that responds to the cAMP-signaling pathway (Brindle & Montminy 1992). Following a follicle stimulating hormone (FSH)-mediated developmental switch in testis that occurs at the time of meiosis, *CREM* expression increases (Sassone-Corsi 1998); we show that

at this time, *CREM* also begins to exhibit biased ASE in favor of the *P. polionotus* allele. Given the function of *CREM* as a master regulator of mammalian spermatogenesis, even low levels of ASE at this locus are likely to cause a cascade of regulatory effects at other genes *in trans*. *DROSHA* is an RNase enzyme that mediates canonical microRNA (miRNA) production, and appears necessary for meiotic sex chromosome inactivation; the seminiferous tubules of *DROSHA* knockout mice are depleted in post-meiotic germ cells (Wu *et al.* 2012). Notably, we see *P. maniculatus*-biased ASE in *DROSHA* only after meiosis, despite high expression of the gene at all time points, suggesting that divergence in *cis*-regulation between species at this locus is contingent on developmental context. Because the miRNAs processed by *DROSHA* regulate the transcription and stability of mRNAs from many other loci, change in regulation of *DROSHA*, like *CREM*, is likely to have widespread downstream effects. In sum, the examples of *CREM* and *DROSHA* illustrate that ASE need not be consistently strong over the entire course of development to signify important regulatory change between species. Additionally, context-specificity yields support to the hypothesis that *cis*-regulatory differences at these loci may have been selected for their developmental consequences, rather than adult phenotype alone.

In conclusion, we find that many significant ASE events are relatively short-lived in the developing testis (on the order of a few days), and that clusters of genes exhibit distinct patterns of differential ASE across spermatogenesis. We have thus illuminated the existence of many *cis*-acting regulatory mutations with effects contingent on developmental context. Hundreds of these evolutionary changes likely combine to

produce notable differences in age to sexual maturity, a life history trait that differs between promiscuous and monogamous wild mice.

CHAPTER 4: DIRECT GAMETE SEQUENCING REVEALS NO EVIDENCE FOR SEGREGATION DISTORTION IN HOUSE MOUSE HYBRIDS

Co-Authors: Russ Corbett-Detig, Daniel Hartl, and Hopi Hoekstra

ABSTRACT

Understanding the molecular basis of species formation is an important goal in evolutionary genetics, and Dobzhansky-Muller incompatibilities are thought to be a common source of postzygotic reproductive isolation between closely related lineages. However, the evolutionary forces that lead to the accumulation of such incompatibilities between diverging taxa are poorly understood. Segregation distorters are believed to be an important source of Dobzhansky-Muller incompatibilities between hybridizing species of *Drosophila* as well as hybridizing crop plants, but it remains unclear if these selfish genetic elements contribute to reproductive isolation in other taxa. Here, we collected viable sperm from first-generation hybrid male progeny of *Mus musculus castaneus* and *M. m. domesticus*, two subspecies of rodent in the earliest stages of speciation. We then genotyped millions of single nucleotide polymorphisms in these gamete pools and tested for a skew in the frequency of parental alleles across the genome. We show that segregation distorters are not measurable contributors to observed infertility in these hybrid males, despite sufficient statistical power to detect even weak segregation

distortion with our novel method. Thus, reduced hybrid male fertility in crosses between these nascent species is attributable to other evolutionary forces.

INTRODUCTION

The Dobzhansky-Muller model (Dobzhansky 1937; Muller 1942) is widely accepted among evolutionary biologists as a primary explanation for the accumulation of intrinsic reproductive incompatibilities between diverging lineages (Coyne & Orr 2004; Presgraves 2010). Briefly, this model posits that genes operating normally in their native genetic background can be dysfunctional in a hybrid background due to epistatic interactions with alleles from a divergent lineage. Although elucidating the molecular basis of speciation has been a central focus for decades, loci contributing to Dobzhansky-Muller incompatibilities (DMIs) have proved challenging to identify primarily because they are, by definition, incompatible in combination (reviewed by Coyne & Orr, 2004; Noor & Feder, 2006; Presgraves, 2010; Wu & Ting, 2004). As a result, the specific genetic changes responsible for the onset of reproductive isolation between lineages remain largely obscure.

The rapid evolution of selfish genetic elements within lineages is thought to be a potent source of DMIs between diverging taxa. Segregation distorters (SDs) are one such selfish element that increase their transmission through heterozygotes by either disabling or destroying gametes that failed to inherit the distorting allele (Lyttle 1991; Taylor & Ingvarsson 2003). Because males heterozygous for a distorter produce fewer

viable sperm, SDs can decrease the fitness of carriers. In this case, other loci in the genome are expected to evolve to suppress distortion (Hartl 1975). This coevolution of drivers and suppressors has been suggested to be a widespread source of DMIs between diverging lineages: hybrids of isolated populations in which such coevolutionary cycles have occurred may suffer lower fertility as drivers become uncoupled from their suppressors in a mixed genome (Frank 1991; Hurst & Pomiankowski 1991; McDermott & Noor 2010). Indeed, there is evidence that SDs contribute to hybrid male sterility in several *Drosophila* species pairs (*e.g.* Phadnis & Orr, 2009; Tao, Masly, Araripe, Ke, & Hartl, 2007; Tao, Araripe, et al., 2007; reviewed in McDermott & Noor 2010; Presgraves 2010) as well as in many crop species (*e.g.* Bohn & Tucker, 1940; Cameron & Moav, 1957; Loegering & Sears, 1963; Sano, Chu, & Oka, 1979; Yang, Zhao, Cheng, Du, & Ouyang, 2012). However, comparatively little is known about genetics of speciation outside of these groups, and a multitude of processes besides SD can contribute to the evolution of DMIs. Hence, it remains unclear if SDs contribute to hybrid sterility in other taxa more generally.

Analyses aimed at identifying the genetic targets of positive selection suggest that SDs may be an important source of DMIs in mammalian lineages. One particularly intriguing finding shows a substantial overrepresentation of loci associated with spermatogenesis and apoptosis within the set of genes with the strongest evidence for recurrent positive selection in mammals (*e.g.* Kosiol et al., 2008; Nielsen et al., 2005). These functions in turn are potentially driven, at least in part, by SDs, which are expected to leave just such a mark of selection as they sweep through a population.

Therefore, mammals are an appealing group in which to test for SD and its role in speciation.

In particular, *Mus musculus domesticus* and *M. m. castaneus* are two subspecies of house mice in the earliest stages of evolving reproductive isolation (Boursot & Auffray 1993; Geraldes *et al.* 2008). Indeed, these subspecies are estimated to be approximately 500,000 years diverged from one another (Geraldes *et al.* 2008). Hybrid males suffer from reproductive deficiencies (Davis *et al.* 2007); specifically, the vas deferens of first-generation hybrid (F_1) males contain more apoptotic sperm cells than either pure strain, and numerous loci affecting fertility in hybrid males have been reported, particularly in F_2 individuals (White *et al.* 2012). Finally, Wagner (2010) identified eight genomic regions that exhibited significant deviations from Mendelian segregation in an F_2 mapping population derived from these two subspecies, which may be consistent with the action of SDs in their hybrids (but see below). In combination with the comparative genomic evidence and phenotypic observations described above, these data suggest that coevolution of SDs and their suppressors may contribute to DMIs in *M. musculus*.

The conventional approach to identifying SD relies on detecting a skew in the allele frequencies of second-generation hybrids in a large genetic cross. However, methods that rely on genotyping progeny unavoidably conflate SD, female effects on sperm function, and differential viability of offspring. Additionally, practical issues limit the power of these experiments—specifically, the ability to produce and genotype hundreds to thousands of individuals in order to detect distorters of small effect in an unbiased, genome-wide assay —particularly in vertebrates. Therefore, as a result of

modest sample sizes, many experiments designed to detect SD using genetic crosses are underpowered and unable to detect even moderate distortion (*e.g.* a typical mammalian cross with a few hundred offspring will likely fail to identify 5-10% distortion). These practical issues impose challenges for speciation research, generally, and for studies of SD, specifically, by limiting our ability to confidently identify SDs within and between natural populations.

Here, we explore a novel approach in which we survey the genome for SD by directly sequencing viable gametes from F_1 hybrid *M. m. domesticus*/*M. m. castaneus* males, allowing us to circumvent the problems outlined above. Briefly, we enriched for viable sperm in hybrids and then sequenced these sperm in bulk preparations, along with control somatic tissues, to identify any skew in the representation of either parental chromosome in the viable sperm relative to the control (Figure 4.1). While we demonstrate via simulation that our experimental design has excellent power, we find no evidence of SD in this cross, suggesting that SDs are not a primary contributor to male infertility in *M. m. castaneus* and *M. m. domesticus* hybrids. Nonetheless, this approach has a number of advantages relative to conventional methods. Specifically, our method is more cost effective, more specific to the identification of SD, and more generally applicable to a wide variety of organisms than conventional pedigree-based approaches. We therefore expect that it will be a useful means to study the frequency and impact of SD in other systems.

METHODS

Reference Genome Assembly

To generate robust genome assemblies for each of the two strains of interest, we aligned all short read data for *M. m. castaneus* strain (CAST/EiJ) and *M. m. domesticus* strain (WSB/EiJ) from a recent large-scale resequencing project (Keane *et al.* 2011) to the MM9 genome assembly using BWA mem v0.7.1 (Li & Durbin 2010) for initial mapping. For reads that failed to map with high confidence, we remapped using stampy v1.0.17 (Lunter & Goodson 2011). We realigned reads that overlap indels, and called SNPs and indels for each strain using the Genome Analysis Tool Kit (GATK (DePristo *et al.* 2011). For each program, we used default parameters, except that during variant calling we used the option '–-sample_ploidy 1,' because the strains are extremely inbred.

We generated a consensus sequence for each strain at sites where both assemblies have high quality data. That is, if both CAST and WSB assemblies had a q30 minimum quality genotype (either indels or SNPs) that site was added to both consensus sequences. Otherwise, if either or both assemblies were below this quality threshold at a given site, we used the MM9 reference allele for both.

Alignment Simulation

Our goal was to align short read data to a single diploid reference genome, comprised of assemblies from the two parental strains. The mapping quality, which indicates the probability that a read is incorrectly mapped in the position indicated by the aligner, should then provide a reliable means of distinguishing whether a read can

be confidently assigned to one of the parental genomes. To confirm the accuracy of this approach and to identify suitable quality thresholds, we performed simulations using SimSeq (https://github.com/jstjohn/SimSeq). We used the sequencing error profiles derived from our mapped data (below) and found qualitatively similar error rates using the default error profile included with the SimSeq software package (data not shown). For both the CAST and WSB genomes, we simulated 10,000,000 pairs of 94-bp paired-end reads, whose size distribution was set to match that of our libraries (below). We then mapped these reads back to the single reference genome containing both CAST and WSB consensus sequences. We scored reads as 'mapping correctly' if they mapped to within 10 bp of their expected location measured by their left-most coordinate and on the correct subspecies' chromosome. If the pair mapped, we required that the insert length be less than 500 bp, which is well within three standard deviations of the mean insert size of our data and should therefore encompass the vast majority of read pairs. If both reads in a pair mapped and met our criteria above, we used the higher mapping quality of the two, and discarded the other read. This filter is important, here and below, as it avoids counting pairs as though their provenance is independent of their pair.

Experimental Crosses and Swim-up Assay

To create first-generation (F_1) hybrids of *Mus* subspecies, we crossed 2 *M. m. castaneus* males to 3 *M. m. domesticus* females and 2 *M. m. domesticus* males to 5 *M. m. castaneus* females in a harem-mating scheme. In total, we produced 8 male F_1s in

each direction of the cross. F_1 males whose sire was *M. m. castaneus* (CAST genome) are referred to as CW, and those whose sire was *M. m. domesticus* (WSB genome) as WC. All males were housed individually for a minimum of two weeks prior to sacrifice between 90 and 120 days of age.

To enrich for viable sperm from each F_1 male, we performed a standard swim-up assay (Holt *et al.* 2010). First, immediately following sacrifice, we collected and flash-froze liver and tail control tissues (liver samples, $N = 16$; tail samples $N = 8$). Then, we removed and lacerated the epididymides of each male, placed this tissue in 1.5 ml of human tubal fluid (Embryomax® HTF, Millipore), and maintained the sample at a constant 37 °C for 10 minutes. Next, we isolated the supernatant, containing sperm that swam out of the epididymides, and spun this sample for 10 minutes at 250 g. We then discarded the supernatant, repeated the wash, and this time allowed sperm to swim up into the solution for an hour to select the most robust cells. Finally, we removed the solution, transferred them to new vial, pelleted these sperm by centrifugation, and froze them at -80 °C.

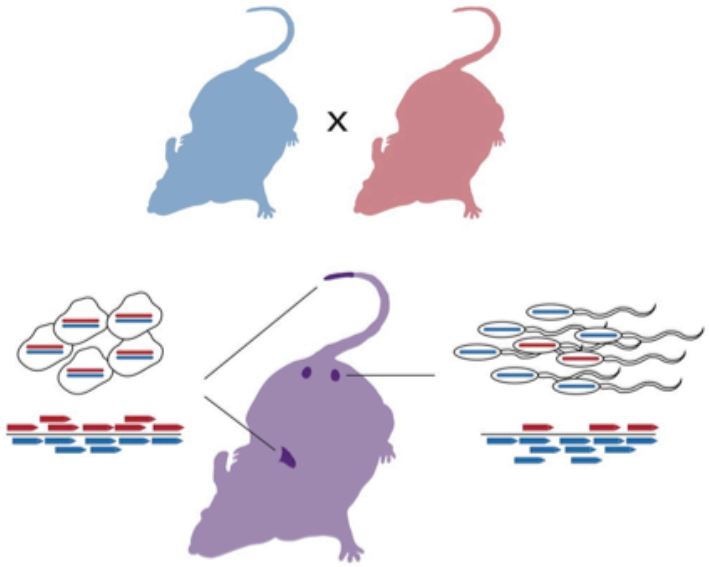

Figure 4.1. Schematic of experimental cross scheme.

Inbred parental strains were crossed, and individual F1 males (purple) sacrificed at between 3 and 6 months, when their sperm were subjected to a swim up assay. Libraries were prepared from liver or tail (control; left) and sperm (experiment; right) samples, sequenced, and then aligned to a diploid reference genome; subspecies of origin was determined for as many sequences as possible.

Library Preparation and Sequencing

For each F_1 hybrid male, we first extracted DNA from sperm, liver, and tail tissues identically using a protocol designed to overcome the difficulty of releasing the tightly packed DNA within sperm nuclei (Qiagen *Purification of total DNA from animal sperm using the DNeasy Blood & Tissue Kit; protocol 2*). We sheared this DNA by sonication to a target insert size of 300 bp using a Covaris S220, then performed blunt-end repair,

adenylation, and adapter ligation following the manufacturer protocol (New England BioLabs). Following ligation, libraries were pooled into two groups of 16 and one group of 8 based on the adapter barcodes. Prior to PCR, each pool was subject to automated size selection for 450-500 bp to account for the addition of 175 bp adapter sequences, using a Pippin Prep (Sage Science) on a 2.0% agarose gel cassette. PCR was performed using six amplification cycles, and then we re-ran the size selection protocol to eliminate adapter dimer prior to sequencing. Finally, we combined the three pools and sequenced them on two lanes of a HiSeq 2500. Each sequencing run consisted of 100 bp paired-end reads, of which the first 6 bp are the adapter barcode sequence, and the remaining 94 bp are derived from randomly-sheared gDNA.

Alignment and Read Counting

We aligned read data to the combined reference genome using 'BWA mem' as described above in the alignment simulation. We removed potential PCR duplicates using Picard v1.73. We then filtered reads based on the alignment filtering criteria described above for the simulated data. Because copy number variations may pose problems for our analysis, we attempted to identify and exclude these regions. Specifically, we broke the genome into non-overlapping 10 kb windows. Then, within each library, we searched for 10 kb regions that had a sequencing depth greater than two standard deviations above the mean for that library. All aberrantly high-depth windows identified were excluded in downstream analyses in all libraries. These regions, representing approximately 7% of the windows in the genome, are reported in

Supplemental Table S1. We exclude high depth regions because translocated duplications that are linked to distant drive alleles could produce a spurious signature of drive in paralogous regions. Importantly, this is unlikely to impact our ability to detect SD that is affected by copy-number variable regions (*e.g.* Merrill et al. 1999; Cocquet et al. 2012) because linked single-copy regions will still display a signature of drive. Although deletions in one parental strain relative to the MM9 genome could also skew the parental allele frequencies for sequenced tissues, these copy number variable regions would affect both somatic tissues and gametes equivalently, and we therefore do not expect copy number variable regions to yield false positive results.

Next, to identify regions showing evidence of SD, we conducted windowed analyses with 1 Mb between the centers of adjacent windows. We counted reads in each window as a decreasing function of their distance from the center of the window, and included no reads at distances greater than 20 cM, thereby placing the most weight in a window on the center of the window. We then analyzed each window in two mixed-effects generalized linear models. Both models included random effects for the libraries and individuals. The first model includes no additional factors. The second had fixed effects for tissue, direction of cross, and an interaction term based on tissue by direction of cross effects, and thus has five fewer degrees of freedom than the first model. Hence, for each window, we assessed the fit of the second model relative to the first using a likelihood ratio test, wherein the log likelihood ratio should be chi-square distributed with 5 degrees of freedom. Afterwards, we applied a false-discovery rate multiple

testing correction to the data (Benjamini & Hochberg 1995). We performed all statistical analyses in R (R Core Team 2014).

To investigate the potential contribution of X or Y linked distorters, we performed an analysis identical to that described above for autosomal windows, with one exception: we compared the number of reads that mapped to the X of each species with the proportion of total reads that mapped to the first chromosome of the corresponding individual. Here, the expectation in the absence of SD is that the X chromosome will have about half as many reads as an autosome (after normalizing for length). We performed a similar analysis contrasting reads mapping to the X versus the Y chromosome (and obtained similar results), but because the Y chromosome is largely repetitive, read mapping is unreliable, and we therefore prefer (and recommend) contrasting depth on the X and an autosomal chromosome.

Power Simulations:

To estimate the power of our method, we simulated distortion data. We began by selecting sites randomly distributed across the genome, and for each site drew a distortion coefficient from a uniform distribution between -0.05 and 0.05. Each read on the parental genome that was susceptible to distortion was counted on the distorting genome with probability equal to the distortion coefficient multiplied by the probability that no recombination events occurred between the distorted locus and the read. We also did the alternative (*i.e.* switching reads from the distorted against genome to the distorting genome) by multiplying by the probability that a recombination event was

expected to occur in the genomic interval between the distorter and the read. We determined recombination probabilities using the genetic map reported in Cox *et al.* (2009). We performed the simulation for both parental genomes, and then again for each parental genome but with the distortion limited to one direction of the cross (*e.g.* only sperm from CW males experienced distortion). A direction-specific effect could occur if, for example, suppressing alleles are present on the Y chromosome of one subspecies and therefore are only present in CW or WC males.

RESULTS

After addressing the possibility of contamination, labeling, and quality issues (see Supplemental Text S1, Supplemental Table S2), we ran our analysis of the data across all autosomes, excluding regions with evidence for copy-number variations (described in Methods). With the exception of windows on chromosome 16 (see below), we found no windows with a statistically significant signature of SD. The lowest uncorrected *p*-value for any window (aside from those on chromosome 16) was 0.0224, which is not significant when we corrected for multiple tests. Thus, we did not find evidence for SDs in any of the autosomal genomic regions considered or on the X and Y chromosomes (Figure 4.2).

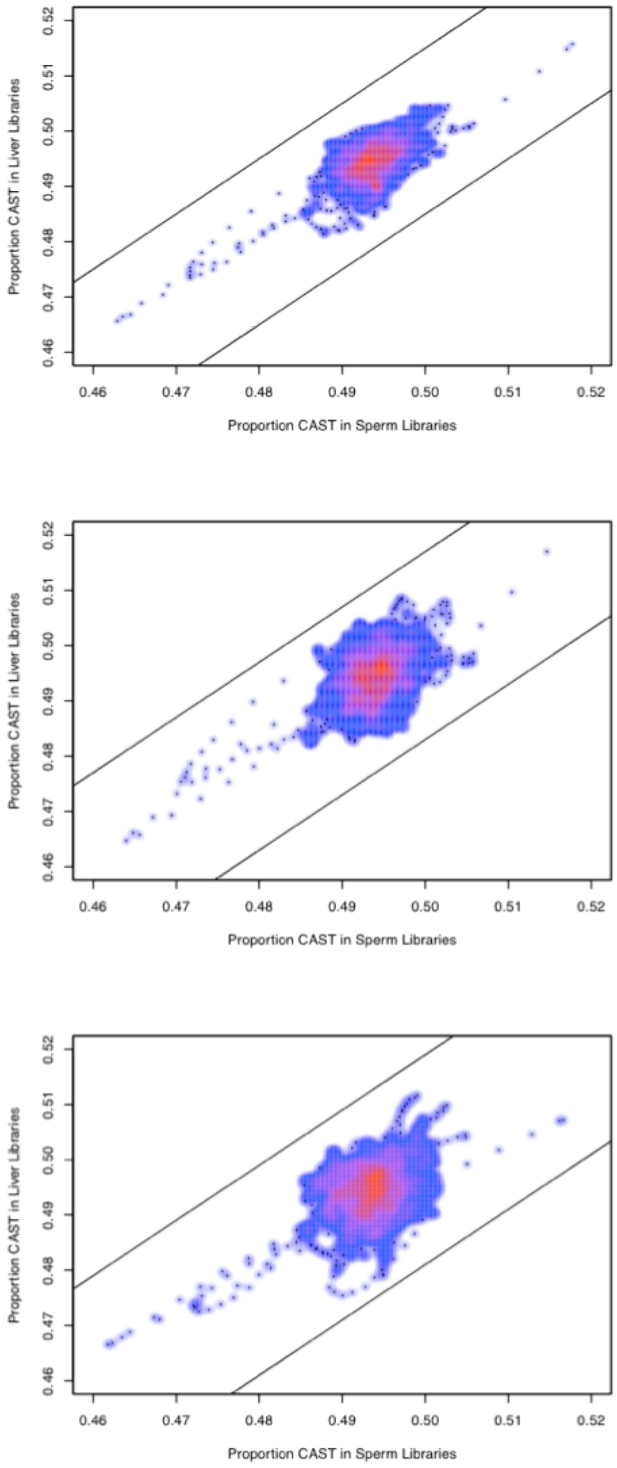

Figure 4.2. Average proportion CAST reads in sperm libraries versus liver libraries.

Using all males (A), using only CW males (B), and using only WC males (C). Lines indicate the approximate threshold at which we would have 50% power to detect distortion at the alpha = 0.0001 level (see Methods for how this threshold was calculated).

By contrast, on chromosome 16, we identified 15 contiguous windows with significantly skewed allele frequencies following correction for multiple comparisons (minimum p = 5.026E-4; Figure 4.3). However, upon closer examination, it appears that this signal is driven almost entirely by a single liver sample, that of individual CW10. If this sample is removed from the dataset, this chromosome no longer shows significant deviation from expectations. When comparing the relative read depths across chromosomes 16 and 1, CW10's liver sample also appears to have disproportionately lower depth on this chromosome relative to the ratio of depths in CW10's sperm sample (p = 3.02E-5; X^2-test). These results suggest that this pattern is likely driven by a somatic aneuploidy event in CW10's liver that occurred relatively early in liver development and is not the result of distortion in the sperm sample.

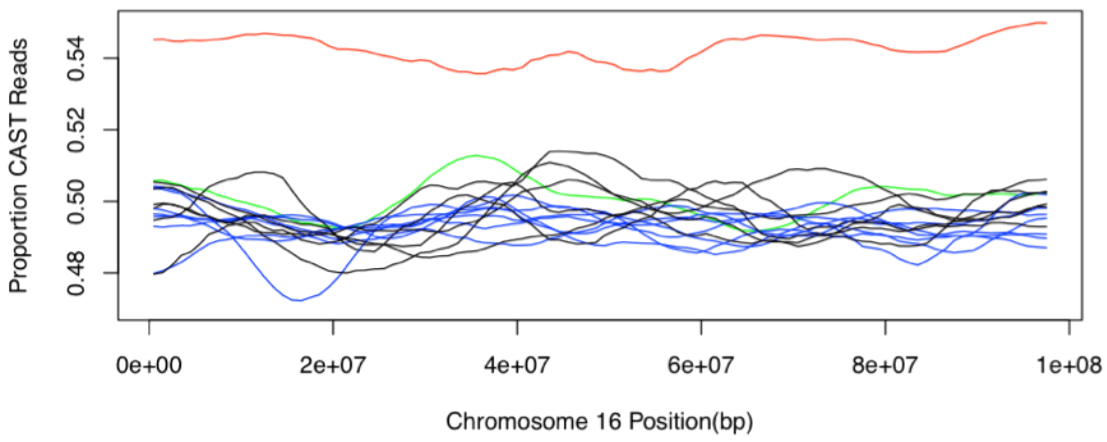

Figure 4.3. Proportion of informative reads that are derived from the CAST genome across chromosome 16.

CW10's liver sample is shown in red, and CW10's sperm sample is shown in green. All other CW libraries are represented in black for liver and in blue for sperm.

Through simulation, we ensured that we have sufficient statistical power, given our experimental design and data quality, to detect SD if it is indeed occurring in hybrid males. We found that we have 50% power to detect SD to approximately 0.014, or 1.4% (this number reflects the positive or negative deviation from the null expectation, 0.5, at $\alpha = 0.001$) if distortion affects CW and WC males equally (Figure 4.4). In other words, we have 50% power to detect distortion that is greater than 51.5% or less than 48.5%. If there is directionality to the distortion effect (*i.e.* only CW or only WC males experience SD), we have 50% power to detect distortion of 0.016 for CW males and 0.018 for WC males (at $\alpha = 0.001$). This significance level was selected for illustrative purposes because it is approximately what would be required for genome-wide significance given our false discovery rate correction. The slight difference in power based on cross direction likely reflects differences in sequencing depth between WC and CW sperm and liver samples. It is also important to note that different regions of the genome will differ slightly in power to detect distortion because read mapping and sequencing as well as divergence between the CAST and WSB strains and their divergence from the reference genome are not uniform across the genome.

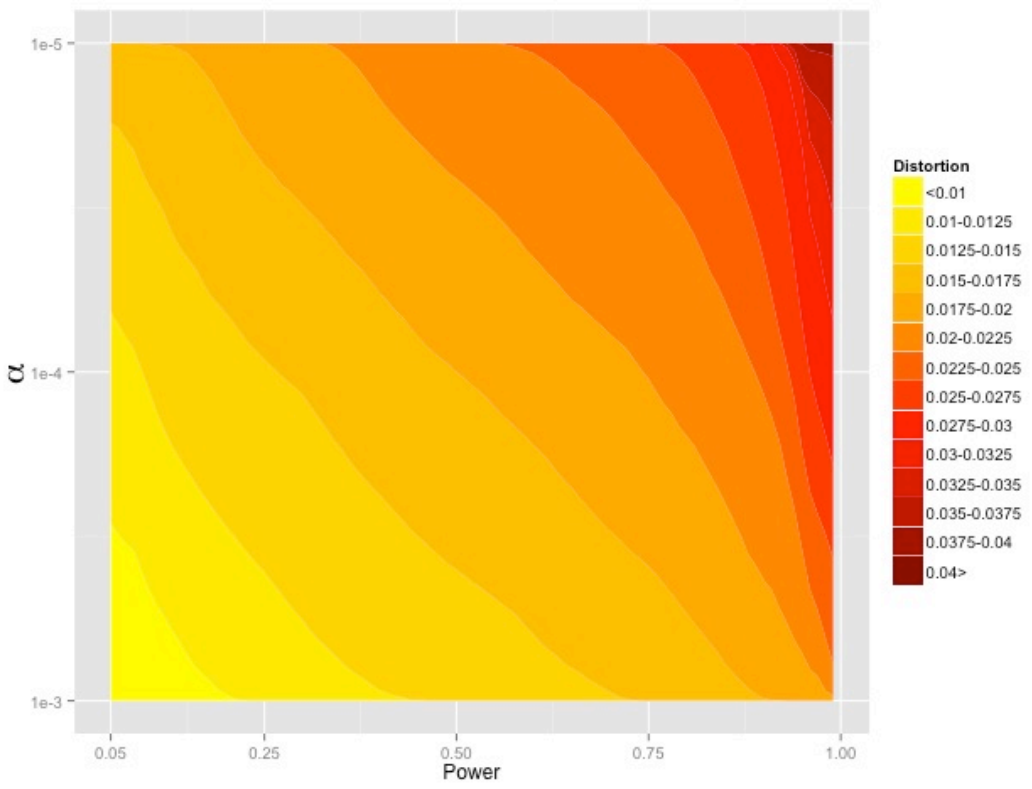

Figure 4.4 Minimum levels of detectable distortion.

Minimum levels of distortion detectable given a specified significance threshold (α, y-axis), and desired power (x-axis).

DISCUSSION

Elucidating the genetic mechanisms underlying species formation is a central goal of evolutionary biology. Although there has been progress in identifying the genetic basis of reproductive isolation in a few elegant instances (*e.g.* (Bradshaw & Schemske 2003; Mihola *et al.* 2009; Lassance *et al.* 2010), including several studies in *Drosophila*

(*e.g.* (Ting *et al.* 1998; Masly *et al.* 2006; Bayes & Malik 2009), it is unclear how general these results are. For example, in the case of SD specifically, we know that SDs contribute to reproductive isolation in several young *Drosophila* species pairs (Tao *et al.* 2007a; b; Phadnis & Orr 2009) but here, to our surprise, we find no evidence for SD between two nascent species of mouse, *M. m. castaneus*/*M. m. domesticus,* despite strong experimental power.

Our conclusion must be qualified to some degree. SDs are generally classified as either gamete disablers or gamete killers depending on their mode of action (reviewed in (Lyttle 1991; Taylor & Ingvarsson 2003). We expect to detect gamete killers with our approach since their victims may not be present in the epididymides, or, if present, these sperm would not be captured in our stringent swim up assay. Our ability to detect gamete- disablers, however, depends on the specific mechanism by which these genetic elements act. If the motility or longevity of a sperm cell is sufficiently impaired, it is likely that this sperm would fail to swim into solution and remain motile over the course of the assay, but if the distortion effect has a very subtle effect on motility or impairs function later in the sperm life cycle (*e.g.* by causing a premature acrosome reaction), it is unlikely that our method could detect these effects. Thus, although gamete killers are not prevalent sources of DMIs in these subspecies, we cannot completely exclude the possibility that gamete disablers contribute to *M. musculus* species formation. However, it is worth noting that disablers cannot explain the reported observation of increased apoptosis of sperm cells in hybrid males (White *et al.* 2012).

Conventional methods of detecting SDs (*i.e.* genotyping the progeny of a cross) will conflate SD, gamete competition, and offspring viability, and due to practical limitations are usually statistically underpowered and thus unable to detect even modest distortion effects. For example, one would need to genotype 3405 offspring to have 80% power to detect 5% distortion ($\alpha = 0.001$), whereas using our method, we have 100% power to detect the same effect in the bulk-sequenced sperm of a single F1 male. Moreover, requiring the presence of offspring from F_1 hybrids unavoidably conflates viability, gamete competition, and segregation distortion effects. By contrast, our simulations demonstrate that by sequencing high quality gametes from individual hybrid males and comparing allele ratios in these gametes to those of somatic tissues, we have excellent power to detect even relatively weak SDs, of approximately one percent. In support of this point, we successfully detected an aneuploidy event that resulted in a four percent difference in allele frequencies relative to expectations within only a single biological replicate. Nonetheless, we found little evidence that SDs are active in F_1 hybrid males, which indicates that segregation distortion (specifically by gamete killers though not necessarily by gamete disablers) is not a primary contributor to reduced F_1 male fertility in these subspecies.

Because our method of determining the allele ratios in bulk preparations of viable gametes relative to somatic tissues is very general, we expect that it will be useful in a wide variety of systems for an array of questions. Provided one can accurately phase the diploid genome of an individual, *e.g.* by using complete parental genotype data when inbred strains are not available, it is straightforward to apply this method to

assay SD in a wide variety of taxa (including humans). Thus, we are now well positioned to survey the prevalence of segregation distortion both within and between a diversity of species. This approach also allows segregation distortion to be weighed against other possible sources of DMIs that may occur during spermatogenesis, oogenesis, fertilization, or embryogenesis, but which leave an identical signature to SD in conventional cross-based experiments. Furthermore, because SDs can increase in frequency in populations despite deleterious consequences for the host, these selfish genetic elements may also be an important source of disease alleles. For example, it has been suggested that SDs contribute to the perpetuation of split-hand/split-foot disease (Jarvik *et al.* 1994; Özen *et al.* 1999), retinal dystrophy (Evans *et al.* 1994) and Machado-Joseph disease (Ikeuchi *et al.* 1996) in humans. Hence, the method introduced here has the potential to improve our understanding of disease evolution in addition to the contribution of SDs to the evolution of reproductive isolation between diverging lineages. When applying this new method to outbred or natural populations, however, one must consider the possibility that SD alleles may be polymorphic. If SD alleles are at low frequency, it will be especially necessary to survey a large number of hybrid individuals to capture the loci of interest.

While segregation distorters may be an important mechanism of speciation in *Drosophila* and crop plants, efforts to detect SD in other diverging lineages—especially studies with high statistical power—have been limited. We find that at least in *M. m. castaneus*/*M. m. domesticus* hybrids, SDs —specifically gamete killers— are not measurable contributors to observed infertility in F1 hybrid males, despite strong

statistical power to detect them, suggesting that reduced hybrid male fertility in these nascent species is attributable to other underlying genetic causes. Further studies using the novel and powerful approach developed here will improve understanding of the role of SDs within and between populations.

CHAPTER 5: THE *TUG1* LOCUS FACILITATES SEPARATION OF SPERMATIDS FROM COLLECTIVE CYTOPLASM DURING SPERMIATION

Co-Authors: Stephen C Liapis, Martin Sauvageau, William Mallard, John L Rinn, and Hopi Hoekstra.

ABSTRACT

Many thousands of long non-coding RNAs (lncRNAs) are transcribed from the genomes of complex organisms such as mice and humans. Evolutionary conservation of sequence, strong promoters, and signatures of active transcription at lncRNA loci suggest that a large subset play important roles in the cell, and indeed, lncRNAs have been implicated in the regulation of transcription, human disease, and development. However, a clear function has been described for only a very small proportion of identified lncRNAs. In particular, though well over ten thousand of these loci are expressed in the mammalian testis alone, only one is currently implicated in spermatogenesis. Here, we examine the role of the *Tug1* lncRNA in male reproduction. *Tug1* male (but not female) knockout mice are infertile or extremely sub-fertile. We show that these animals produce few mature sperm, and that their sperm exhibit a suite of abnormalities, some of which have been previously linked to the process of cytoplasmic removal during spermiation. Our histological examination of male reproductive tissues from *Tug1* knockout males confirms that in the absence of *Tug1* lncRNA, spermatids fail to separate from the collective cytoplasm shared by all

daughter cells of single progenitor spermatogonia, though they are released into the testis lumen and travel together to the epididymis. *Tug1* is thus critical to sperm individualization, the genetic basis of which has not been previously characterized in mammals.

INTRODUCTION

Long non-coding RNAs (lncRNAs) are transcribed from DNA, but unlike mRNA, transmission of the biological information they carry is not contingent upon translation into protein. Instead, lncRNAs may act alone or with protein, DNA, or RNA molecular partners (Guttman & Rinn 2012), to perform a variety of functions within the cell (reviewed in Yang et al. 2014). Specifically, recent research implicates lncRNAs in human disease (Wapinski & Chang 2011; Qiu *et al.* 2013), genetic and epigenetic regulation (Lee 2012; Rinn & Chang 2012; Mercer & Mattick 2013), and development and cell differentiation (Pauli *et al.* 2011; Sauvageau *et al.* 2013; Fatica & Bozzoni 2014). Although our knowledge of most lncRNA functions is still very recent, a few lncRNAs have been well characterized, e.g. Xist, which directs X-chromosome inactivation *in cis* (Kay *et al.* 1993), and HOTAIR, which represses transcription *in trans* at the HOXD locus (Rinn *et al.* 2007).

Although studies have identified thousands of transcribed, long noncoding RNA sequences (Derrien *et al.* 2012), some of these may represent transcriptional noise (Struhl 2007; Louro *et al.* 2009). In contrast, functional lncRNAs are often, but not

always, evolutionarily conserved (Ponjavic *et al.* 2007), are typically associated with strong promoters, carry signatures of active transcription, and are frequently transcribed in a tissue-specific manner. Additionally, the presence of lncRNAs is associated with increasing organismal complexity. In sum, although not all non-coding RNA transcripts have important functions within the cell, a subset certainly do. Many of these can be clearly identified by a combination of the attributes mentioned above, and although their evolution suggests intriguing functions, most are uncharacterized.

In the testes, the number of expressed lncRNAs may exceed the number of mRNAs (Bao *et al.* 2013). Over one-thousand of these noncoding transcripts show differential expression over the course of spermatogenesis in mice (Laiho *et al.* 2013) and in rats (Chalmel *et al.* 2014). However, the male reproductive function of only one (to date) is known (reviewed in Mukherjee et al. 2014; Luk & Lee 2013). This lncRNA, *mrhl*, regulates Wnt signaling in mouse spermatogonial cells, resulting in perturbations to differentiation and development (Arun *et al.* 2012). In females, only one lncRNA, *Neat1*, is currently known for a direct effect on fertility (Nakagawa *et al.* 2014; Shen & Zhong 2015). Collectively, these results suggest that more work needs to be done to identify the role of additional lncRNAs in gonad development.

The lncRNA *Taurine Upregulated Gene 1* (*Tug1*) was identified in a screen for loci up-regulated by taurine in murine retinal cells (Young *et al.* 2005). Although *Tug1* was implicated originally in the formation of photoreceptors (Young *et al.* 2005), it is expressed in multiple mouse tissues. Additionally, the *Tug1* gene has a human homolog, TUG1 (Sauvageau *et al.* 2013). Multiple lines of evidence suggest that *Tug1* is not

protein coding: it has no conserved open reading frames, does not engage ribosomes in profiling assays, and does not appear in mass spectrometry data from relevant tissues (Sauvageau *et al.* 2013). Similarly, there is strong support for *Tug1* lncRNA function: it is highly expressed in tissues throughout the murine body (including brain, testes, liver, lung, kidney, spleen, colon, heart, and skeletal muscle (Sauvageau *et al.* 2013)), and the chromatin at its locus contains canonical features of active transcription but lacks signatures common to DNA enhancers (S. Liapis, personal communication).

Although *Tug1* knockout adult mice do not have obvious outward physical deficits, males, but not females, have not been observed to sire pups, despite producing mating plugs in many pairs (S. Liapis, unpublished data). Thus, we became interested in the role that the *Tug1* lincRNA might play in male fertility. Here, we examine the reproductive morphology, sperm morphology, and testis and epididymis histology in *Tug1* knockout, heterozygous, and wild type male mice. We characterize the timing and location of expression from the *Tug1* locus, and determine the cellular consequences of *Tug1* absence in spermatogenesis.

METHODS

Tug1 *knockout model*

The *Tug1* knockout model was created as described previously (Figure 5.1; (Sauvageau *et al.* 2013). Briefly, the second, third, and fourth exons of *Tug1* were replaced with a *LacZ* expression cassette, preceded by a start codon with strong Kozak

sequence context. The approximate location and timing of *Tug1* expression can therefore be visualized in knockouts (and heterozygotes) with X-gal staining for the β-galactosidase product of the *LacZ* gene.

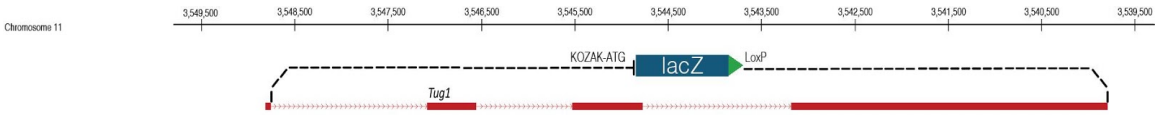

Figure 5.1. Genetic construct replacing the *Tug1* locus with a *LacZ* expression cassette

Tug1 exons are shown in red. Position of LacZ expression cassette is indicated with dashed lines and a blue bar.

Tug1 -/-, +/-, and +/+ male phenotypes

We sacrificed Tug1 knockout, heterozygous, and wild-type males between 60 and 400 days of age, weighed each animal, and dissected out the entire male reproductive tract into phosphate buffered saline (PBS). We next removed and weighed one testis and collected sperm from one cauda epididymis by bisecting it and suspending the tissue in a solution of Biggers-Whitten-Whittingham (BWW) sperm media (Biggers *et al.* 1971) at 37 degrees Celsius. To examine motility after approximately 15 minutes' incubation, we took a five-second video of sperm solution mounted between a plastic slide and coverslip on an upright microscope (AxioImager.A1, Zeiss, Jena, Germany). We then fixed sperm in 2% paraformaldehyde (PFA) in PBS.

To examine morphology, we mounted 20 uL of suspended cells in Fluoromount

media (Southern Biotech), and scanned each slide in a linear transect, recording for each cell encountered whether morphology was normal or abnormal, and if abnormal, which of 15 observed sperm morphological abnormalities (headless, head angle aberrant, head bent back to midpiece, debris on head, debris on hook, head mishapen, midpiece curled, midpiece kinked, midpiece stripped, debris on midpiece, tail-less, tail curled, tail kinked, tail broken, multiple cells annealed together) were present. To determine sperm count, we used a Countess automated cell counter (Life Technologies). We performed all statistical comparisons of *Tug1* +/+, +/-, and -/- testis size, sperm morphology, and sperm count using R (Kruskal-Wallis one-way analysis of variance with Bonferroni correction, Wilcoxon rank-sum test with Bonferroni correction, and principal component analysis (PCA); R Core Team 2014).

Location and timing of Tug1 *expression in male reproductive tissues*

To investigate the timing of Tug1 expression and the cellular basis of *Tug1* knockout male infertility, we examined testis and epididymis histology. We fixed testis and epididymis tissues from *Tug1* knockout and wild-type males in 4% PFA, and stained these whole organs with X-gal to reveal the timing and position of expression driven by the *Tug1* promoter (replaced in knockout animals with a *LacZ* reporter construct; see above). We then embedded both organs in paraffin, sectioned blocks at 6 micron thickness, and mounted tissue sections onto glass microscope slides. To visualize cell types and stages, we additionally stained testis sections with Mayer's hematoxylin, Periodic Acid, and Schiff's Reagent (VWR), and epididymis sections with eosin (VWR).

RESULTS

Male reproductive phenotypes

To determine the phenotypic basis of *Tug1* knockout male infertility, we first explored the possibility that *Tug1* -/- animals fail to develop or maintain testis tissue. We measured *Tug1* -/-, Tug1 +/- , and Tug1 +/+ male testis mass, and found significant differences among these strains (Kruskal-Wallis one-way analysis of variance with Bonferroni correction, $p = 0.035$; Figure 5.2A). Specifically, Tug1 knockout males' testes (mean ± SE = 0.084 ± 0.003g, n = 7) were on average 78 percent of the size of wild type males' testes (mean ± SE = 0.107 ± 0.007g, n = 9), but wild type and heterozygote testes (mean ± SE = 0.099 ± 0.008g, n = 3) did not differ significantly in size (Wilcoxon rank sum tests with Bonferroni correction, $p_{-/- \text{ v. } +/+} = 0.035$, $p_{+/- \text{ v. } +/+} = 1.000$).

To assess the possibility that *Tug1* plays a critical role in spermatogenesis, we next quantified the sperm production (count) of *Tug1* -/-, +/-, +/+ males. We found that sperm count does differ significantly among genotypes (Kruskal-Wallis one-way analysis of variance with Bonferroni correction, $p = 0.003$; Figure 5.2B), and that *Tug1* knockout males (mean ± SE = $2.48 \times 10^6 \pm 5.00 \times 10^5$ cells/mL, n = 7) on average produce only 40 percent as many sperm as wild type males (mean ± SE = $6.13 \times 10^6 \pm 6.36 \times 10^5$ cells/mL, n = 9; Wilcoxon rank sum test with Bonferroni correction, $p_{-/- \text{ v. } +/+} = 0.009$). *Tug1* heterozygous males have an intermediate sperm count (mean ± SE = $3.8 \times 10^6 \pm 4.00 \times 10^5$ cells/mL, n = 3) and do not differ significantly from wild type males (Wilcoxon rank sum test with Bonferroni correction $p_{+/- \text{ v. } +/+} = .1227$).

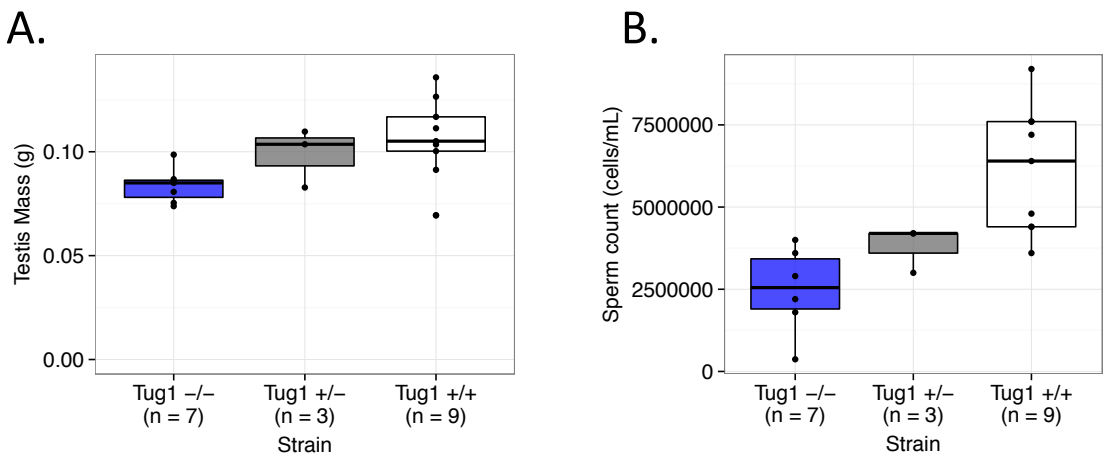

Figure 5.2. Testis mass and sperm count in wild type and *Tug1* knockout animals

Blue elements denote Tug1 -/- (knockout), grey elements denote Tug1 +/- (heterozygote), and white elements denote Tug1+/+ (wild type). Boxes denote median (horizontal line) and interquartile range; all points are shown. Sample sizes are given below each strain. A. Average mass of two testes from adult males. B. Sperm count in a standard dilution of cells from adult male cauda epididymis.

Sperm abnormalities

Although *Tug1* knockout males produce fewer sperm than wild type animals, we found none that were completely azoospermic. We examined the existing sperm of *Tug1* -/- males to identify abnormalities that might illuminate the role of *Tug1* in spermatogenesis. In a principle components analysis (PCA) of the proportion of each male's sperm displaying each of 15 morphological abnormalities, the sperm of *Tug1* wild type and heterozygous males cluster together on the first axis (PC1), to the exclusion of

Tug1 knockout animals (Figure 5.3). Additionally, the proportion of morphologically normal cells is significantly greater in wild type males (mean ± SE = 0.502 ± 0.092, n = 9) relative to *Tug1* knockouts (mean ± SE = 0.064 ± 0.030, n = 8), but not heterozygotes (mean ± SE = 0.36 ± 0.042, n = 5; Wilcoxon rank sum tests with Bonferroni correction, $p_{-/- \text{ v. } +/+} = 0.0037$, $p_{+/- \text{ v. } +/+} = 1.000$).

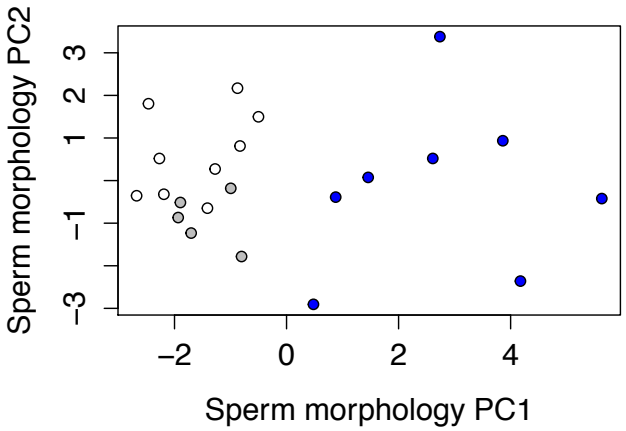

Figure 5.3. PCA of *Tug1*-associated sperm morphological aberrations

PC1 (x-axis) and PC2 (y-axis) from a PCA of sperm morphological aberrations present in Tug1 -/- (blue), Tug1 +/- (grey) and Tug1+/+ (white) males.

To determine which sperm abnormalities best describe differences between Tug1 genotypes, we identified the top loadings on PC1. These were the proportion of sperm with no head, mishapen head, head bent back to contact midpiece, stripped midpiece, kinked midpiece, and the presence of multiple sperm attached along the midpiece. All of these traits, with the exception of mishapen head, differed significantly

between the Tug1 knockout and wild type males (Figure 5.4A-F), but not between wild type and heterozygous animals (Wilcoxon rank sum tests with Bonferroni correction, means and p-values in Table 5.1).

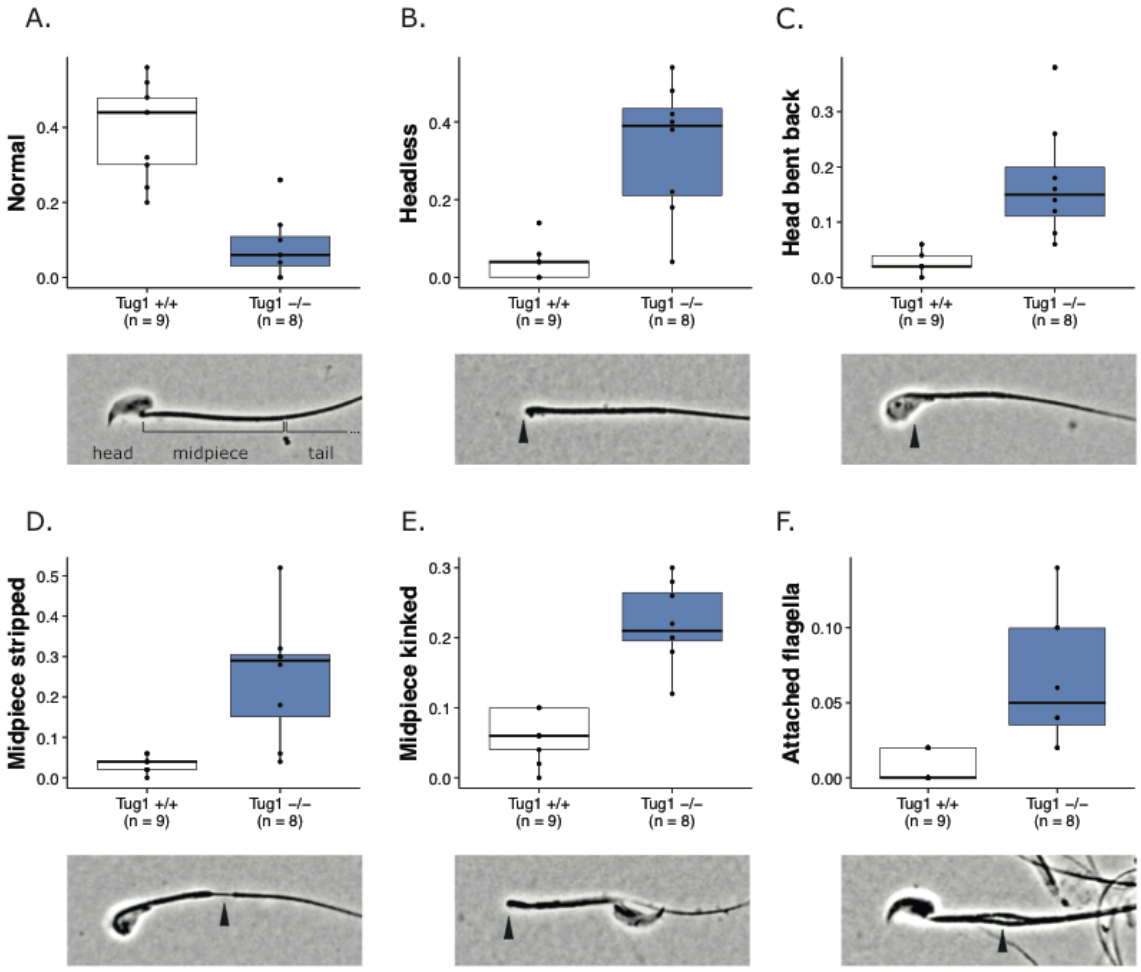

Figure 5.4. *Tug1*-associated sperm morphological aberrations

Proportion normal sperm, and proportion sperm exhibiting six morphological abnormalities in Tug1 -/- (blue) and Tug1+/+ (white) males. Representative images of normal and of morphologically aberrant cells significantly more common in Tug1 -/-

than in Tug1 +/+ males are shown beneath the box plot for the relevant sperm type. A. Normal sperm. B. Headless sperm. C. Sperm with head bent back to the midpiece. D. Sperm with stripped midpiece. E. Sperm with kinked midpiece. F. Sperm with flagella attached to that of other cells, typically at the midpiece region.

Table 5.1. **Means and p-values associated with the proportion of selected morphological abnormalities *Tug1* -/-, +/-, and +/+ males' sperm.**

Significant p-values after Bonferroni correction are shown in bold, with a single asterisk.

Trait: *Proportion of sperm…*	Mean -/-	Mean +/-	Mean +/+	Wilcoxon -/- v. +/+ (α = 0.008)	Wilcoxon +/+ v. +/- (α = 0.008)
Headless	.333	.032	.036	**0.0055 ***	1.000
Head bent back	.173	.036	.027	**0.0024 ***	0.9818
Midpiece stripped	.25	.044	.033	**0.0076 ***	1.000
Midpiece kinked	.22	.076	.06	**0.0018 ***	1.000
Attached flagella	.065	.036	.009	**0.005 ***	0.287
Head mishapen	.15	.04	.05	0.11	1.000

Timing and location of Tug1 *expression*

To determine the developmental basis of these sperm morphological abnormalities, we compared histological sections of male reproductive tissues from *Tug1* -/- and *Tug1* +/+ individuals. In the testis, *Tug1* expression in stages 9-11 was restricted to residual bodies traveling towards the basement membrane (Figure 5.5A; Russell & Ettlin 1990), and was absent in stages 12-14. Diffuse and faint expression then appeared in stage 15 spermatids. By stage 16, staining was strong and localized to

aggregates of mature spermatids clustered at the edge of the testis lumen. These spermatids appear attached by their collective cytoplasm (shared amongst the progenitors of a single spermatogonia in mammals).

In wild type epididymides, individual sperm appeared to migrate freely throughout the lumen (Figure 5.5B). In contrast, in Tug1 -/- epididymides, the sperm aggregates observed in testis were present, though without staining for *Tug1* expression. These bodies were detectable in all three regions of *Tug1* -/- male epididymides (caput, corpus, and cauda), and the epididymides of knockout males also contained many fewer individual sperm than wild type epididymides, in keeping with these animals' lower sperm count.

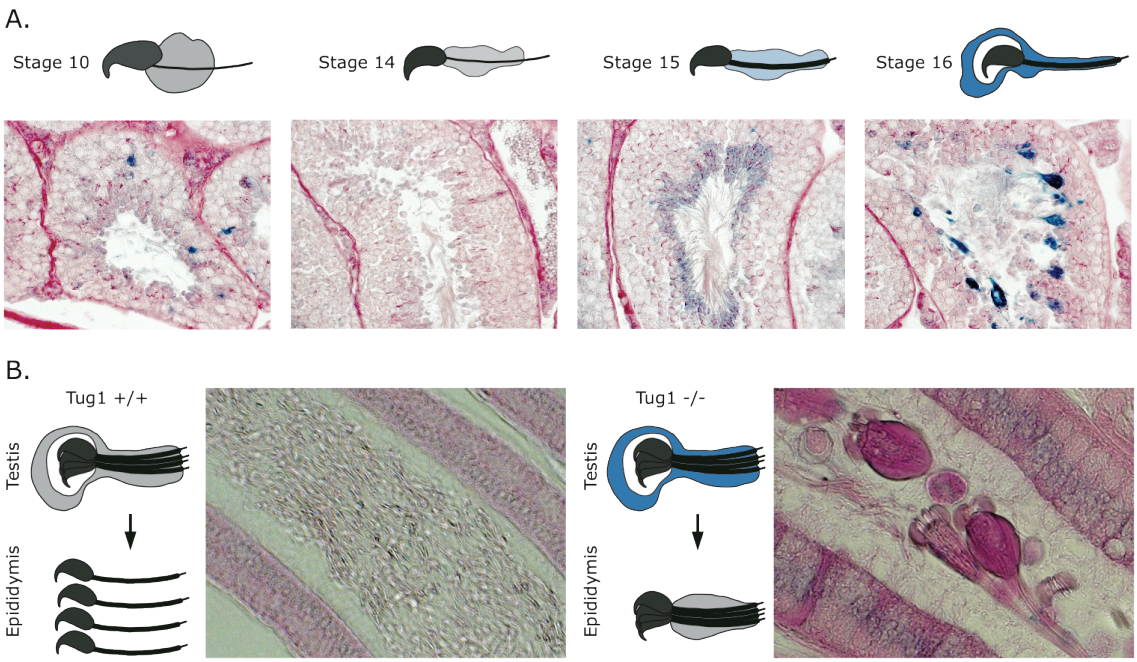

Figure 5.5. Location and timing of *Tug1* expression in testis and epididymis tissue

A. Representative cartoons and images of testis tubules from *Tug1* knockout males in stages 10, 14, 15, and 15, each stained with periodic acid, Schiff's reagent, and X-gal. B. Representative cartoons and images of epididymis tubules from *Tug1* wild type (left) and knockout (right) males in stages 10, 14, 15, and 15, each stained with eosin, and X-gal.

DISCUSSION

Tug1 *function in male reproduction*

We have characterized the nature of *Tug1* function in male reproduction by examining quantitative and qualitative differences in the sperm, testes, epididymides of *Tug1* -/-, +/-, and +/+ individuals. Although significant, the small decrease in testis size of knockout relative to wild type males (Figure 5.2A) is likely insufficient to explain the infertility of these animals. Disparities in sperm counts (Figure 5.2B) are more dramatic, however, and the relatively small numbers of sperm produced by knockout males display a particular suite of morphological abnormalities which suggest that full deficiency of this lncRNA in knockouts (but not in heterozygotes) causes mechanical strain on the midpiece region of the sperm, including the point of attachment with both head and tailpiece (Figure 5.4B-F). Similar aberrant sperm phenotypes have been described previously in association with defects of cytoplasm removal during spermiation (Zheng *et al.* 2007; Rainey *et al.* 2010).

Expression from the *Tug1* locus occurs very late in spermatogenesis, long after the vast majority of transcription ceases in sperm cells (Monesi 1964; Kierszenbaum & Tres 1975), and a single copy of *Tug1* is sufficient to produce testes and sperm that are statistically indistinguishable from those of wild type animals. Together, these lines of evidence suggest two likely scenarios: 1) *Tug1* transcripts are produced by developing spermatids at or before stage 10 (at which time transcription shuts down), and are stored in the collective spermatid cytoplasm until stages 15 and 16, or 2) *Tug1* transcripts are produced by Sertoli cells prior to stage 15 and then transferred to spermatids' shared cytoplasm via the extensive contacts between these cell types (including the ectoplasmic specialization and the tubulobulbar complex (O'Donnell *et al.* 2011)). In either case, because most transcripts are shared amongst developing spermatids in the cytoplasm during development, it is unsurprising that a single copy of the lncRNA *Tug1* is sufficient to produce normal testes and sperm in heterozygotes.

The late and confined localization of strong expression from the *Tug1* locus to abnormal aggregates of stage 16 spermatids in knockout animals (Figure 5.5A) demonstrates that *Tug1* is essential to the process by which spermatids dissociate from their collective cytoplasm. The appearance of unstained sperm aggregates in knockout epididymides (Figure 5.5B), however, indicates that *Tug1* is likely not essential to the separation of spermatids from Sertoli cells (spermiation), and that *Tug1* action occurs at the end of spermiogenesis within the testis, but does not directly control sperm maturation within the epididymides. Thus, *Tug1* appears to play a relatively circumscribed but critical role in spermatogenesis by promoting sperm individualization

(a term borrowed from *Drosophila* spermatogenesis (Fabrizio *et al.* 1998) because individualization lacks a term in common use in mammals).

To our knowledge, *Tug1* is also the only mammalian gene directly implicated in sperm individualization. The collective cytoplasm from which sperm dissociate during this process is particularly fascinating from an evolutionary standpoint, because it is thought to be an adaptation of males to reduce meiotic drive (Haig & Bergstrom 1995). In brief, during meiosis, haploid daughter spermatids inherit only one allele from their progenitors (either maternal or paternal); therefore, mutations allowing one sperm to incapacitate a neighbor carrying the other allele may spread rapidly through a population (Sandler & Novitski 1957; Lyttle 1991). However, such 'driving' mutations may be disadvantageous to the individuals that carry them if sperm are limited or if sperm competition favors males with higher counts (Taylor & Ingvarsson 2003). The presence of shared cytoplasm containing adjacent spermatids may reduce the opportunity for meiotic drivers to evolve, by ensuring that all sperm must interact physically with any 'poison' they might produce. The timing and mechanism by which sperm are permitted to leave the collective cytoplasm during individualization is thus likely highly regulated, but extremely poorly characterized in mammals. Our implication of *Tug1* is an important step towards a more comprehensive understanding of this process.

In conclusion, we propose here that the lncRNA *Tug1* facilitates dissociation of spermatids from their shared cytoplasm. Our work thus describes a critical function for *Tug1*, now the second lncRNA with a known role in spermatogenesis, though thousands

are thought to participate. Future work will further probe the mechanism of *Tug1* action and will identify the partners with which this gene promotes sperm individualization in mammals.

APPENDIX 1: SUPPLEMENTARY MATERIALS, CHAPTER 1

Supplementary Table S1.1. Fine-scale mapping assay, primers and probe for 10 loci

Locus	Assay*	Primers (5'-3')	Probe (5'-3')
Foxj1	TaqMan	GCTCCACTCAGCCTTGTATTCT CTGCTCCTCAAAGTCATTCATGTCT	**CTTCCTTGC(G/A)TTCTTAG**
Kcnj16	TaqMan	CGATGGCCCCAGAGAATTTCC CTGGGACATCCCACCAGTC	**TAGAAGTTCCTA(C/T)GTCCCC**
Amz2[†]	sequence	ATGGCTCAAGGGCTACTGTG AAGAACGCCAGGATGTGC	-
Prkar1a	TaqMan	CCTGCCAACATTGAGTTAGGTTTT TGGTCATACAGTATTGTTCGTTTCACA	**ATAGGCC(T/C)CAGGCATT**
Abca8b[†]	sequence	TTGTTGGCATGTCTGTGAGGCA ACTGGCTTGCCCTGGTTTGCT	-
Prkca	TaqMan	CCCATCCCTGCACAGACA ACAAATCCTGGTAAACCAAGTCACT	**CCTGT(G/C)AAACAGAAGC**
Fmnl1	TaqMan	TATTCTGTCCAATGGTGTTCTGTCA TGGGCTCAACACTGTC	**AGAGCTAAGGTCGTT(G/A)GT**
Slc25a39	TaqMan	GTGGACTGCTCAGTGTAGGAA GTTACGGTTATTGTTTTGATTCTCAGCAT	**CCTGAA(T/C)GAATCCC**
Klhl10	TaqMan	GGTCAAGTTTAGTTATTCTTTGCAAATGCT CTCTCATTAAGCCCTGGGATCTG	**AGGGACTGT(C/-)CCCAAGAG**
Ttll6	Enzyme Kpn1	GGTTTACGTGCTGGTGACCT GCTGCCAGAATGAGCATCTT	-

*****Assay indicates whether SNP genotype was assessed using a TaqMan® SNP Genotyping Assay, Sanger sequencing of the DNA fragment, or with an informative restriction enzyme.

[†] Only F_2 hybrids that showed evidence of a recombination event between *Foxj1* and *Fmnl1* (*n* = 13) were genotyped at *Amz2* and *Abca8b*.

Supplementary Table S1.2. Fine-scale mapping of sperm midpiece length

F_2 males that showed a recombination event in the surrounding region ordered by mean midpiece length (μm). Genotypes at each marker: "*Aa*" denotes heterozygous genotypes for the *P. maniculatus* and *P. polionotus* alleles, "*aa*" for homozygous *P. polionotus* alleles. Box drawn in dashed line denotes the *Prkar1a* genotype, which show a perfect association with midpiece length variation unlike any neighboring loci. By excluding a strong association with *Abca8a* and *Amz2,* the implicated region of the genome is reduced to ~1 cM.

F_2 male	midpiece	*Foxj1*	*Kcnj16*	*Abca8a*	*Prkar1a*	*Amz2*	*Prkca*	*Fmnl1*
353	15.38	*Aa*	*Aa*	*aa*	*aa*	*aa*	*aa*	*aa*
876	15.40	*Aa*	*Aa*	*aa*	*aa*	*aa*	*aa*	*aa*
914	15.59	*aa*	*aa*	*aa*	*aa*	*Aa*	*Aa*	*Aa*
958	15.71	*Aa*	*Aa*	*Aa*	*aa*	*aa*	*aa*	*aa*
971	15.80	*Aa*	*aa*	*aa*	*aa*	*aa*	*aa*	*aa*
339	15.97	*Aa*	*aa*	*aa*	*aa*	*aa*	*aa*	*aa*
411	16.14	*aa*	*Aa*	*Aa*	*Aa*	*Aa*	*aa*	*aa*
919	16.14	*aa*	*aa*	*aa*	*Aa*	*Aa*	*Aa*	*Aa*
588	16.17	*Aa*	*Aa*	*Aa*	*Aa*	*Aa*	*aa*	*aa*
915	16.35	*aa*	*Aa*	*Aa*	*Aa*	*Aa*	*aa*	*aa*
942	16.37	*Aa*	*Aa*	*Aa*	*Aa*	*Aa*	*aa*	*aa*
603	16.42	*aa*	*Aa*	*Aa*	*Aa*	*Aa*	*aa*	*aa*
457	16.52	*aa*	*Aa*	*Aa*	*Aa*	*Aa*	*aa*	*aa*

Supplementary Table S1.3. Annotated genes residing in 1cM genomic region associated sperm midpiece length

Gene symbol	Gene	Position*	Description of gene function	Human disease phenotype(s)	References
Slc16a6	Solute carrier family 16, member 6	11: 109,450,855-109,473,598	Catalyzes rapid cross-membrane transport of monocarboxylates	-	(Halestrap & Meredith 2004)
Arsg	Arylsulfatase G	11: 109,473,374-109,573,330	Catalyzes hydrolysis of sulfate esters	hypertension (high blood pressure)	(Ferrante *et al.* 2002)
Wipi1	WD repeat domain, phosphoinositide interacting 1	11: 109,573,331-109,611,967	Degrades cytosolic components (autophagy)	-	(Zhou & Zhang 2012)
Prkar1a	Protein kinase, cAMP-dependent, regulatory, type I, alpha	11: 109,649,405-109,669,656	Regulates metabolism, proliferation, differentiation, and apoptosis	Carney Complex (cancer of connective tissue) and associated male infertility	(Bossis 2004; Veugelers 2004; Burton & McKnight 2007)
Fam20a	Family with sequence similarity 20, member A	11: 109,669,749-109,722,279	Involved in biomineralization of enamel and tooth eruption	hypoplastic amelogenesis imperfecta (dental enamel defects)	(Nalbant *et al.* 2005; Cho *et al.* 2012)

* Position in base pairs in *Mus musculus* based on Mouse Genome Database (Eppig *et al.* 2012).

† Functional and transcriptional literature review of all known genes found in the region was conducted to identify those associated with male fertility, spermatogenesis, sperm motility, and/or specifically or more highly expressed in the testes or during spermatogenesis. Review preformed in PubMed (using each of those terms as search items, as well as “sperm”, gene name and symbol) and several online databases: UCSC Genome Browser (Karolchik *et al.* 2014), UniProt (The Uniprot Consortium 2014), Mouse

Genome Database (Eppig *et al.* 2012), Rat Genome Database (Shimoyama *et al.* 2015), and EMBL-EBI (Kanz *et al.* 2005).

Supplementary Table S1.4. Primers for *Prkar1a* cDNA sequencing

Location	Forward primer (5’-3’)	Location	Reverse primer (5’-3’)
Exon 1c	GCCATGGTTCCTCTGTCTTG	Exon 8	AGAACTCATCCCCTGGCTCT
Exon 7	ATGTGAAACTGTGGGGCATT	3' UTR	ACGACCCAGTACTTGCCATC

Supplementary Table S1.5. Gene expression assays (qPCR) primers for *Prkar1a*, three specific *Prkar1a* transcripts and five neighboring loci in *Peromyscus*

Locus	Forward primer (5'-3')		Reverse primer (5'-3')	
Prkar1a all transcripts	Exon 2	TCCAGAAGCACAACATCCAG	Exon 3	TTCATCCTCCCTGGAGTCAG
Prkar1a E1a	Exon 1a	TGAGACCTCCCAACAACAGA	Exon 2	CTCTTCCTCACTGGCGGTAG
Prkar1a E1b	Exon 1b	CTAGCGCTGAGTGGAGTGAG	Exon 2	CTCTTCCTCACTGGCGGTAG
Prkar1a E1c	Exon 1c	GGTCGTGATACTCGGCTGTC	Exon 2	CTCTTCCTCACTGGCGGTAG
Slc16a6	Exon 4	GTCGCTTCTACGGGAGAGTG	Exon 5	TGATGATTGGTCGAAGCAAG
Arsg	Exon 1	TGGCTTCTGAAGGAATGAGG	Exon 2	CTACAGACGTGACGGCAAAG
Wipi1	Exon 9	GGACATGATGAACCAGGACA	Exon 10	CATCCTGAGGGTCCAGATTG
Fam20a	Exon 2	CAGCAAGCTCCTCCATGAC	Exon 4	CCAAAGTCCGAGAACCTCAG
ActB	Exon 4	TGCCCATCTATGAGGGCTAC	Exon 4	TGAAGCTATAGCCACGCTCA

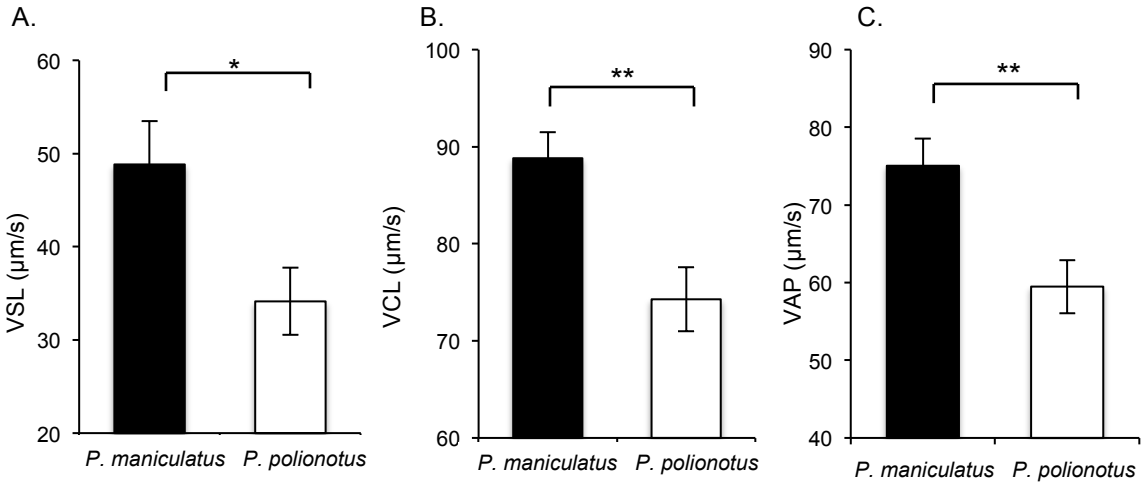

Supplementary Figure S1.1. *Peromyscus* sperm velocity

Mean±SE sperm velocity measured in *P. maniculatus* and *P. polionotus* (*n* = 9 males; *n* = 76-549 sperm/male) males in three ways: (a) straight-line velocity (VSL), (b) curvilinear velocity (VCL), and (c) average path velocity (VAP). All three measures show that *P. maniculatus* sperm cells are significantly faster than *P. polionotus* cells. Note truncated y-axis. **P*<0.05, ***P*<0.005.

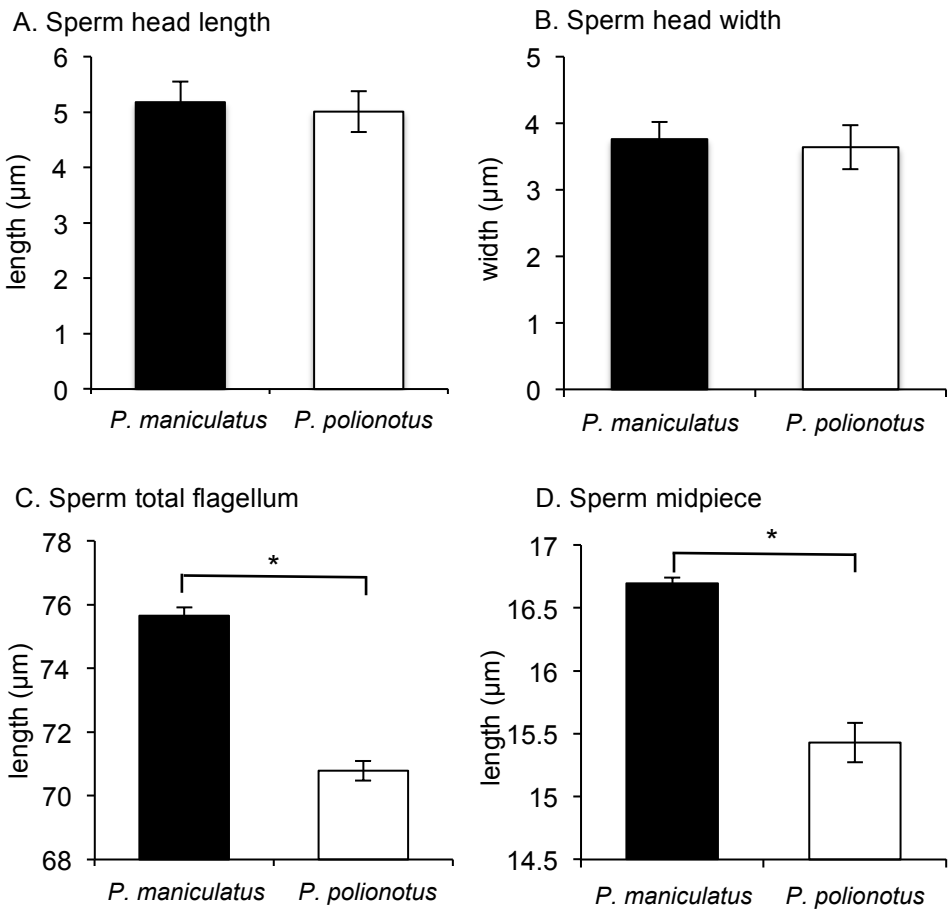

Supplementary Figure S1.2. *Peromyscus* sperm morphology

Mean±SE of *P. maniculatus* and *P. polionotus* (*n* = 10 males; *n* = 10 sperm/male) sperm cells. Sperm head and width do not differ significantly, yet *P. maniculatus* total flagellum and midpiece length are significantly longer than those in *P. polionotus* sperm. Note truncated y-axis. **P* <0.0001

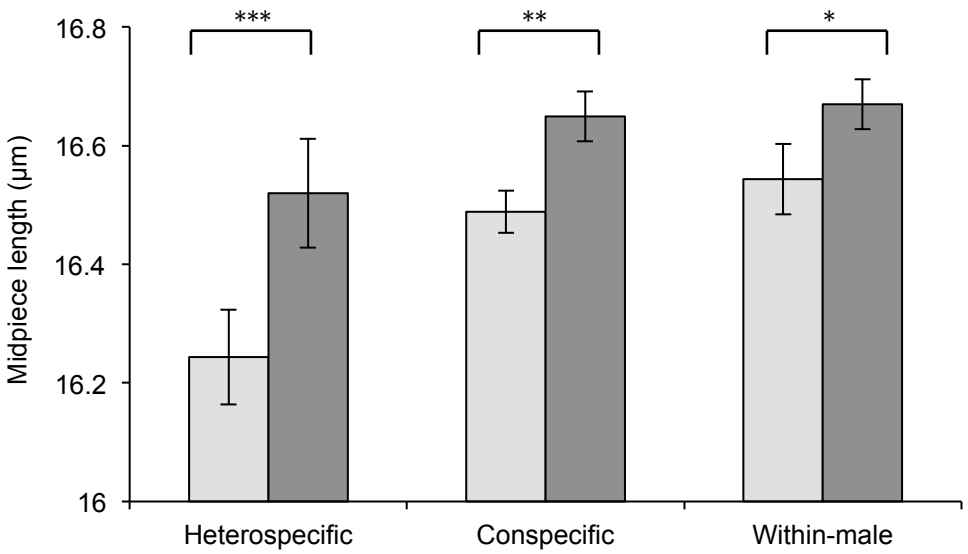

Supplementary Figure S1.3. Competitive sperm swim-up assays

Mean±SE of sperm collected prior to spinning (pre-spin; light grey bars) and from the centrifuged sample surface (post-spin; dark grey bars) in heterospecific (*P. maniculatus* vs. *P. polionotus*; *n* = 12), conspecific (*P. maniculatus* vs. *P. maniculatus*; *n* = 15), and within-male (*P. maniculatus*; *n* = 19) competitive swim-up assays. The mean midpiece regions (*n* = 20 sperm) of competitive sperm collected following centrifugation were significantly longer than those entering all three assays. Note truncated y-axis. *P<0.05, **P<0.005, ***P<0.0005

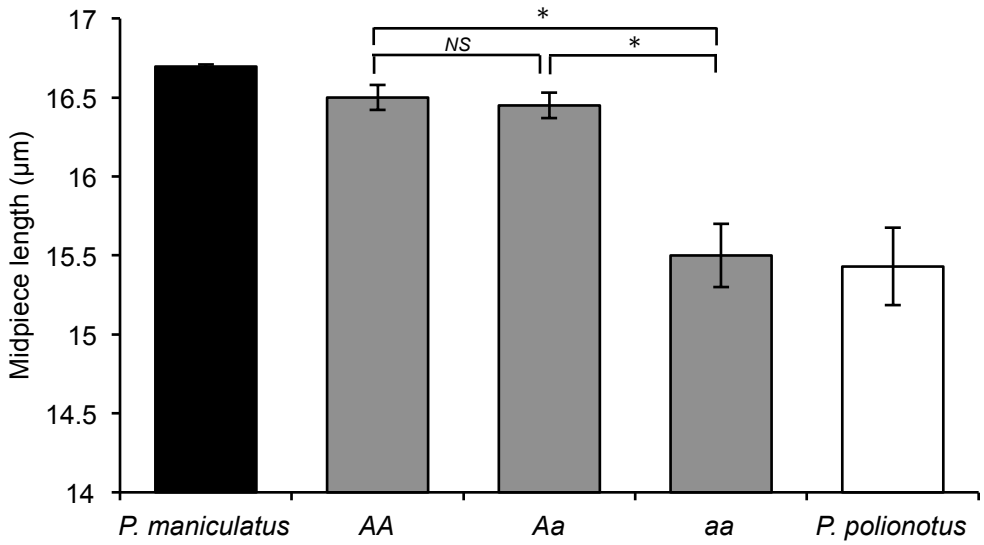

Supplementary Figure S1.4. Midpiece difference between *Prkar1a* genotypes in hybrids relative to parental phenotypes

Mean±SE midpiece length (*n* = 10 sperm/male) of sperm harvested from F_2 hybrid offspring (*P. maniculatus* [*n* = 10; indicated as black bar] x *P. polionotus* [*n* = 10; white bar], redrawn from Supplementary Figure S1.2D for reference here). "*AA*" denotes males homozygous for the *P. maniculatus* allele at the *Prkr1a* locus (*n* = 61), "*Aa*" for heterozygous males (*n* = 130), and "*aa*" for males homozygous for the *P. polionotus* allele (*n* = 50). Note truncated y-axis. **P* <0.0001, *NS* = not significant.

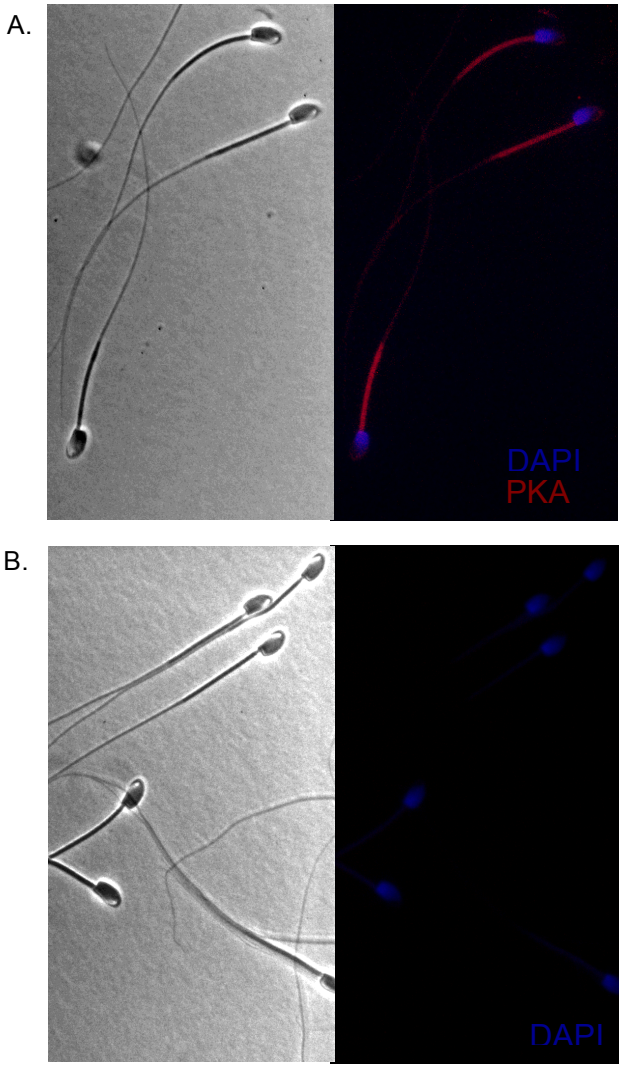

Supplementary Figure S1.5. PKA R1α localization in *Peromyscus* sperm cells

Phase-contrast images of epididymal sperm cells from *P. maniculatus* at 1000X magnification (left) and the same cells with DAPI staining, (a) with and (b) without PKA R1α antibody staining (right). Both treatment (a) and control (b) cells were subjected to identical manipulation (except that control cells were not exposed to the PKA R1α primary antibody) including exposure to the secondary antibody, Alexa Fluor 546.

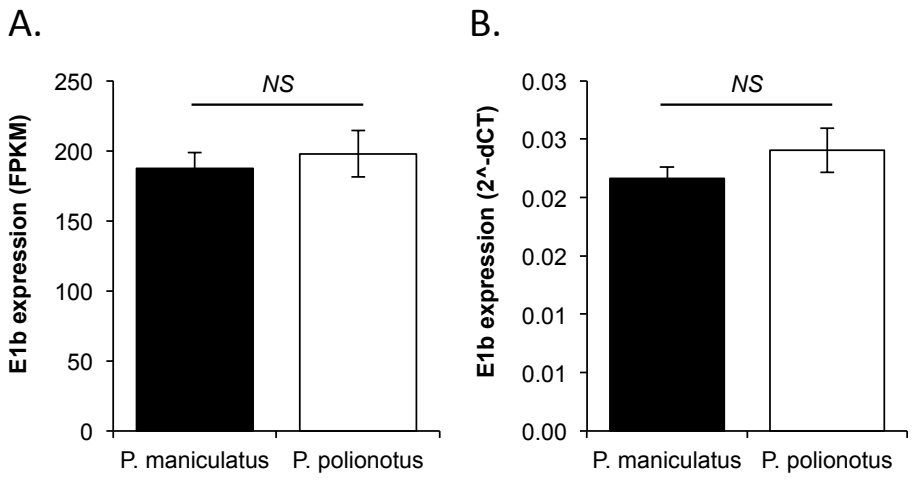

Supplementary Figure S1.6. *Prkar1a 1b* expression in somatic tissues

A. Mean±SE expression of Prkar1a E1b transcript (RPKM) in *P. maniculatus* (black) and *P. polionotus* (white) hypothalamus by RNA-Seq. B. Mean±SE expression of Prkar1a E1b transcript (*n* = 4) relative to a housekeeping gene, *beta actin*, in *P. maniculatus* (black) and *P. polionotus* (white) spleen by qPCR. *NS* = not significant.

APPENDIX 2: SUPPLEMENTARY MATERIALS, CHAPTER 2

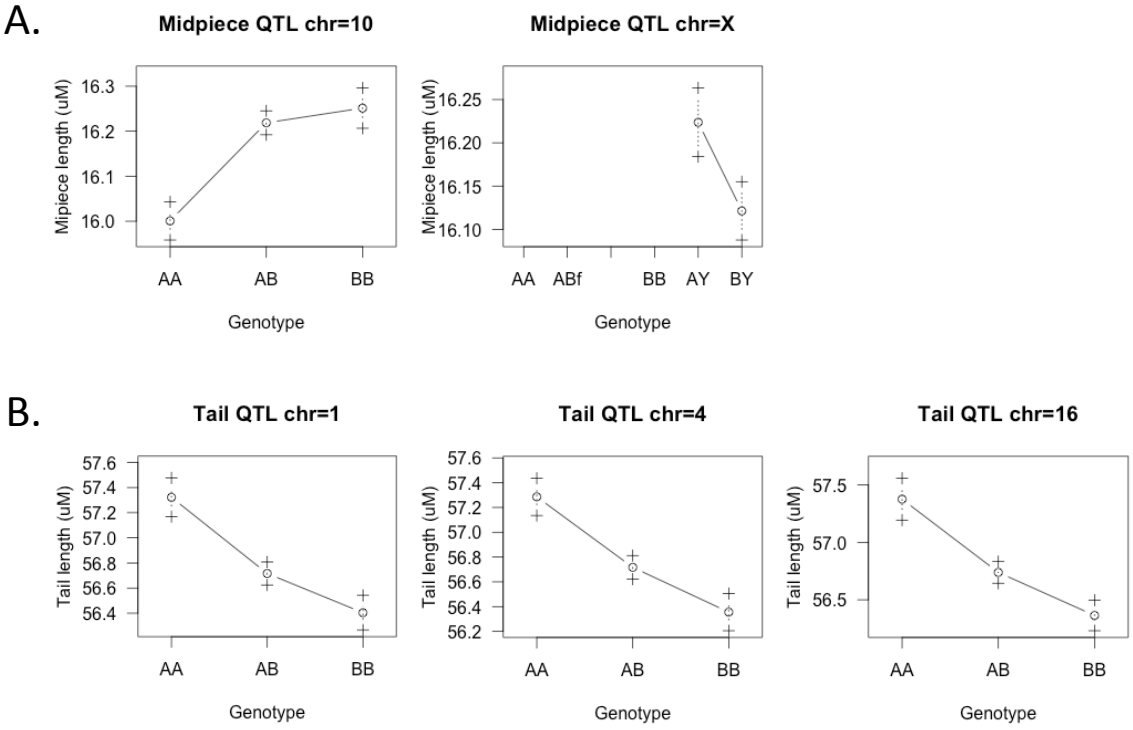

Supplementary Figure S2.1: Individual intraspecific QTL effects

AA: *P. m. bairdii* genotype; BB: *P. m. nubiterrae* genotype

APPENDIX 3: SUPPLEMENTARY MATERIALS, CHAPTER 3

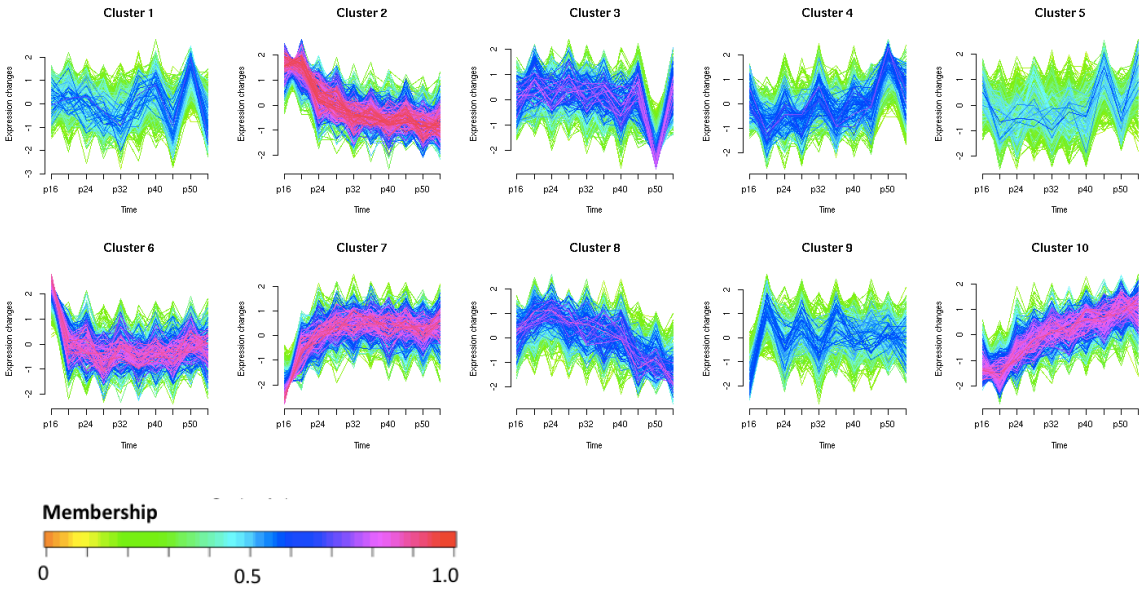

Supplementary Figure S3.1. Soft clusters for ASE patterns across spermatogenesis

Ten clusters were produced with m = 1.33; c = 10. Clusters 2, 6, 7, and 10 contain many genes with high (≥0.75) membership.

Supplementary Table S3.1. Datasets used for *P. maniculatus* x *P. polionotus* SNP variant calling

Individual	Species	Tissue	Owner
BW 1513	*P. maniculatus*	testis	H. Fisher
BW 1518	*P. maniculatus*	testis	H. Fisher
BW 1519	*P. maniculatus*	testis	H. Fisher
BW 1525	*P. maniculatus*	testis	H. Fisher
BW 1529	*P. maniculatus*	testis	H. Fisher
BW 6249	*P. maniculatus*	whole brain	H. Metz
BW 6250	*P. maniculatus*	whole brain	H. Metz
PO 127	*P. polionotus*	testis	H. Fisher
PO 129	*P. polionotus*	testis	H. Fisher
PO 134	*P. polionotus*	testis	H. Fisher
PO 139	*P. polionotus*	testis	H. Fisher
PO 140	*P. polionotus*	testis	H. Fisher
PO 6228	*P. polionotus*	whole brain	H. Metz
PO 6229	*P. polionotus*	whole brain	H. Metz
D16_1	*P. maniculatus* x *P. polionotus* F1 hybrid	testis	E. Jacobs-Palmer
D16_2	*P. maniculatus* x *P. polionotus* F1 hybrid	testis	E. Jacobs-Palmer
D20_1	*P. maniculatus* x *P. polionotus* F1 hybrid	testis	E. Jacobs-Palmer
D20_2	*P. maniculatus* x *P. polionotus* F1 hybrid	testis	E. Jacobs-Palmer
D24_1	*P. maniculatus* x *P. polionotus* F1 hybrid	testis	E. Jacobs-Palmer
D24_2	*P. maniculatus* x *P. polionotus* F1 hybrid	testis	E. Jacobs-Palmer
D28_1	*P. maniculatus* x *P. polionotus* F1 hybrid	testis	E. Jacobs-Palmer
D28_2	*P. maniculatus* x *P. polionotus* F1 hybrid	testis	E. Jacobs-Palmer
D32_1	*P. maniculatus* x *P. polionotus* F1 hybrid	testis	E. Jacobs-Palmer
D32_2	*P. maniculatus* x *P. polionotus* F1 hybrid	testis	E. Jacobs-Palmer
D36_1	*P. maniculatus* x *P. polionotus* F1 hybrid	testis	E. Jacobs-Palmer
D36_2	*P. maniculatus* x *P. polionotus* F1 hybrid	testis	E. Jacobs-Palmer
D40_1	*P. maniculatus* x *P. polionotus* F1 hybrid	testis	E. Jacobs-Palmer
D40_2	*P. maniculatus* x *P. polionotus* F1 hybrid	testis	E. Jacobs-Palmer
D44_1	*P. maniculatus* x *P. polionotus* F1 hybrid	testis	E. Jacobs-Palmer
D44_2	*P. maniculatus* x *P. polionotus* F1 hybrid	testis	E. Jacobs-Palmer
D50_1	*P. maniculatus* x *P. polionotus* F1 hybrid	testis	E. Jacobs-Palmer
D50_2	*P. maniculatus* x *P. polionotus* F1 hybrid	testis	E. Jacobs-Palmer
D64_1	*P. maniculatus* x *P. polionotus* F1 hybrid	testis	E. Jacobs-Palmer
D64_2	*P. maniculatus* x *P. polionotus* F1 hybrid	testis	E. Jacobs-Palmer
BWxPO_6120	*P. maniculatus* x *P. polionotus* F1 hybrid	brain	H. Metz
BWxPO_6121	*P. maniculatus* x *P. polionotus* F1 hybrid	brain	H. Metz
BWxPO_6122	*P. maniculatus* x *P. polionotus* F1 hybrid	brain	H. Metz
BWxPO_6331	*P. maniculatus* x *P. polionotus* F1 hybrid	brain	H. Metz
BWxPO_F1_3	*P. maniculatus* x *P. polionotus* F1 hybrid	brain	H. Metz
BWxPO_F1_4	*P. maniculatus* x *P. polionotus* F1 hybrid	brain	H. Metz

APPENDIX 4: SUPPLEMENTARY MATERIALS, CHAPTER 4

Supplemental Text S4.1.

Supplemental methods describing quality control steps to ensure samples are not contaminated or mislabeled.

Based on the alignment properties of simulated reads from each genome, we selected an *ad hoc* mapping quality cutoff of q20 (Supplemental Table S3). This implies an error rate of less than 0.008 for either genome. Although undoubtedly our simulation does not account for all sources of error that are present in real data, it is reasonable to suppose that a q20 cutoff will reduce the error due to erroneously assigning reads to the alternative parental chromosome. Moreover, even if some error in chromosome assignment persists, in the absence of segregation distortion, we expect the error to affect the mapping properties of reads derived from somatic tissue and gametes equivalently, and will therefore contribute only to type 2, but not type 1 error.

Libraries appear to be very high quality. Notably, the rate of putative PCR-duplicates is quite low, and the relative representation of individuals varies little. Reference bias is a property wherein those reads that contain reference alleles are more likely to align to the genome. Consistent with this, we observe a slight skew in all libraries towards WSB alleles on average. Although some methods exist for circumventing reference bias via local *de novo* assembly (e.g. Schneeberger et al. 2009, Corbett-Detig and Hartl 2012), these require a multiple sequence alignment step

subsequent to *de novo* assembly for consideration of orthologous regions. This is computationally expensive and time consuming when applied to whole mammalian-sized genome datasets. As with the error profile associated with assigning reads to parental chromosomes, the presence of somatic tissues controls for this low-level residual reference bias.

Prior to downstream analyses, we excluded the possibility of contamination or mislabeling of samples or individuals. First, we checked that alleles aligned to the X chromosome, Y chromosome, and mtDNA are consistent with the expected parentage of the cross. That is, we checked that for all CW males the vast majority of their Y-aligned reads attributed to the CAST/EiJ consensus Y chromosome sequence, and that X-chromosome and mtDNA aligned reads were mostly attributed to WSB/EiJ consensus sequences. We confirmed that the opposite is true for WC males. We further used relative mtDNA abundance to confirm that tissues were correctly labeled throughout. That is, we checked that the mtDNA abundance in sperm samples, liver samples, and tail samples are all most similar to other samples of the same tissue type and different between tissue types. For example, sperm has very little mtDNA in the sequencing preparations compared to tail and liver (an approximately 3 fold difference on average, Supplemental Table S2).

Supplemental Table S4.1.

List of genomic windows excluded from all downstream analyses due to detection of individual libraries with unusually high depth.

Available online at: http://biorxiv.org/content/early/2014/12/23/008672.figures-only

Supplemental Table S4.2.

Quality control results for the quantity of reads in each library derived from the *Y* chromosome, *X* chromosome, and mtDNA.

Library	Tissue	Total_Aligned	mt_cast	mt_wsb	x_cast	x_wsb	y_cast	y_wsb
CW10L	L	789925	1.14E-05	0.011412476	0.000432952	0.021074153	2.53E-05	5.32E-05
CW10S	S	4259992	7.04E-07	1.29E-05	0.000429109	0.020788771	2.86E-05	5.73E-05
CW11L	L	1302650	7.68E-07	0.00812037	0.000438337	0.019941657	3.61E-05	5.22E-05
CW11S	S	4340869	4.61E-07	1.80E-05	0.000446685	0.020838454	2.74E-05	5.37E-05
CW11T	T	1323452	3.02E-06	0.001351768	0.000402735	0.021148481	2.57E-05	5.74E-05
CW3L	L	216397	1.85E-05	0.019394908	0.000471356	0.020374589	2.77E-05	4.62E-05
CW3S	S	2171209	0	6.77E-05	0.000450901	0.020999821	3.32E-05	5.62E-05
CW4L	L	2578641	3.49E-06	0.003710869	0.000432011	0.020379727	3.22E-05	4.61E-05
CW4S	S	3506512	2.85E-07	2.62E-05	0.000442035	0.020684372	2.97E-05	4.45E-05
CW5L	L	506048	1.98E-05	0.023313994	0.000464383	0.020322183	2.96E-05	5.14E-05
CW5S	S	3651884	5.48E-07	5.18E-05	0.00041239	0.020785436	3.29E-05	5.26E-05
CW7L	L	1563351	8.32E-06	0.009392644	0.000400422	0.020257127	4.09E-05	4.93E-05
CW7S	S	1762177	1.70E-06	2.33E-05	0.000426745	0.020969517	3.12E-05	5.45E-05
CW7T	T	3030603	1.32E-06	0.001159835	0.000434897	0.020952266	3.00E-05	4.72E-05
CW8L	L	2497562	5.21E-06	0.007538952	0.000397187	0.019781291	3.56E-05	4.32E-05
CW8S	S	3533909	0	2.89E-05	0.000424459	0.020766239	2.97E-05	5.60E-05
CW8T	T	3494677	5.72E-07	0.001303983	0.000448396	0.021141868	2.80E-05	5.52E-05
CW9L	L	819902	9.76E-06	0.012592968	0.000398828	0.020463421	2.68E-05	5.00E-05
CW9S	S	3643365	2.74E-07	4.67E-05	0.000450957	0.021106038	3.21E-05	4.94E-05
CW9T	T	2177073	1.84E-06	0.001190589	0.000408346	0.020692462	3.40E-05	5.47E-05
WC1L	L	2068510	0.010179791	3.53E-05	0.019690018	0.000540002	2.08E-05	3.43E-05
WC1S	S	1549522	0.000192317	2.58E-06	0.020488254	0.000622773	2.07E-05	2.90E-05
WC2L	L	1219086	0.009977147	2.87E-05	0.019550713	0.000489711	2.05E-05	2.95E-05
WC2S	S	1820514	0.000222465	0	0.020462902	0.000607521	2.36E-05	3.52E-05
WC3L	L	278081	0.019206634	9.35E-05	0.019638163	0.00050345	3.24E-05	2.88E-05
WC3S	S	709204	0.000256626	0	0.02055685	0.000564013	2.40E-05	3.67E-05
WC3T	T	4020369	0.000775551	9.95E-07	0.019778781	0.00051836	2.41E-05	3.16E-05
WC4L	L	999550	0.013323996	8.20E-05	0.020116052	0.000626282	1.80E-05	3.60E-05
WC4S	S	2024248	6.13E-05	4.94E-07	0.020647174	0.000533037	2.17E-05	3.85E-05
WC4T	T	1609726	0.00150274	3.73E-06	0.02003695	0.000531146	1.99E-05	2.48E-05
WC5L	L	1277781	0.023531419	6.89E-05	0.018957083	0.000502434	1.80E-05	3.76E-05
WC5S	S	3178918	3.55E-05	0	0.020197124	0.000531627	2.45E-05	3.46E-05
WC7L	L	281190	0.043849355	0.000106689	0.017952274	0.000444539	1.78E-05	5.69E-05
WC7S	S	2195967	5.60E-05	4.55E-07	0.020216606	0.000544179	3.01E-05	3.32E-05
WC7T	T	2775322	0.001130319	4.68E-06	0.020162705	0.00050913	2.38E-05	2.63E-05
WC8L	L	1924417	0.014270296	4.26E-05	0.019235956	0.000515481	2.39E-05	3.12E-05
WC8S	S	2600197	9.46E-05	7.69E-07	0.020052711	0.000546497	2.92E-05	3.50E-05
WC8T	T	3226947	0.000818111	1.55E-06	0.01976946	0.000515038	2.39E-05	3.13E-05
WC9L	L	1616820	0.017384124	4.70E-05	0.018880271	0.000522012	2.54E-05	3.22E-05
WC9S	S	3965923	5.27E-05	2.52E-07	0.020207906	0.000547666	2.45E-05	3.61E-05

Supplemental Table S4.3.

Alignment simulation results showing the relationship between the reported mapping quality for a read and its probability of correct assignment to the genomic location from which it was derived.

mapq	reads_aligned_correctly	reads_aligned_incorrectly	proprotion_aligned_incorrectly
0	1636676	362828	0.181459002
1	1368445	6845	0.004977132
2	1368220	6765	0.004920054
3	1368115	6718	0.004886412
4	1350344	2611	0.00192985
5	1350099	2456	0.001815823
6	1349884	2367	0.001750415
7	1349664	2311	0.001709351
8	1349473	2275	0.001683006
9	1349337	2237	0.001655107
10	1336708	1928	0.001440272
11	1336396	1624	0.001213734
12	1335929	1422	0.001063296
13	1335452	1344	0.001005389
14	1334943	1261	0.000943718
15	1334456	1217	0.000911151
16	1321858	1075	0.000812588
17	1321253	1037	0.000784246
18	1320678	1003	0.000758882
19	1320116	971	0.000735001
20	1319409	939	0.000711176
21	1318584	903	0.000684357
22	1302793	803	0.000615988
23	1301529	773	0.000593564
24	1300787	755	0.000580081
25	1298340	725	0.000558094
26	1296451	697	0.000537333
27	1296386	697	0.00053736
28	971659	115	0.00011834
29	971555	107	0.000110121
30	971471	105	0.000108072
31	971303	103	0.000106032
32	971101	101	0.000103995
33	971034	99	0.000101943
34	949494	92	9.69E-05

35	949398	86	9.06E-05
36	949277	86	9.06E-05
37	949067	84	8.85E-05
38	948846	80	8.43E-05
39	948753	80	8.43E-05
40	921805	76	8.24E-05
41	728041	25	3.43E-05
42	722314	23	3.18E-05
43	717506	22	3.07E-05
44	710018	18	2.54E-05
45	572796	15	2.62E-05
46	493079	12	2.43E-05
47	485797	12	2.47E-05
48	476401	12	2.52E-05
49	471959	12	2.54E-05
50	471654	11	2.33E-05
51	471572	11	2.33E-05
52	464960	10	2.15E-05
53	450323	8	1.78E-05
54	442467	8	1.81E-05
55	365068	7	1.92E-05
56	302940	6	1.98E-05
57	282328	6	2.13E-05
58	268548	5	1.86E-05
59	260393	5	1.92E-05
60	246114	4	1.63E-05

REFERENCES

Aitken RJ, Baker M a (2004) Oxidative stress and male reproductive biology. *Reproduction, Fertility and Development*, **16**, 581–588.

Anders S, Huber W (2010) Differential expression analysis for sequence count data. *Genome biology*, **11**, R106.

Anderson JT, Willis JH, Mitchell-Olds T (2011) Evolutionary genetics of plant adaptation. *Trends in Genetics*, **27**, 258–66.

Andersson M (1994) *Sexual Selection*. Princeton University Press, Princeton, NJ.

Arnqvist G, Nilsson T (2000) The evolution of polyandry: multiple mating and female fitness in insects. *Animal Behaviour*, **60**, 145–164.

Arun G, Akhade VS, Donakonda S, Rao MRS (2012) mrhl RNA, a long noncoding RNA, negatively regulates Wnt signaling through its protein partner Ddx5/p68 in mouse spermatogonial cells. *Molecular and Cellular Biology*, **32**, 3140–52.

Avise JC, Lansman RA, Shade RO (1979) The use of restriction endonuceleases to measure mitochondrial DNA sequence relatedness in natural populations. I. Population structure and evolution in the genus Peromyscus. *Genetics*, 279–295.

Avise J, Shapira J, Daniel S (1983) Mitochondrial DNA differentiation during the speciation process in Peromyscus. *Molecular Biology and Evolution*, **1**, 38–56.

Bao J, Wu J, Schuster AS, Hennig GW, Yan W (2013) Expression profiling reveals developmentally regulated lncRNA repertoire in the mouse male germline. *Biology of Reproduction*, **89**, 107.

Bateman AJ (1948) Intra-sexual selection in Drosophila. *Heredity*, **2**, 349–368.

Bayes J, Malik H (2009) Altered heterochromatin binding by a hybrid sterility protein in Drosophila sibling species. *Science*, **326**, 1538–1541.

Benjamini Y, Hochberg Y (1995) Controlling the false discovery rate: a practical and powerful approach to multiple testing. *Journal of the Royal Statistical Society. Series B (Methodological)*, **57**, 289–300.

Berndh (2005) Ophrys apifera var. aurita. *Wikimedia Commons*.

Biggers JD, Whitten WK, Whittingham DG (1971) The culture of mouse embryos in vitro. In: *Methods of Mammalian Embryology*, p. 86. San Francisco, CA.

Birdsall DA, Nash D (1973) Occurrence of Successful Multiple Insemination of Females in Natural Populations of Deer Mice (Peromyscus maniculatus). *Evolution*, **27**, 106–110.

Birkhead TR (2010) How stupid not to have thought of that: post-copulatory sexual selection. *Journal of Zoology*, **281**, 78–93.

Birkhead TR, Hosken D, Pitnick S (2008) *Sperm Biology: an Evolutionary Perspective*. Elsevier, New York.

Birkhead TR, Pizzari T (2002) Postcopulatory sexual selection. *Nature Reviews Genetics*, **3**, 262–273.

Bjork A, Dallai R, Pitnick S (2007) Adaptive modulation of sperm production rate in Drosophila bifurca, a species with giant sperm. *Biology letters*, **3**, 517–9.

Blair WF (1948) Population Density, Life Span, and Mortality Rates of Small Mammals in the Blue-Grass Meadow and Blue-Grass Field Associations of Southern Michigan. *American Midland Naturalist*, **40**, 395–419.

Bohn GW, Tucker CM (1940) Studies of Fusarium wilt of the Tomato. I. Immunity in Lycopersicon pimpinellifolium Mill, and its inheritance in hybrids. *Research Bulletin, Missouri Agricultural Experiment Station*, **311**.

Bossis I (2004) Minireview: PRKAR1A: Normal and Abnormal Functions. *Endocrinology*, **145**, 5452–5458.

Boursot P, Auffray J (1993) The evolution of house mice. *Annual Review of Ecology, Evolution, and Systematics*, **24**, 119–152.

Bradbury JW, Davies NB (1987) Relative roles of intra-and intersexual selection. In: *Sexual selection: testing the alternatives*, pp. 143–163.

Bradshaw HDJ, Schemske D (2003) Allele substitution at a flower colour locus prodices a pollinator shift in monkeyflowers. *Nature*, **426**, 176–178.

Brennan PLR, Prum RO, McCracken KG *et al.* (2007) Coevolution of male and female genital morphology in waterfowl. *PloS One*, **2**, e418.

Brindle PK, Montminy MR (1992) The CREB family of transcription activators. *Current Biology*, **2**, 207.

Broman KW (2006) The new summary.scantwo and plot.scantwo.

Broman KW, Wu H, Sen S, Churchill G a. (2003) R/qtl: QTL mapping in experimental crosses. *Bioinformatics*, **19**, 889–890.

Bronson FH (1979) The reproductive ecology of the house mouse. *Quarterly Review of Biology*, **54**, 265–299.

Brunner S, Colman D, Travis AJ *et al.* (2008) Overexpression of RPGR leads to male infertility in mice due to defects in flagellar assembly. *Biology of Reproduction*, **79**, 608–17.

Bruseo JA, Vessey SH, Graham JS (1999) Discrimination between Peromyscus leucopus noveboracensis and Peromyscus maniculatus nubiterrae in the field. *Acta Theriologica*, **44**, 151–160.

Burton KA (2006) Haploinsufficiency at the Protein Kinase A RI Gene Locus Leads to Fertility Defects in Male Mice and Men. *Molecular Endocrinology*, **20**, 2504–2513.

Burton KA, McKnight GS (2007) PKA, germ cells, and fertility. *Physiology*, **22**, 40–46.

Cameron DR, Moav RM (1957) Inheritance in Nicotiana tabacum XXVII. Pollen killer, an alien genetic locus inducing abortion of microspores not carrying it. *Genetics*, **42**, 326–355.

Cardullo R, Baltz JM (1991) Metabolic regulation in mammalian sperm: mitochondrial volume determines sperm length and flagellar beat frequency. *Cell Motility and the Cytoskeleton*, **19**, 180–8.

Cesari F, Rennekampff V, Vintersten K *et al.* (2004) Elk-1 knock-out mice engineered by Flp recombinase-mediated cassette exchange. *Genesis*, **38**, 87–92.

Chalmel F, Lardenois A, Evrard B *et al.* (2014) High-resolution profiling of novel transcribed regions during rat spermatogenesis. *Biology of Reproduction*, **91**, 5.

Chalmel F, Rolland AD, Niederhauser-Wiederkehr C *et al.* (2007) The conserved transcriptome in human and rodent male gametogenesis. *Proceedings of the National Academy of Sciences*, **104**, 8346–8351.

Chapman T, Arnqvist G, Bangham J, Rowe L (2003) Sexual conflict. *Trends in Ecology & Evolution*, **18**, 41–47.

Chenoweth SF, McGuigan K (2010) The Genetic Basis of Sexually Selected Variation. *Annual Review of Ecology, Evolution, and Systematics*, **41**, 81–101.

Cho SH, Seymen F, Lee K-E *et al.* (2012) Novel FAM20A mutations in hypoplastic amelogenesis imperfecta. *Human Mutation*, **33**, 91–94.

Clark F (1938) Age of sexual maturity in mice of the genus Peromyscus. *Journal of Mammalogy*, **19**, 230–234.

Clarkson J, Herbison AE (2006) Postnatal development of kisspeptin neurons in mouse hypothalamus; sexual dimorphism and projections to gonadotropin-releasing hormone neurons. *Endocrinology*, **147**, 5817–25.

Cocquet J, Ellis PJI, Mahadevaiah SK *et al.* (2012) A Genetic Basis for a Postmeiotic X Versus Y Chromosome Intragenomic Conflict in the Mouse (MW Nachman, Ed,). *PLoS Genetics*, **8**, e1002900.

Colosimo PF, Hosemann KE, Balabhadra S *et al.* (2005) Widespread parallel evolution in sticklebacks by repeated fixation of Ectodysplasin alleles. *Science*, **307**, 1928–33.

Cox A, Ackert-Bicknell CL, Dumont BL *et al.* (2009) A new standard genetic map for the laboratory mouse. *Genetics*, **182**, 1335–44.

Coyne JA (1985) Genetic studies of three sibling species of Drosophila with relationship to theories of speciation. *Genetical Research*, **46**, 169–192.

Coyne JA, Orr HA (2004) *Speciation*. Sinauer Associates, Sunderland, MA.

Dahle MK, Reinton N, Orstavik KA, Tasken KA, Tasken K (2001) Novel alternatively spliced mRNA (1c) of the protein kinase A RI alpha; subunit is implicated in haploid germ cell specific expression. *Molecular Reproduction and Development*, **59**, 11–16.

Dapson RW (1972) Age structure of six populations of old-field mice, Peromyscus polionotus. *Researches on Population Ecology*, **8**, 161–169.

Darwin C (1859) *On the Origin of Species*. John Murray, Albemarle St., London, UK.

Darwin C (1871) *The Descent of Man and Selection in Relation to Sex*. John Murray, Albemarle St., London, UK.

Davis RC, Jin A, Rosales M *et al.* (2007) A genome-wide set of congenic mouse strains derived from CAST/Ei on a C57BL/6 background. *Genomics*, **90**, 306–13.

Dawe HR (2005) The Parkin co-regulated gene product, PACRG, is an evolutionarily conserved axonemal protein that functions in outer-doublet microtubule morphogenesis. *Journal of Cell Science*, **118**, 5421–5430.

Dawson W (1965) Fertility and Size Inheritance in a Peromyscus Species Cross. *Evolution*, **19**, 44–55.

DePristo M a, Banks E, Poplin R *et al.* (2011) A framework for variation discovery and genotyping using next-generation DNA sequencing data. *Nature Genetics*, **43**, 491–8.

Derrien T, Johnson R, Bussotti G *et al.* (2012) The GENCODE v7 catalog of human long noncoding RNAs: analysis of their gene structure, evolution, and expression. *Genome Research*, **22**, 1775–89.

Dewsbury DA (1981) An exercise in the prediction of monogamy in the field from laboratory data on 42 species of muroid rodents. *Biologist*, **63**, 138–162.

Dewsbury DA (1985) Interactions between males and their sperm during multi-male copulatory episodes of deer mice (Peromyscus maniculatus). *Animal Behaviour*, **33**, 1266–1274.

Dobin A, Davis C a, Schlesinger F *et al.* (2013) STAR: ultrafast universal RNA-seq aligner. *Bioinformatics*, **29**, 15–21.

Dobzhansky T (1937) *Genetics and the origin of species*. Columbia University Press, New York, NY.

Eberhard W (1996) *Female control: sexual selection by cryptic female choice*. Princeton University Press, Princeton, NJ.

Eberhard WG (1998) Female roles in sperm competition. In: *Sperm Competition and Sexual Selection*, pp. 91–115.

Eden E, Lipson D, Yogev S, Yakhini Z (2007) Discovering motifs in ranked lists of DNA sequences. *PLoS Computational Biology*, **3**, e39.

Eden E, Navon R, Steinfeld I, Lipson D, Yakhini Z (2009) GOrilla: a tool for discovery and visualization of enriched GO terms in ranked gene lists. *BMC bioinformatics*, **10**, 48.

Eppig JT, Blake J a, Bult CJ, Kadin J a, Richardson JE (2012) The Mouse Genome Database (MGD): comprehensive resource for genetics and genomics of the laboratory mouse. *Nucleic Acids Research*, **40**, D881–6.

Erezyilmaz DF, Stern DL (2013) Pupariation site preference within and between Drosophila sibling species. *Evolution*, **67**, 2714–27.

Evans K, Fryer A, Inglehearn C (1994) Genetic linkage of cone-rod retinal dystrophy to chromosome 19q and evidence for segregation distortion. *Nature Genetics*, **6**, 210–213.

Fabian L, Brill JA (2012) Drosophila spermiogenesis: Big things come from little packages. *Spermatogenesis*, **2**, 197–212.

Fabrizio JJ, Hime G, Lemmon SK, Bazinet C (1998) Genetic dissection of sperm individualization in Drosophila melanogaster. *Development*, **1843**, 1833–1843.

Fatica A, Bozzoni I (2014) Long non-coding RNAs: new players in cell differentiation and development. *Nature reviews. Genetics*, **15**, 7–21.

Ferrante P, Messali S, Meroni G, Ballabio A (2002) Molecular and biochemical characterisation of a novel sulphatase gene: Arylsulfatase G (ARSG). *European Journal of Human Genetics*, **10**, 813–818.

Firman RC, Simmons LW (2010) Sperm midpiece length predicts sperm swimming velocity in house mice. *Biology Letters*, **6**, 513–516.

Fisher RA (1930) *The Genetical Theory of Natural Selection*.

Fisher HS, Hoekstra HE (2010) Competition drives cooperation among closely related sperm of deer mice. *Nature*, **463**, 801–803.

Foltz DW (1981) Genetic Evidence for Long-Term Monogamy in a Small Rodent, Peromyscus polionotus. *The American Naturalist*, **117**, 665.

Frank S (1991) Divergence of meiotic drive-suppression systems as an explanation for sex-biased hybrid sterility and inviability. *Evolution*, **45**, 262–267.

Freour T, Com E, Barriere P *et al.* (2013) Comparative proteomic analysis coupled with conventional protein assay as a strategy to identify predictors of successful testicular sperm extraction in patients with non-obstructive azoospermia. *Andrology*, **1**, 414–420.

Futschik M (2014) Mfuzz: Soft clustering of time series gene expression data.

Genner MJ, Seehausen O, Lunt DH *et al.* (2007) Age of cichlids: new dates for ancient lake fish radiations. *Molecular Biology and Evolution*, **24**, 1269–82.

Geraldes A, Basset P, Gibson B *et al.* (2008) Inferring the history of speciation in house mice from autosomal, X-linked, Y-linked and mitochondrial genes. *Molecular Ecology*, **17**, 5349–63.

Gleason JM, Nuzhdin S V, Ritchie MG (2002) Quantitative trait loci affecting a courtship signal in Drosophila melanogaster. *Heredity*, **89**, 1–6.

Gleason JM, Ritchie MG (2004) Do Quantitative Trait Loci (QTL) for a Courtship Song Difference Between Drosophila simulans and D . sechellia Coincide With Candidate Genes. , **1311**, 1303–1311.

Gomendio M, Roldan ERS (2008) Implications of diversity in sperm size and function for sperm competition and fertility. *International Journal of Developmental …*.

Groot a. T, Staudacher H, Barthel a. *et al.* (2013) One quantitative trait locus for intra- and interspecific variation in a sex pheromone. *Molecular Ecology*, **22**, 1065–1080.

Guttman M, Rinn JL (2012) Modular regulatory principles of large non-coding RNAs. *Nature*, **482**, 339–46.

Haig D, Bergstrom CT (1995) Multiple mating, sperm competition and meiotic drive. *Journal of Evolutionary Biology*, **8**, 265–282.

Halestrap AP, Meredith D (2004) The SLC16 gene family - from monocarboxylate transporters (MCTs) to aromatic amino acid transporters and beyond. *European Journal of Physiology*, **447**, 619–628.

Hall ER, Kelson KR (1959) *The Mammals of North America*. The Ronald Press Co.

Hartl D (1975) Modifier theory and meiotic drive. *Theoretical population biology*, **174**, 168–174.

Harvey P, Zammuto R (1985) Patterns of mortality and age at first reproduction in natural populations of mammals. *Nature*, **315**.

Hoekstra HE, Hirschmann RJ, Bundey RA, Insel PA, Crossland JP (2006) A single amino acid mutation contributes to adaptive beach mouse color pattern. *Science*, **313**.

Hoekstra HE, Hoekstra JM, Berrigan D *et al.* (2001) Strength and tempo of directional selection in the wild. *Proceedings of the National Academy of Sciences of the United States of America*, **98**, 9157–60.

Hoekstra HE, Price T (2004) Evolution. Parallel evolution is in the genes. *Science*, **303**, 1779–81.

Holt W V, Hernandez M, Warrell L, Satake N (2010) The long and the short of sperm selection in vitroand in vivo: swim-up techniques select for the longer and faster swimming mammalian sperm. *Journal of Evolutionary Biology*, **23**, 598–608.

Hosken DJ, Stockley P (2004) Sexual selection and genital evolution. *Trends in ecology & evolution*, **19**, 87–93.

Howard WE (1949) Dispersal, amount of inbreeding, and longevity in a local population of prairie deermice on the George Reserve, southern Michigan.

Hurst L, Pomiankowski A (1991) Causes of Sex Ratio Bias May Account for Unisexual Sterility in Hybrids: a new explanation of Haldane's Rule and Related Phenomena. *Genetics*.

Ikeuchi T, Igarashi S, Takiyama Y *et al.* (1996) Non-Mendelian transmission in dentatorubral-pallidoluysian atrophy and Machado-Joseph disease: the mutant allele is preferentially transmitted in male meiosis. *American Journal of Human Genetics*, **58**, 730–733.

Immler S, Birkhead TR (2007) Sperm competition and sperm midpiece size: no consistent pattern in passerine birds. *Proceedings. Biological sciences / The Royal Society*, **274**, 561–568.

Jamsai D, Bianco DM, Smith SJ *et al.* (2008) Characterization of gametogenetin 1 (GGN1) and its potential role in male fertility through the interaction with the ion channel regulator, cysteine-rich secretory protein 2 (CRISP2) in the sperm tail. *Reproduction*, **135**, 751–9.

Jarvik G, Patton M, Homfray T, Evans JP (1994) Non-Mendelian Transmission in a Human Developmental Disorder : Split Hand/Split Foot. *American Journal of Human Genetics*, **55**, 710–713.

Johanson U, West J, Lister C *et al.* (2000) Molecular Analysis of FRIGIDA , a Major Determinant of Natural Variation in Arabidopsis Flowering Time. , **290**, 344–348.

Johnson J (2012) Closeup of male secondary feather. *Wikimedia Commons*.

Kanz C, Aldebert P, Althorpe N *et al.* (2005) The EMBL Nucleotide Sequence Database. *Nucleic acids research*, **33**, D29–33.

Karolchik D, Barber GP, Casper J *et al.* (2014) The UCSC Genome Browser database: 2014 update. *Nucleic acids research*, **42**, D764–70.

Kay G, Penny G, Patel D, Ashworth A (1993) Expression of Xist during mouse development suggests a role in the initiation of X chromosome inactivation. *Cell*, **72**, 171–182.

Keane TM, Goodstadt L, Danecek P *et al.* (2011) Mouse genomic variation and its effect on phenotypes and gene regulation. *Nature*, **477**, 289–94.

Kierszenbaum A, Tres L (1975) Structural and transcriptional features of the mouse spermatid genome. *The Journal of cell biology*, **65**.

Kim D, Pertea G, Trapnell C *et al.* (2013) TopHat2: accurate alignment of transcriptomes in the presence of insertions, deletions and gene fusions. *Genome biology*, **14**, R36.

Kingsolver JG, Hoekstra HE, Hoekstra JM (2001) The strength of phenotypic selection in natural populations. *The American Naturalist*.

Kleiman DG (1977) Monogamy in mammals. *Quarterly Review of Biology*, **52**, 39–69.

Knight J (2002) Sexual stereotypes. *Nature*, **415**, 17–19.

Kopp A, Graze R, Xu S, Carroll S, Nuzhdin S (2003) Quantitative trait loci responsible for variation in sexually dimorphic traits in Drosophila melanogaster. *Genetics*, **787**, 771–787.

Korstanje R, Paigen B (2002) From QTL to gene: the harvest begins. *Nature genetics*, **31**, 235–236.

Kosiol C, Vinar T, da Fonseca RR *et al.* (2008) Patterns of positive selection in six Mammalian genomes. *PLoS genetics*, **4**, e1000144.

Kotaja N (2004) Abnormal sperm in mice with targeted deletion of the act (activator of cAMP-responsive element modulator in testis) gene. *Proceedings of the National Academy of Sciences*, **101**, 10620–10625.

Laiho A, Kotaja N, Gyenesei A, Sironen A (2013) Transcriptome profiling of the murine testis during the first wave of spermatogenesis. *PloS one*, **8**, e61558.

Lande R (1981) Models of speciation by sexual selection on polygenic traits. *Proceedings of the National Academy of Sciences*, **78**, 3721–3725.

Larracuente AM, Presgraves DC (2012) The selfish Segregation Distorter gene complex of Drosophila melanogaster. *Genetics*, **192**, 33–53.

Lassance J-M, Groot AT, Liénard M a *et al.* (2010) Allelic variation in a fatty-acyl reductase gene causes divergence in moth sex pheromones. *Nature*, **466**, 486–9.

Lee J (2012) Epigenetic Regulation by Long Noncoding RNAs. *Science*, **338**, 1435–1440.

Lemos B, Araripe L (105AD) Dominance and the evolutionary accumulation of cis-and trans-effects on gene expression. *Proceedings of the National Academy of Sciences*, **2008**, 14471–14476.

Li H, Durbin R (2010) Fast and accurate long-read alignment with Burrows-Wheeler transform. *Bioinformatics*, **26**, 589–95.

Li J, Wang S, Huang S, Cheng D (2009) Attractin Gene Deficiency Contributes to Testis Vacuolization and Sperm Dysfunction in Male Mice. *Journal of Huazhong University Science Technology*, **29**, 750–754.

Linzey A V, Layne JN (1969) Comparative morphology of the male reproductive tract in the rodent genus Peromyscus (Muridae). American Museum novitates ; no. 2355.

Linzey A V, Layne JN (1974) Comparative morphology of spermatozoa of the rodent genus Peromyscus (Muridae). American Museum novitates ; no. 2532.

Loegering WQ, Sears ER (1963) Distorted inheritance of stem-rust resistance of Timstein wheat caused by a pollen-killing gene. *Canadian Journal of Genetics and Cytology*, **5**, 65–72.

Louro R, Smirnova AS, Verjovski-Almeida S (2009) Long intronic noncoding RNA transcription: expression noise or expression choice? *Genomics*, **93**, 291–8.

Lu Q, Gore M, Zhang Q *et al.* (1999) Tyro-3 family receptors are essential regulators of mammalian spermatogenesis. *Nature*, **398**, 723–728.

Lu Q, Lemke G (2001) Homeostatic Regulation of the Immune System by Receptor Tyrosine Kinases of the Tyro 3 Family. , **293**, 306–311.

Luk AC-S, Lee T-L (2013) The Interplay of Coding and Non-Coding Regulations in Mouse Spermatogenesis. *Reproductive System & Sexual Disorders*, **S1**, 1–6.

Lunter G, Goodson M (2011) Stampy: a statistical algorithm for sensitive and fast mapping of Illumina sequence reads. *Genome research*, 936–939.

Lyttle TW (1991) Segregation distorters. *Annual review of genetics*, **25**, 511–57.

Manceau M, Domingues VS, Linnen CR, Rosenblum EB, Hoekstra HE (2010) Convergence in pigmentation at multiple levels: mutations, genes and function. *Philosophical transactions of the Royal Society of London. Series B, Biological sciences*, **365**, 2439–50.

Manser A, Lindholm AK, Barbara K, Bagheri HC (2011) Polyandry and the decrease of a selfish genetic element in a wild house mouse population. *Evolution*, **65**, 2435–2447.

Masly JP, Dalton JE, Srivastava S, Chen L, Arbeitman MN (2011) The genetic basis of rapidly evolving male genital morphology in Drosophila. *Genetics*, **189**, 357–74.

Masly JP, Jones CD, Noor M a F, Locke J, Orr HA (2006) Gene transposition as a cause of hybrid sterility in Drosophila. *Science*, **313**, 1448–50.

Matzuk MM, Lamb DJ (2008) The biology of infertility: research advances and clinical challenges. *Nature medicine*, **14**, 1197–1213.

McDermott SR, Noor M a F (2010) The role of meiotic drive in hybrid male sterility. *Philosophical transactions of the Royal Society of London. Series B, Biological sciences*, **365**, 1265–72.

McKenna A, Hanna M, Banks E *et al.* (2010) The Genome Analysis Toolkit: a MapReduce framework for analyzing next-generation DNA sequencing data. *Genome Research*, **20**, 1297–303.

McManus CJ, Coolon JD, Duff MO *et al.* (2010) Regulatory divergence in Drosophila revealed by mRNA-seq. *Genome research*, **20**, 816–25.

McNeil CL, Bain CL, Macdonald SJ (2011) Multiple Quantitative Trait Loci Influence the Shape of a Male-Specific Genital Structure in Drosophila melanogaster. *G3 (Bethesda, Md.)*, **1**, 343–51.

Mercer TR, Mattick JS (2013) Structure and function of long noncoding RNAs in epigenetic regulation. *Nature structural & molecular biology*, **20**, 300–7.

Merrill C, Bayraktaroglu L, Kusano A, Ganetzky B (1999) Truncated RanGAP encoded by the Segregation Distorter locus of Drosophila. *Science*, **283**, 1742–1746.

Mihola O, Trachtulec Z, Vlcek C, Schimenti J, Forejt J (2009) A mouse speciation gene encodes a meiotic histone H3 methyltransferase. *Science*, **323**, 373–375.

Mikolcevic P, Sigl R, Rauch V *et al.* (2012) Cyclin-dependent kinase 16/PCTAIRE kinase 1 is activated by cyclin Y and is essential for spermatogenesis. *Molecular and cellular biology*, **32**, 868–79.

Mizuno K, Kojima Y, Kurokawa S *et al.* (2009) Identification of Differentially Expressed Genes in Human Cryptorchid Testes Using Suppression Subtractive Hybridization. *The Journal of Urology*, **181**, 1330–1337.

Moller AP (1988) Testes size, ejaculate quality and sperm competition in birds. *Biological Journal of the Linnean Society*, 273–283.

Moller A (1989) Ejaculate quality, testes size and sperm production in mammals. *Functional Ecology*, **3**, 91–96.

Monesi V (1964) Ribonucleic acid synthesis during mitosis and meiosis in the mouse testis. *The Journal of cell biology*, 521–532.

Montoto LG, Arregui L, Sánchez NM, Gomendio M, Roldan ERS (2012) Postnatal testicular development in mouse species with different levels of sperm competition. *Reproduction*, **143**, 333–46.

Montoto LG, Magaña C, Tourmente M, Martín-Coello J (2011) Sperm Competition, Sperm Numbers and Sperm Quality in Muroid Rodents. *PLoS ONE*, **6**, e18173.

Moore H, Dvoráková K, Jenkins N, Breed W (2002) Exceptional sperm cooperation in the wood mouse. *Nature*, **418**.

Mukai C, Okuno M (2004) Glycolysis plays a major role for adenosine triphosphate supplementation in mouse sperm flagellar movement. *Biology of reproduction*, **71**, 540–7.

Mukherjee a, Koli S, Reddy KVR (2014) Regulatory non-coding transcripts in spermatogenesis: shedding light on “dark matter”. *Andrology*, **2**, 360–9.

Muller HJ (1942) Isolating mechanisms, evolution and temperature. *Biological Symposia*, **6**.

Nachman MW, Hoekstra HE, D’Agostino SL (2003) The genetic basis of adaptive melanism in pocket mice. *Proceedings of the National Academy of Sciences of the United States of America*, **100**, 5268–73.

Nadeau NJ, Jiggins CD (2010) A golden age for evolutionary genetics? Genomic studies of adaptation in natural populations. *Trends in genetics*, **26**, 484–92.

Nakagawa S, Shimada M, Yanaka K *et al.* (2014) The lncRNA Neat1 is required for corpus luteum formation and the establishment of pregnancy in a subpopulation of mice. *Development (Cambridge, England)*, **141**, 4618–27.

Nalbant D, Youn H, Nalbant SI *et al.* (2005) FAM20: an evolutionarily conserved family of secreted proteins expressed in hematopoietic cells. *BMC genomics*, **6**, 11.

Nef S, Parada LF (2000) Hormones in male sexual development. , 3075–3086.

Nielsen R, Bustamante C, Clark AG *et al.* (2005) A scan for positively selected genes in the genomes of humans and chimpanzees. *PLoS biology*, **3**, e170.

Noguchi T, Koizumi M, Hayashi S (2011) Sustained elongation of sperm tail promoted by local remodeling of giant mitochondria in Drosophila. *Current biology*, **21**, 805–14.

Noor M a F, Feder JL (2006) Speciation genetics: evolving approaches. *Nature reviews. Genetics*, **7**, 851–61.

Nuzhdin S, Reiwitch S (2000) Are the same genes responsible for intra- and interspecific variability for sex comb tooth number in Drosophila ? *Heredity*, **84**, 97–102.

O'Donnell L, Nicholls PK, O'Bryan MK, McLachlan RI, Stanton PG (2011) Spermiation: The process of sperm release. *Spermatogenesis*, **1**, 14–35.

O'Donnell L, Rhodes D, Smith SJ *et al.* (2012) An essential role for katanin p80 and microtubule severing in male gamete production. *PLoS genetics*, **8**, e1002698.

Obbard DJ, Maclennan J, Kim K-W *et al.* (2012) Estimating divergence dates and substitution rates in the Drosophila phylogeny. *Molecular biology and evolution*, **29**, 3459–73.

Okuwaki M, Sumi a., Hisaoka M *et al.* (2012) Function of homo- and hetero-oligomers of human nucleoplasmin/nucleophosmin family proteins NPM1, NPM2 and NPM3 during sperm chromatin remodeling. *Nucleic Acids Research*, **40**, 4861–4878.

Özen R, Baysal B, Devlin B, Farr J (1999) Fine Mapping of the Split-Hand/Split-Foot Locus (SHFM3) at 10q24 : Evidence for Anticipation and Segregation Distortion. *The American Journal of Human Genetics*, **64**, 1646–1654.

Parker GA (1970) Sperm competition and its evolutionary consequences in the insects. *Biological Reviews*, **45**, 525–567.

Parker GA, Partridge L (1998) Sexual conflict and speciation. *Philosophical transactions of the Royal Society of London. Series B, Biological sciences*, **353**, 261–274.

Pauli A, Rinn JL, Schier AF (2011) Non-coding RNAs as regulators of embryogenesis. *Nature reviews. Genetics*, **12**, 136–49.

Pazour GJ, Agrin N, Walker BL, Witman GB (2006) Identification of predicted human outer dynein arm genes: candidates for primary ciliary dyskinesia genes. *Journal of medical genetics*, **43**, 62–73.

Peterson BK, Weber JN, Kay EH, Fisher HS, Hoekstra HE (2012) Double digest RADseq: an inexpensive method for de novo SNP discovery and genotyping in model and non-model species. *PloS One*, **7**, e37135.

Petrie M, Kempenaers B (1998) species and populations. , **13**, 52–58.

Phadnis N, Orr H (2009) A single gene causes both male sterility and segregation distortion in Drosophila hybrids. *science*, **323**, 376–379.

Piomboni P, Focarelli R, Stendardi a, Ferramosca a, Zara V (2012) The role of mitochondria in energy production for human sperm motility. *International journal of andrology*, **35**, 109–24.

Pizzari T, Foster KR (2008) Sperm sociality: cooperation, altruism, and spite. *PLoS biology*, **6**, e130.

Ponjavic J, Ponting CP, Lunter G (2007) Functionality or transcriptional noise ? Evidence for selection within long noncoding RNAs. , 556–565.

Ponting CP (2006) A novel domain suggests a ciliary function for ASPM, a brain size determining gene. *Bioinformatics (Oxford, England)*, **22**, 1031–5.

Presgraves DC (2010) The molecular evolutionary basis of species formation. *Nature reviews. Genetics*, **11**, 175–80.

Prieto AL, Weber JL, Lai C (2000) Expression of the Receptor Protein- Tyrosine Kinases Tyro-3 , Axl , and Mer in the Developing Rat Central Nervous System. , **314**, 295–314.

Qiu M-T, Hu J-W, Yin R, Xu L (2013) Long noncoding RNA: an emerging paradigm of cancer research. *Tumour biology : the journal of the International Society for Oncodevelopmental Biology and Medicine*, **34**, 613–20.

R Core Team (2014) R: A Language and Environment for Statistical Computing. *R Foundation for Statistical Computing*, **1**, 409.

Rainey M a, George M, Ying G *et al.* (2010) The endocytic recycling regulator EHD1 is essential for spermatogenesis and male fertility in mice. *BMC developmental biology*, **10**, 37.

Ramm SA, Parker GA, Stockley P (2005) Sperm competition and the evolution of male reproductive anatomy in rodents. *Proceedings. Biological sciences / The Royal Society*, **272**, 949–955.

Rashid S, Grzmil P, Drenckhahn J-D *et al.* (2010) Disruption of the murine dynein light chain gene Tcte3-3 results in asthenozoospermia. *Reproduction (Cambridge, England)*, **139**, 99–111.

Rave E, Holler N (1992) Population Dynamics of Beach Mice (Peromyscus polionotus ammobates) in Southern Alabama. *Journal of Mammalogy*, **73**, 347–355.

Rehschuh J (2011) Melanochromis Maingano Malawi cyaneorhabdos. *Wikimedia Commons*.

Reiter JF, Blacque OE, Leroux MR (2012) The base of the cilium: roles for transition fibres and the transition zone in ciliary formation, maintenance and compartmentalization. *EMBO reports*, **13**, 608–18.

Rinn J, Chang H (2012) Genome regulation by long noncoding RNAs. *Annual review of biochemistry*, 8–12.

Rinn JL, Kertesz M, Wang JK *et al.* (2007) Functional demarcation of active and silent chromatin domains in human HOX loci by noncoding RNAs. *Cell*, **129**, 1311–23.

Ritchie MG (2007) Sexual Selection and Speciation. *Annual Review of Ecology, Evolution, and Systematics*, **38**, 79–102.

Rood JP (1972) Ecological and Behavioural Comparisons of Three Genera of Argentine Cavies. *Animal Behaviour Monographs*, **5**, 1–IN4.

Rosenblum EB, Römpler H, Schöneberg T, Hoekstra HE (2010) Molecular and functional basis of phenotypic convergence in white lizards at White Sands.

Russell LD, Ettlin R (1990) *Histological and histopathological evaluation of the testis*. Cache River Press.

Sadleir R (1965) The relationship between agonistic behaviour and population changes in the deermouse, Peromyscus maniculatus (Wagner). *The Journal of Animal Ecology*, **34**, 331–352.

Saito K, Kageyama Y, Okada Y *et al.* (2004) Localization of Aquaporin-7 in Human Testis and Ejaculated Sperm: Possible Involvement in Maintenance of Sperm Quality. *The Journal of Urology*, **172**, 2073–2076.

Sandler L, Novitski E (1957) Meiotic drive as an evolutionary force. *American Naturalist*, **91**, 105–110.

Sano Y, Chu YE, Oka HI (1979) Genetic studies of speciation in cultivated rice. 1. Genic analysis for the F1 sterility between Oryza sativa L. and Oryza glaberrima Steud. *Japanese Journal of Genetics*, **54**, 121–132.

Sassone-Corsi P (1998) ScienceDirect.com - Seminars in Cell & Developmental Biology - CREM: a master–switch governing male germ cells differentiation and apoptosis. *Seminars in Cell & Developmental Biology*.

Sauvageau M, Goff L a, Lodato S *et al.* (2013) Multiple knockout mouse models reveal lincRNAs are required for life and brain development. *eLife*, **2**, e01749.

Schiestl FP, Ayasse M, Taylor RP, Micolich AP (1999) Orchid pollination by sexual swindle. , 421–422.

Shaw KL, Lesnick SC (2009) Genomic linkage of male song and female acoustic preference QTL underlying a rapid species radiation. *Proceedings of the National Academy of Sciences*, **106**, 9737–9742.

Sheck a L, Groot a T, Ward CM *et al.* (2006) Genetics of sex pheromone blend differences between Heliothis virescens and Heliothis subflexa: a chromosome mapping approach. *Journal of evolutionary biology*, **19**, 600–17.

Shen C, Zhong N (2015) Long non-coding RNAs: the epigenetic regulators involved in the pathogenesis of reproductive disorder. *American journal of reproductive immunology (New York, N.Y. : 1989)*, **73**, 95–108.

Shima JE, McLean DJ, McCarrey JR, Griswold MD (2004) The murine testicular transcriptome: characterizing gene expression in the testis during the progression of spermatogenesis. *Biology of reproduction*, **71**, 319–330.

Shimoyama M, De Pons J, Hayman GT *et al.* (2015) The Rat Genome Database 2015: genomic, phenotypic and environmental variations and disease. *Nucleic acids research*, **43**, D743–50.

Smith M, Carmon J, Gentry J (1972) Pelage Color Polymorphism in Peromyscus polionotus. *Journal of mammalogy*, **53**, 824–833.

Soulsbury CD (2010) Genetic patterns of paternity and testes size in mammals. *PloS one*, **5**, e9581.

Stapley J, Reger J, Feulner PGD *et al.* (2010) Adaptation genomics: the next generation. *Trends in ecology & evolution*, **25**, 705–12.

Stern DL (2013) The genetic causes of convergent evolution. *Nature reviews. Genetics*, **14**, 751–64.

Stockley P, Gage M, Parker G, Møller A (1997) Sperm Competition in Fishes: The Evolution of Testis Size and Ejaculate Characteristics. *The American Naturalist*, **149**, 933–954.

Stoltz J a, Neff BD (2006) Sperm competition in a fish with external fertilization: the contribution of sperm number, speed and length. *Journal of evolutionary biology*, **19**, 1873–81.

Struhl K (2007) Transcriptional noise and the fidelity of initiation by RNA polymerase II. *Nature structural & molecular biology*, **14**, 103–5.

Swanson W, Vacquier V (2002) The rapid evolution of reproductive proteins. *Nature Reviews Genetics*, **3**.

Tao Y, Araripe L, Kingan SB *et al.* (2007a) A sex-ratio meiotic drive system in Drosophila simulans. II: an X-linked distorter. *PLoS biology*, **5**, e293.

Tao Y, Masly JP, Araripe L, Ke Y, Hartl DL (2007b) A sex-ratio meiotic drive system in Drosophila simulans. I: an autosomal suppressor. *PLoS biology*, **5**, e292.

Tatsuta H, Takano-Shimizu T (2006) Genetic architecture of variation in sex-comb tooth number in Drosophila simulans. *Genetical research*, **87**, 93–107.

Taylor D, Ingvarsson P (2003) Common features of segregation distortion in plants and animals. *Genetica*, **117**, 27–35.

The Heliconius Genome Consortium (2012) Butterfly genome reveals promiscuous exchange of mimicry adaptations among species. *Nature*, **487**, 94–8.

The Uniprot Consortium (2014) Activities at the Universal Protein Resource (UniProt). *Nucleic acids research*, **42**, D191–8.

Ting C, Tsaur S, Wu M, Wu C (1998) A rapidly evolving homeobox at the site of a hybrid sterility gene. *Science*, **282**, 1501–1504.

Toure A, Rode B, Hunnicutt GR, Escalier D, Gacon G (2011) Septins at the annulus of mammalian sperm. *Biological chemistry*, **392**, 799–803.

Tourmente M, Gomendio M, Roldan ERS (2011) Sperm competition and the evolution of sperm design in mammals. *BMC evolutionary biology*, **11**, 12.

Tourmente M, Gomendio M, Roldan ERS, Giojalas LC, Chiaraviglio M (2009) Sperm competition and reproductive mode influence sperm dimensions and structure among snakes. *Evolution; international journal of organic evolution*, **63**, 2513–24.

True J, Liu J, Stam L, Zeng Z, Laurie C (1997) Quantitative genetic analysis of divergence in male secondary sexual traits between Drosophila simulans and Drosophila mauritiana. *Evolution*, **51**, 816–832.

Uller T, Olsson M (2008) Multiple paternity in reptiles: patterns and processes. *Molecular ecology*, **17**, 2566–80.

Veugelers M (2004) Comparative PRKAR1A genotype-phenotype analyses in humans with Carney complex and prkar1a haploinsufficient mice. *Proceedings of the National Academy of Sciences*, **101**, 14222–14227.

Vrana PB, Guan X, Ingram RS, Tilghman SM (1998) Genomic imprinting is disrupted in interspecific Peromyscus hybrids. , **20**, 362–365.

Wagner J (2010) Transmission Ratio Distortion in the Hybrid Offspring of Three Mouse Subspecies. University of Wisconsin-Madison.

Wagner CE, Harmon LJ, Seehausen O (2012) Ecological opportunity and sexual selection together predict adaptive radiation. *Nature*, **487**, 366–9.

Wapinski O, Chang HY (2011) Long noncoding RNAs and human disease. *Trends in cell biology*, **21**, 354–61.

White MA, Stubbings M, Dumont BL, Payseur BA (2012) Genetics and Evolution of Hybrid Male Sterility in House Mice. *Genetics*.

Williams TM, Selegue JE, Werner T *et al.* (2008) The regulation and evolution of a genetic switch controlling sexually dimorphic traits in Drosophila. *Cell*, **134**, 610–23.

Willis BS, Niswender CM, Su T, Amieux PS, McKnight GS (2011) Cell-Type Specific Expression of a Dominant Negative PKA Mutation in Mice. *PLoS ONE*, **6**, e18772.

Wittkopp PJ, Stewart EE, Arnold LL *et al.* (2009) Intraspecific Polymorphism to Interspecific Divergence : Genetics of Pigmentation in Drosophila. , 540–545.

Wittkopp PJ, Williams BL, Selegue JE, Carroll SB (2002) Drosophila pigmentation evolution : Divergent genotypes underlying convergent phenotypes. , **2002**.

Wolff JO, Cicirello DM (1991) Comparative paternal and infanticidal behavior of sympatric white-footed mice (Peromyscus leucopus noveboracensis) and deermice (P. Maniculatus nubiterrae). *Behavioral Ecology*, **2**, 38–45.

Workman C, Dalen L, Vartanyan S *et al.* (2011) Population-level genotyping of coat colour polymorphism in woolly mammoth (Mammuthus primigenius). *Quaternary Science Reviews*, **30**, 2304–2308.

Wu Q, Song R, Ortogero N *et al.* (2012) The RNase III enzyme DROSHA is essential for microRNA production and spermatogenesis. *The Journal of biological chemistry*, **287**, 25173–90.

Wu C-I, Ting C-T (2004) Genes and speciation. *Nature reviews. Genetics*, **5**, 114–22.

Xiong W, Chen Y, Wang H *et al.* (2008) Gas6 and the Tyro 3 receptor tyrosine kinase subfamily regulate the phagocytic function of Sertoli cells. *Reproduction (Cambridge, England)*, **135**, 77–87.

Yang L, Froberg JE, Lee JT (2014) Long noncoding RNAs: fresh perspectives into the RNA world. *Trends in biochemical sciences*, **39**, 35–43.

Yang J, Zhao X, Cheng K, Du H, Ouyang Y (2012) A killer-protector system regulates both hybrid sterility and segregation distortion in rice. *Science*, **337**, 1336–1340.

Young TL, Matsuda T, Cepko CL (2005) The noncoding RNA taurine upregulated gene 1 is required for differentiation of the murine retina. *Current biology : CB*, **15**, 501–12.

Yuan S, Stratton CJ, Bao J *et al.* (2015) Spata6 is required for normal assembly of the sperm connecting piece and tight head-tail conjunction. *Proceedings of the National Academy of Sciences of the United States of America*, **112**, E430–9.

Van Zant JL, Wooten MC (2007) Old mice, young islands and competing biogeographical hypotheses. *Molecular Ecology*, **16**, 5070–5083.

Zhang X, Borevitz JO (2009) Global analysis of allele-specific expression in Arabidopsis thaliana. *Genetics*, **182**, 943–54.

Zheng H, Stratton CJ, Morozumi K *et al.* (2007) Lack of Spem1 causes aberrant cytoplasm removal , sperm deformation , and male infertility.

Zhou X-J, Zhang H (2012) Autophagy in immunity: Implications in etiology of autoimmune/autoinflammatory diseases. *Autophagy*, **8**, 1286–1299.